UNIVERSITY OF CALIFORNIA,
IRVINE

N-acetylcysteine for the Prevention of Cisplatin Chemotherapy-Related Cognitive Impairments

DISSERTATION

submitted in partial satisfaction of the requirements
for the degree of

DOCTOR OF PHILOSOPHY

in Biomedical Sciences

by

Naomi Lomeli

Dissertation Committee:
Associate Professor Daniela A. Bota, MD, PhD, Chair
Professor Cristina M. Kenney, MD, PhD
Professor Edwin S. Monuki, MD, PhD

2019

TABLE OF CONTENTS

LIST OF FIGURES AND TABLES

ACKNOWLEDGMENTS

I would like to express my sincerest appreciation for my mentor and committee chair, Dr. Daniela Bota, for the incredible opportunity to work with a strong visionary scientist/clinician. I greatly value her support in me, immersing me in grant writing, including me in critical meetings with collaborators, and trusting that my research will provide new insight to direct our translational studies. Her mentorship has given me the independence to grow as a scientist and person, and the valuable experiences I have gained in the Bota Lab, I will carry throughout my life.

I would like to thank my dissertation committee members, Dr. Christina Kenney, and Dr. Edwin Monuki; their critical insight, expertise, and feedback have been vital in shaping my scientific skills and advancing my projects. Thank you for all your encouragement, support, and time throughout this journey.

Thank you to all my fellow lab members (current and past) of the Bota Lab for all that they have helped me throughout my studies. I would like to thank Drs. Kaijun Di, Tami John, Diana Pearre, Michelle Pulley; and Howard Nguyen, Michael Au, Annie Chung, Chris Douglas, and Javier Lepe.

A special thank you to Drs. Tami John and Diana Pearre, who have been indispensable to this work. I have gained clinical perspectives into chemotherapy-related cognitive impairments through them, their friendship, support, and advice has been especially meaningful to me.

Thank you to Drs. John Guzowski and Jennifer Czerniawski for a fruitful collaboration, support, and advice, their expertise have been instrumental in setting up our behavioral studies.

Thank you to Dr. Marlene de la Cruz and Dr. Luis Mota-Bravo for introducing me to biomedical research as an undergraduate, and their continued support since then.

Thank you to School of Medicine Graduate Director Leora Fellus, for her support and advice throughout my graduate career. I would also like to acknowledge Stefani Ching from the Pathology Department and Briana Sara from Neurology for all their administrative help and support behind the scenes. I would also like to thank Drs. Michael McClelland and Dan Mercola, and fellow Pathology graduate students for our insightful Pathology Journal Club discussions.

Finally, I would like to thank my family, my grandmother Ella, and friends for their unwavering support throughout this entire journey.

The studies presented in this dissertation were supported by NIH grants TG GM055246 and T32 NS082174. I am very thankful to have been supported by Dr. Lorna Carlin and to have received the Founding President's ARCS Foundation Scholar Award. I am also

very honored to have been awarded the University of California President's Dissertation Year Fellowship, which supported my final year of graduate school.

CURRICULUM VITAE

Naomi Lomeli

Department of Pathology & Laboratory Medicine
839 Health Sciences Road
Sprague Hall B200
University of California, Irvine
Irvine, CA 92697

EDUCATION

2009-2013 Bachelor of Science in Biological Sciences
University of California, Irvine, Irvine, California, 92697

2013-2019 Doctor of Philosophy in Biomedical Sciences
University of California, Irvine, Irvine, California, 92697
Advisor: Daniela A. Bota, MD, PhD

HONORS AND AWARDS

2011-2012 NIH MBRS-IMSD Initiative for Maximizing Student Development for Undergraduates Grant R25GM055246

2012 NIH Minority Health and Health Disparities International Research Training (MHIRT) Grant T37MD001485

2012-2013 NIH Minority Access to Research Careers (MARC) Grant T34GM069337

2013-2015 NIH MBRS-IMSD Graduate Training Grant GM055246

2015 Ford Foundation Pre-Doctoral Fellowship Competition Honorable Mention

2016-2017 NINDS/NIH Training Grant in Stem Cell Translational Medicine for Neurological Disorders T32NS082174

2016 Seahorse Bioscience Travel Award – AACR 2016

2016 UCI School of Medicine Travel Award – AACR 2016

2017 Stanley Behrens Foundation Honorable Mention

2017 Founding President's ARCS Foundation Scholar Award

2018-2019 University of California President's Dissertation Year Fellowship

2018 UCI School of Medicine Travel Award – Society for Neuro-Oncology 2018

TEACHING EXPERIENCE

Fall, 2015 Teaching Assistant: Scientific Writing, Bio 100

Fall, 2017 Teaching Assistant: Scientific Writing, Bio 100

Winter, 2018 Teaching Assistant: Ecology and Evolution, Bio Sci 94

PROFESSIONAL SOCIETIES

2012-2013 Member, American Association for the Advancement of Science (AAAS)

2016-2017 Member, American Association for Cancer Research (AACR)

2017-present Member, Society for Neuro-Oncology (SNO)

PUBLICATIONS

Peer Reviewed Manuscripts

1. Di K, **Lomeli N**, Wood SD, Vanderwal CD, Bota DA. Mitochondrial Lon is over-expressed in high-grade gliomas, and mediates hypoxic adaptation: potential role of Lon as a therapeutic target in glioma. Oncotarget. 2016;7(47):77457-77467.

2. John T, **Lomeli N**, Bota DA. Systemic cisplatin exposure during infancy and adolescence causes impaired cognitive function in adulthood. Behav Brain Res. 2017; 319: 200-206.

3. **Lomeli N**, Di K, Czerniawski J, Guzowski JF, Bota DA. Cisplatin-induced mitochondrial dysfunction is associated with impaired cognitive function in rats. Free Radic Biol Med. 2017;102: 274-286.

4. **Lomeli N**, Bota DA, Davies KJA. The role of diminished stress resistance and defective adaptive homeostasis in age-related diseases. Clinical Sciences Res. 2017; 131(21):2573-2599.

5. **Lomeli N**, Bota DA. Targeting HSP90 in malignant gliomas: onalespib as a potential therapeutic. Transl Cancer Res. 2018; 7 (4): S460-S462.

6. Di K, **Lomeli N**, Bota DA, Das BC. Magmas inhibition as a potential treatment strategy in malignant glioma. J Neuro-oncol. 2018. 1-10.

7. **Lomeli N**, Di K, Pearre DC, Chung TF, Bota DA. Mitochondrial-associated impairments of Temozolomide on Neural Stem/Progenitor Cells and Hippocampal Neurons. 2019. *Manuscript submitted.*

Abstracts

1. **Lomeli N,** Mota-Bravo L. Screening of Antimicrobial Compounds in California Native Plants. American Association for the Advancement of Science (AAAS) 2012. February 16-20; Vancouver, Canada. Poster Presentation.

2. **Lomeli N,** Bateman J. Modeling MtDNA Damage in Motor Neurons Using RNA Interference. Annual Biomedical Research Conference for Minority Students (ABRCMS) 2012. November 7-10; San Jose, CA. Poster Presentation.

3. **Lomeli N**, Andres AL, Gong X, Di K, Bota DA. Low-doses of cisplatin injure hippocampal synapses: A mechanism for 'chemo' brain? Institute for Clinical and Translational Research (ICTS) Translational Research Day 2014. June 27; Irvine, CA. Poster Presentation.

4. **Lomeli N**, Andres AL, Gong X, Di K, Bota DA. Low-doses of cisplatin injure hippocampal synapses: A mechanism for 'chemo' brain? UC Irvine Cancer Center Retreat 2014. September 26-27; Palm Springs, CA. Poster Presentation.

5. **Lomeli N**. Cisplatin causes mitochondrially mediated hippocampal damage. AAAS 2015. February 12-16; San Jose, CA. Poster Presentation.

6. **Lomeli N**, Czerniawski J, Di K, Guzowski J, Bota DA. Cisplatin induces mitochondrial damage and hippocampal neurotoxicity: a potential mechanism for chemotherapy-related cognitive impairment. American Association for Cancer Research (AACR) 2016. April 16-20; New Orleans, LA. Poster Presentation.

7. **Lomeli N**, Czerniawski J, Di K, Guzowski J, Bota DA. N-acetylcysteine (NAC) treatment can reverse cisplatin-induced cognitive damage in rats. ReMIND 8th Annual Emerging Scientists Symposium 2017. February 16. Irvine, CA. Poster Presentation.

8. **Lomeli N**, Di K, Czerniawski J, Guzowski JF, Bota DA. Investigation of N-acetylcysteine for the prevention of cisplatin chemotherapy-related cognitive impairments. Society for Neuro-oncology (SNO) 2017. November 16-19; San Francisco, CA. Oral Presentation.

9. **Lomeli N**, Pearre DC, Di K, Bota DA. BDNF enhancement via ampakines as a potential treatment for chemotherapy-related cognitive impairments. Society for Neuro-oncology (SNO) 2018. November 15-18. New Orleans, LA. Poster Presentation.

10. Pearre DC, **Lomeli N**, Bota DA. A Novel Rat Ovarian Cancer Model to Examine Chemotherapy-Related Cognitive Impairments. Western Association of Gynecologic Oncologists (WAGO) 2019. June 12-15; Huntington Beach, CA. Oral Presentation.

ABSTRACT OF THE DISSERTATION

N-acetylcysteine for the Prevention of Cisplatin Chemotherapy-Related Cognitive Impairments

Naomi Lomeli
Doctor of Philosophy in Biomedical Sciences
University of California, Irvine, 2019
Department of Pathology and Laboratory Medicine
Dr. Daniela A. Bota, MD, PhD, Chair

Chemotherapy-related cognitive impairments (CRCI) are commonly reported during and after completion of chemotherapy treatment. CRCI includes changes across various cognitive domains such as working memory, executive function, attention, and processing speed. While up to 75% of cancer patients experience cognitive impairments during chemotherapy treatment, up to 34% of survivors experience long-term CRCI years after treatment completion. Clinical studies have found structural brain changes, including hippocampal atrophy, and reduction in gray and white matter density, which correlate with impaired cognitive function in the affected brain regions in cancer survivors following chemotherapy treatment. Earlier studies from our lab have examined the effects of cisplatin chemotherapy on cultured hippocampal neurons and neural stem/progenitor cells (NSCs) and found that at doses lower than those required to kill cancer cells, cisplatin induces severe hippocampal dendritic spine damage and neural cell death, suggesting that neural injury/death including a loss of excitatory synapses may underlie the cellular basis of cisplatin-induced CRCI.

Here we provide evidence for mitochondrial dysfunction as a candidate mechanism for cisplatin-induced CRCI, and the therapeutic potential of the antioxidant N-

acetylcysteine to prevent cisplatin-induced neural damage and cognitive impairments in an adult rat model. Since cisplatin is used to treat pediatric as well as adult malignancies, and the risk and extent of cisplatin-induced CRCI on the developing brain have not been well characterized, we also developed two pediatric rat models of CRCI to examine the long-term effects of systemic cisplatin administration on cognitive function when administered during infancy or adolescence. We employed clinically relevant doses of cisplatin to develop our rat models of cisplatin-induced CRCI and used hippocampus-dependent behavioral tasks to assess neurocognitive function. Lastly, we developed an ovarian cancer xenograft rat model, in which we determined that delayed NAC administration could prevent cisplatin-induced CRCI without interfering with its anti-cancer efficacy.

CHAPTER 1

Introduction

This dissertation is divided into chapters that focus on different rat models of chemotherapy-related cognitive impairments (CRCI) caused by the chemotherapeutic drug cisplatin. Chapter 2 focuses on mitochondrial dysfunction as a mechanism for cisplatin-induced CRCI, and a model of cisplatin-induced CRCI in adult male Sprague Dawley rats. CRCI in adulthood following cisplatin-treatment in infant and adolescent Sprague Dawley rats is described in Chapter 3. Chapter 4 is the latest project I worked on to develop an ovarian cancer xenograft model of cisplatin-induced CRCI. Lastly, Chapter 5 is a separate *in-vitro* study of neurotoxicity in NSCs and hippocampal neurons associated with the chemotherapeutic drug temozolomide.

Chemotherapy-Related Cognitive Impairments (CRCI)

Chemotherapy-related cognitive impairments (CRCI), also referred to commonly as chemo-fog or chemobrain, is defined as neurocognitive deficits experienced by cancer survivors associated with chemotherapy. Cognitive decline is associated with impairments in learning and memory, executive function, and processing speed. Executive function is the control system that manages other cognitive processes, it is regulated by the prefrontal cortex, and allows one to mentally organize information, and to regulate the information to modulate a response based on the environment. Impairments in executive function may result in difficulties planning, organizing, verbal fluency, difficulties processing, storing, and or retrieving information[1].

The earliest reports of cognitive impairments in cancer patients date back to the 1970s. Initial studies attributed the behavioral changes in cancer patients to psychiatric depression and anxiety due to the patient's emotional distress associated with the cancer diagnosis, and not the use of chemotherapeutic agents[2]. Two studies on psychiatric referrals of hospitalized cancer patients found that although over 55% of patients were diagnosed with depression, neurocognitive impairments which were reported as 'organic brain syndrome,' were often misdiagnosed as depression and underreported[3,4]. Weiss et al. provided one of the first detailed reports on the clinical manifestations, incidence, and neurological complications associated with commonly used antineoplastic drugs for treatment of non-central nervous system (CNS) malignancies, suggesting that the prevalence of neurological complications in cancer patients would continue to rise as advances in cancer treatment increased patient survival[5,6]. Silberfarb et al. conducted cognitive and psychological assessments in admitted oncology patients and found that cancer patients receiving chemotherapy demonstrated lower cognitive functioning compared to non-chemotherapy cancer patients, which was not attributed to depression and/or anxiety[7]. However, studies of prospective longitudinal neuroimaging and cognitive assessments of cancer survivors did not appear in the literature until the early 2000s[8,9], with research on the neural molecular and cellular mechanisms associated with CRCI coming to focus much more recently[10-14].

Clinical neuroimaging and cognitive studies

The majority of clinical studies on CRCI have focused on breast cancer survivors, as this population regularly reports experiencing cognitive impairments during and after

treatment. Acute declines in cognitive function during chemotherapy have been reported to occur in 60% - 75% of chemotherapy-treated cancer patients, with 34% of survivors experiencing cognitive impairments years after chemotherapy completion[15,16]. Notably in one report, a subset of patients (29%) experienced delayed cognitive decline, which was not present at the time of neurocognitive testing during chemotherapy treatment[17]. In this same study, 21% of patients demonstrated cognitive impairments at baseline cognitive testing, prior to systemic chemotherapy or other treatments, compared to age-matched controls. This finding highlights the need to conduct pre-treatment baseline evaluations in clinical studies of CRCI but also suggests that there are additional contributing factors that may influence cognitive decline, such as cancer or diminished cognitive reserve which may predispose patients to CRCI[17]. Cognitive reserve is defined as overall cognitive capacity, which is influenced by genetic and epigenetic factors, education, training, and environmental factors[18].

Clinical studies have revealed that declines in neurocognitive function correlate with structural brain changes, including reduced gray and white matter density in frontal and temporal brain regions, and hippocampal atrophy. Magnetic resonance diffusion tensor imaging (DTI), a technique used to map white matter connectivity via the diffusion of water molecules, has been used to examine white matter integrity in chemotherapy-treated patients. A longitudinal study of young premenopausal (43 years at baseline) breast cancer patients, found microstructural white matter changes which significantly correlated with decreased performance on attention and verbal memory tests 3-4 months after chemotherapy completion compared to baseline assessment[19]. A follow-up study in the same cohort of patients 3-4 years after chemotherapy completion revealed a recovery

to baseline performance in neurocognitive tasks and white matter alterations[20]. Other longitudinal studies have reported a time-dependent improvement in cognitive performance 1-4 years after chemotherapy completion[21,22]. Whereas other studies examining the late-effects of adjuvant chemotherapy (cyclophosphamide, methotrexate, and fluorouracil) on neurocognitive function in breast cancer survivors (n=196) 20 years after treatment found that they performed worse on tests measuring delayed verbal memory, processing speed, and psychomotor speed compared to a large population-based group without a history of cancer (n=1,509)[23], suggesting that some cancer survivors experience long-term neurological sequelae that detrimentally affect their quality of life years after completing chemotherapy treatment.

Several studies have also examined hippocampal volume alterations and their association with cognitive function. Apple et al. performed a cross-sectional study, which examined hippocampal volume in 16 breast cancer survivors 18 months after adjuvant chemotherapy (doxorubicin, taxane, cyclophosphamide) and estrogen-blockade therapy (tamoxifen) relative to 18 healthy controls[24]. Compared to the controls, the cancer survivors had significantly smaller hippocampal volumes, increased levels of self-reported cognitive difficulties, and impairments in episodic memory. Episodic memory is the ability to learn and retain novel context-dependent information and is mediated by the medial temporal lobes and prefrontal cortex[16]. Given the cross-sectional design of the study it is not clear whether the breast cancer survivors experienced cognitive decline or hippocampal atrophy following chemotherapy completion relative to before treatment. In addition, it is not clear whether chemotherapy, tamoxifen, or a combination of both, contributed to changes in hippocampal volume as tamoxifen has been shown to impair

working memory and induce structural changes in the prefrontal cortex and hippocampus independently of chemotherapy[16,25]. Bergouignan et al. also observed hippocampal atrophy (8% volume reduction) and impairments in episodic memory in breast cancer survivors, 18-36 months after treatment completion (surgery, chemotherapy, radiation) relative to controls[26]. Functional neuroimaging studies of breast cancer survivors revealed altered hippocampal connectivity following chemotherapy completion (5-6 months after commencing chemotherapy) using resting-state functional magnetic resonance imaging (Rs-fMRI), which correlated with impairments in executive function, planning, and working memory[27,28].

The clinical evidence shows that there is a neurobiological basis for the cognitive impairments; in particular, these neurocognitive impairments are consistent with dysfunction in the hippocampal and frontal cortex brain regions[29]. From these studies, it is also evident that there are multiple factors that may influence the development of CRCI, including age, class of chemotherapeutic agents used, other therapeutic strategies (radiation, hormone-blockade therapies, surgery). However, there are discrepancies in the literature regarding clinical neuropsychological assessments, which should be addressed using neuroscientific approaches to investigate CRCI[18]. In the clinical CRCI literature, subjective reports of cognitive impairments may not correlate with objective neuropsychological testing results. Horowitz et al. attribute this to the diffuse damage in the brain associated with CRCI, which may be under-detected given that these tests were initially designed to detect focal lesions[18]. The effects of cognitive reserve, cancer, epigenetic, and genetic factors on cognition may be masked in cross-sectional comparisons (e.g., to cancer patients not treated with chemotherapy, or healthy controls)

in contrast to longitudinal assessments where comparisons are made to a patient's pretreatment baseline. The lack of a standardized battery of cognitive tests to examine CRCI also contributes to the broad estimate (17% - 75%) of CRCI prevalence in the literature.

Animal models of CRCI

Research using primary neural cell cultures and rodents has allowed the study of candidate mechanisms of CRCI, providing direct evidence of the neurotoxicity of specific chemotherapeutic agents to brain cells and resulting effects on cognition, in the absence of confounding factors associated with the clinical studies. *In-vitro* exposure of primary neural cells (rat and human), neural stem/precursors cells (NSCs), neuron-restricted precursor (NRP) cells, glial-restricted precursor (GRP) cells, oligodendrocyte-type-2 astrocytes/oligodendrocyte precursor cells (O-2A/OPCs), astrocytes, and oligodendrocytes to clinically relevant doses of DNA cross-linking agents (BCNU, cisplatin) and human cancer cell lines revealed that these agents were much more toxic to neural cells than the cancer cells (**Figure 1.1**). Exposure to 1 μM cisplatin or 25 μM BCNU (48 h) reduced viability of O-2A/OPCs and NRP cells by 60-90%, in contrast these doses had negligible effects on cancer cell line viability[10]. *In-vivo*, chronic systemic BCNU and cisplatin administration significantly increased apoptotic cell death 6 weeks post-treatment. Confocal microscopic analysis of immunolabeling and terminal deoxynucleotidyl transferase-mediated biotinylated UTP nick end labeling (TUNEL) staining was used to quantify vulnerable neural populations following treatment. In the subventricular zone (SVZ) the majority of apoptotic cells (TUNEL+ cells) after BCNU

treatment were neuronal progenitors positive for doublecortin (DCX+), astrocytes/NSCs positive for glial fibrillary acidic protein (GFAP+), and O-2A/OPCs positive for NG2 proteoglycan (NG2+), and in the dentate gyrus (DG) of the hippocampus, mature neurons positive for neuronal nuclear antigen (NeuN+). The *in-vivo* vulnerability of neural progenitor cell populations to chemotherapeutic agents are in agreement with the *in-vitro* experiments, reflecting the validity of both methods to study the neurobiological mechanisms of CRCI.

A large body of work in the field of CRCI has focused on the mechanisms associated with the alkylating agents cyclophosphamide in combination with the topoisomerase II inhibitor doxorubicin[30-32], the antimetabolites methotrexate (inhibitor of dihydrofolate reductase)[33,34] and 5-fluorouracil (5-FU) which interferes with DNA biosynthesis and repair by inhibiting thymidylate synthase[35,36]. Methotrexate-induced cognitive impairments are associated with decreased neurogenesis and tri-glial dysfunction initiated by chronic microglial activation, which activates astrocytes, depletes OPCs, reduces myelin thickness of mature oligodendrocytes, and neuronal death [33,37].

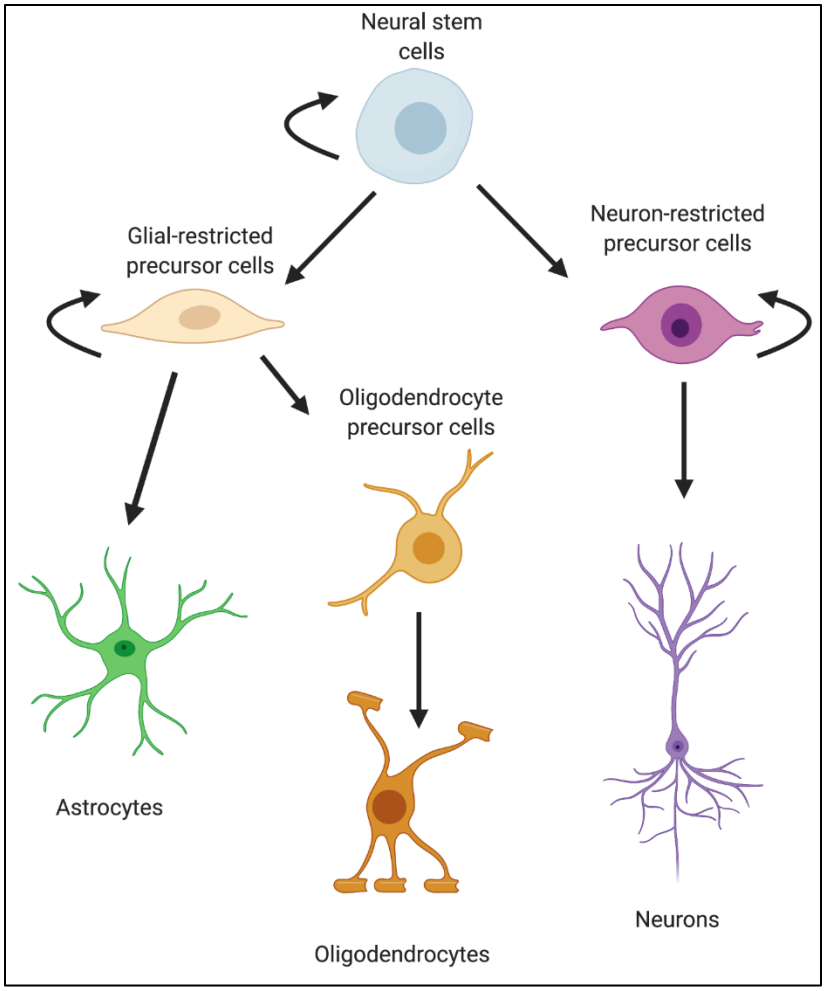

Figure 1.1. Simplified schematic illustration of the NSC differentiation lineage. NSCs are undifferentiated precursor cells with the capacity for multi-potency and self-renewal. NSCs give rise to glial-restricted precursor (GRP) cells and neuron-restricted precursor (NRP) cells. GRP cells give rise to astrocytes, and oligodendrocyte-type-2 astrocytes/oligodendrocyte precursor cells (O-2A/OPCs), which in turn give rise to oligodendrocytes. NRP cells give rise to neurons. Created with BioRender.com.

Oxidative Stress and Role in Neurological Disorders

Among the CRCI candidate mechanisms, DNA damage and oxidative stress have been described for various chemotherapeutic agents including cisplatin, doxorubicin, carmustine, methotrexate, and cyclophosphamide[38-41]. Doxorubicin results in oxidative stress by producing superoxide ions that damage complex I of the electron transport chain (ETC), in addition, it increases levels of tumor necrosis factor-alpha (TNFα) in the plasma, which crosses the blood-brain barrier and activates apoptotic pathways resulting in neural death[42]. Diminished antioxidant capacity and low levels of key antioxidants glutathione (GSH) and superoxide dismutase (SOD) have been observed in the blood of chemotherapy-treated cancer patients[43,44] as well as in the blood and brain tissue of chemotherapy-treated rodents[45,46].

Cells and organisms are regularly exposed to oxidative stress. Oxidative stress is a major type of stress which is defined on the basis of a pro-oxidizing shift in the thiol-redox state and the resulting dysfunction of redox-sensitive proteins. Oxidative stress occurs when the equilibrium of oxidant/antioxidant balance is disrupted, and there is a shift towards an oxidative status, this is accompanied by detrimental effects on cell survival including lipid peroxidation and oxidative modification of DNA, RNA, and proteins[47]. Free radicals play a vital role in physiological processes in signaling pathways, gene regulation, and cellular differentiation[48].

During periods of high oxidative stress, the ability of cells and organisms to cope with such stress can be transiently altered to meet changing demands through a process called oxidative stress adaptation[49-51]. Oxidative damage to mitochondrial enzymes and the mitochondrial genome is implicated in the pathogenesis of various neurodegenerative

disorders[52]. Mitochondria contain an ETC, that transfers high energy electrons to a series of membrane protein complexes, before final acceptance by oxygen. Unfortunately, this process also generates reactive oxygen species (ROS) as by-products, including superoxide and hydrogen peroxide, which can cause damage to surrounding macromolecules. Superoxide is dismutated to hydrogen peroxide by SOD. Hydrogen peroxide is converted to water by glutathione peroxidase (GPx) with the concomitant oxidation of reduced glutathione (GSH) to oxidized glutathione (GSSG). As mitochondria are one of the major producers of cellular ROS, removal of mitochondrial oxidatively damaged proteins is crucial for mitochondrial homeostasis and normal cellular function[53,54]. Since mitochondrial DNA (*mt*DNA) encodes thirteen protein components of the ETC, under conditions of oxidative stress, damage to *mt*DNA can impair ATP production, and elicit a vicious cycle in which ROS damages DNA and mitochondrial proteins, resulting in impaired ETC function, which may further increaseROS generation (**Figure 1.2**).

The brain is highly susceptible to damage induced by oxidative stress and ROS production, as most of neuronal ATP is generated by mitochondrial oxidative phosphorylation (OXPHOS), only 10% of brain ATP is produced by glycolysis[55]. High levels of ROS and diminished antioxidant capacity is implicated in aging and neurological disorders that compromise cognitive function. In addition, its high lipid content makes the brain vulnerable to lipid peroxidation. Mitochondrial dysfunction reduces neuronal capacity to respond to bioenergetic challenges, which impair brain metabolism and may contribute to neuronal death. Oxidative stress lesions in *mt*DNA, along with mitochondrial respiratory dysfunction, apoptosis, and impaired antioxidant defense systems are

involved in the pathology of neurodegenerative disorders, including but not limited to Alzheimer's disease, Parkinson's disease, Huntington's disease, Amyotrophic Lateral Sclerosis, Stroke, and major depressive disorder[52,56].

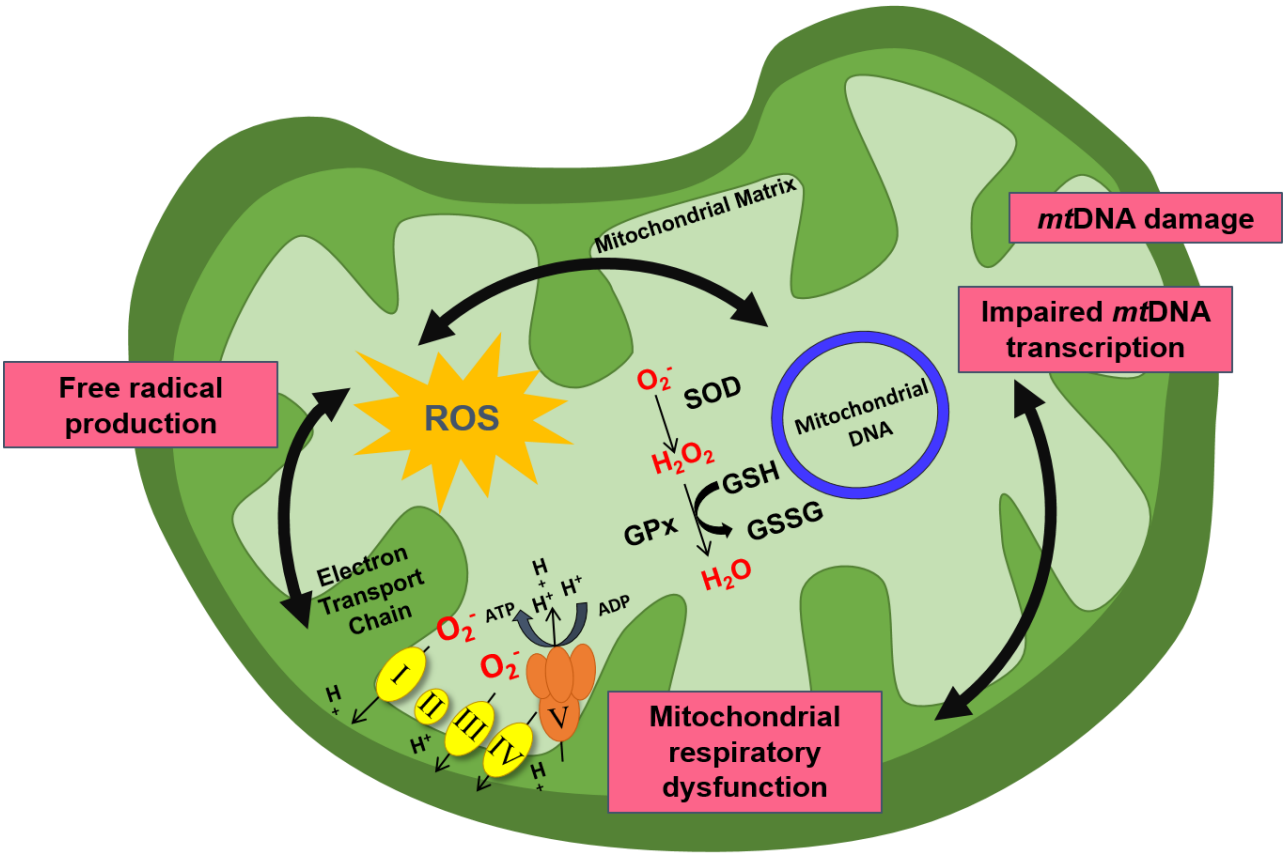

Figure 1.2. Schematic representation of antioxidant responses to mitochondrial reactive oxygen species.
The figure shows a mitochondrion with electron transport complexes I, II, III, and IV in the inner membrane, along with the ATP synthase complex V. The mitochondrial respiratory chain can generate stressful levels of superoxide, which is quickly dismutated to hydrogen peroxide by SOD. Despite effective removal of hydrogen peroxide, by GPx with the concomitant oxidation of GSH to GSSG some protein damage still occurs. During such oxidative stress conditions, antioxidant capacity decreases, which results in a cycle of increased ROS generation that may result in *mt*DNA damage, impair *mt*DNA transcription, and respiratory dysfunction. (Adapted from Lomeli et al., 2017)

Role of NSCs in CRCI

Hippocampal neurogenesis has been shown to decrease following chemotherapy treatment in humans and rodents and may contribute to cognitive changes associated with CRCI[57]. Chemotherapy is associated with neurocognitive deficits that include working memory, concentration difficulties, executive function, and speed of information processing. The subgranular zone (SGZ) of the dentate gyrus in the hippocampus is one of the main neurogenic niches in the adult brain. In the SGZ, NSCs differentiate into dentate granular neurons, which then functionally incorporate into the hippocampal circuitry. As NSCs are crucial for intact memory and hippocampal function throughout life, toxicity to NSCs and decrease in neurogenesis may contribute to the neurocognitive impairments experienced by cancer survivors[11].

Postmortem analysis of human hippocampal tissue from medulloblastoma or leukemia patients, 2-23 years following the completion of chemotherapy revealed a profound reduction in neurogenesis. The number of immature neurons (DCX+) was decreased 10 to 100-fold in patients receiving chemoradiation relative to age- and sex-matched control subjects[58].

Animal studies have elucidated the effects of chemotherapy on hippocampal NSCs and neurons. Work in such models has demonstrated that exposure to clinically relevant doses of chemotherapy results in increased apoptosis in the hippocampus, decreased NSC proliferation, and decreased neuronal differentiation in the SGZ of the dentate gyrus[30,37,38]. Our studies and those of others have shown both *in-vitro* and *in-vivo* that neural progenitor cells and post-mitotic neural cells including neurons and oligodendrocytes are preferentially susceptible to damage by diverse types of

chemotherapeutic agents, as compared to human cancer cell lines[10,38,59,60]. At clinically relevant concentrations that kill 40-80% of cancer cells, the DNA targeting chemotherapeutic, cisplatin, has been shown to reduce the viability of human and rat primary CNS progenitor cells by 70-100%[10]. Unexpectedly, sub-lethal doses of cisplatin and other DNA-targeting agents reduce the self-renewal of neural progenitor cells, decrease the number SOX2+ cells in the dentate gyrus, and reduce the dendritic spine density of hippocampal neurons[10,38,59].

Christie et al. developed a model of cyclophosphamide and doxorubicin-induced CRCI and showed that chronic treatment with clinically relevant doses of either chemotherapeutic agent in rats impaired performance on hippocampus-dependent behavioral paradigms (novel place recognition tasks, and contextual fear conditioning), compared to untreated controls. Assessment of hippocampal neurogenesis at three weeks post-treatment revealed a 47% - 53% decrease in DCX+ neurons, and an 81%-88% drop in BrdU-NeuN+ cells compared to the saline-treated controls. The DCX+ neurons displayed abnormal dendritic morphology and ectopic migration. These results suggest that decline in hippocampal neurogenesis is associated with disrupted hippocampal-based cognitive function in CRCI and that neuroprotective strategies that preserve hippocampal neurogenesis may be useful in ameliorating CRCI[30]. As a follow-up study to support this hypothesis, human NSC transplantation in the rat model of chronic cyclophosphamide-treatment ameliorated the cognitive impairmen. The grafted NSCs survived (8%) and differentiated along neuronal and astroglial lineages, and importantly enhanced neuronal dendritic arborization and spine density. As only 8% of transplanted NSCs survived, a plausible mechanism for reversing the harmful effects of

CRCI with stem cells may be through trophic support through secretion of neurotrophic factors that preserve neuronal integrity.

Our work and others on cisplatin-induced CRCI have shown that hippocampal mitochondrial dysfunction, oxidative stress, and reduction in neuronal arborization are associated with cognitive impairments in rodent models of CRCI[38,59,61-63]. Using a cellular approach, Chiu et al. have demonstrated that following nasal administration of mesenchymal stem cell (MSC) at 48 hours and 96 hours post-cisplatin cessation, MSCs migrated into the brain, restored white matter integrity, and reversed cisplatin-induced cognitive impairments including deficits in working memory, spatial recognition, and executive functioning[64]. Cisplatin altered the brain transcription profiles of genes involved in oxidative phosphorylation and mitochondrial dysfunction. In addition, MSC administration restored mitochondrial respiratory function and morphology following cisplatin treatment in brain synaptosomes. Further studies revealed that MSC nasal administration prevented cisplatin-induced loss of DCX+ neural progenitor cells in the SGZ of the hippocampal dentate gyrus in mice. *In-vitro* studies using co-cultures of MSCs and NSCs revealed that MSC transferred healthy mitochondria to cisplatin-damaged NSCs via actin-based intercellular structures, which was enhanced by overexpression of the mitochondrial motor protein Rho-GTPase 1 (Miro1) in MSCs. Mitochondrial transfer to NSCs restored cisplatin-induced changes in mitochondrial integrity by normalizing the membrane potential, respiratory function, and promoting NSC survival[61]. Although further investigation on how MSC-derived mitochondria communicate with the damaged acceptor NSC cellular machinery to improve NSC survival and rescue mitochondrial

function is needed, these studies along with others crucially demonstrate the role of NSCs and mitochondrial dysfunction in cisplatin-induced CRCI.

Notably, the regenerative effects of mitochondrial-based strategies, using either small molecules such as the antioxidant N-acetylcysteine, which is presented in this dissertation, or biologics such as MSC mitochondrial transfer, demonstrate the therapeutic potential of these strategies at ameliorating cisplatin-induced CRCI.

CHAPTER 2

Cisplatin-induced Mitochondrial Dysfunction is Associated with Impaired Cognitive Function in Rats

Abstract

Chemotherapy-related cognitive impairment (CRCI) is commonly reported following the administration of chemotherapeutic agents and comprises a wide variety of neurological problems. No effective treatments for CRCI are currently available. Here we examined the mechanisms involving cisplatin-induced hippocampal damage following cisplatin administration in a rat model, and cultured rat hippocampal neurons and neural stem/progenitor cells (NSCs). We also assessed the protective effects of the antioxidant, N-acetylcysteine in mitigating these damages.

Adult male rats received 6 mg/kg cisplatin in the acute studies. In chronic studies, rats received 5 mg/kg cisplatin or saline injections once per week for four weeks. N-acetylcysteine (250 mg/kg/day) or saline was administered for five consecutive days during cisplatin treatment. Cognitive testing was performed five weeks after treatment cessation. Cisplatin-treated cultured hippocampal neurons and NSCs were tested for changes in mitochondrial function, reactive oxygen species production, caspase-9 activation, and neuronal dendritic spine density.

Acute cisplatin treatment reduced dendritic branching and spine density, induced mitochondrial degradation. Rats receiving the chronic cisplatin regimen showed impaired performance in contextual fear conditioning, context object discrimination, and novel

object recognition tasks compared to controls. Cisplatin induced mitochondrial DNA damage, impaired respiratory activity, increased oxidative stress, and activated caspase-9 in cultured hippocampal neurons and NSCs. N-acetylcysteine treatment prevented free radical production, ameliorated apoptotic cell death and dendritic spine loss, and partially reversed the cisplatin-induced cognitive impairments.

Our results suggest that mitochondrial dysfunction and increased oxidative stress are involved in cisplatin-induced cognitive impairments. Therapeutic agents, such as N-acetylcysteine, may be effective in mitigating the harmful effects of cisplatin.

2.1. Introduction

Chemotherapy causes short-term memory loss and concentration difficulties, which severely diminishes quality of life. Chemotherapy-related cognitive impairment (CRCI) encompasses a broad range of neurological problems, such as impairments in memory, attention, clarity of thought, executive functioning, and information processing speed[65,66]. CRCI is an ever-increasing problem of significant clinical concern; up to 34% of patients experience persistent cognitive problems years after completing chemotherapy[16]. The underlying mechanisms of CRCI are not well understood, and no effective treatments are currently available.

Cisplatin (CDDP) is one of the most widely used cancer drugs; it is used to treat advanced ovarian and testicular cancer among other malignancies. CDDP can cross through the blood-brain barrier and accumulates in the hippocampus[67,68]. CDDP is a DNA targeting agent, forming toxic platinum DNA adducts, inducing DNA damage, and apoptosis[69]. In addition, CDDP forms adducts with mitochondrial DNA (*mt*DNA) and

inhibits *mt*DNA replication and mitochondrial gene transcription[70,71]. Unlike nuclear DNA, mitochondria lack nucleotide excision repair mechanisms for *mt*DNA[72]. Studies examining the mechanisms of CDDP-induced peripheral neuropathy in dorsal root ganglion neurons and ototoxicity in the cochlea show that CDDP induces *mt*DNA damage and generation of reactive oxygen species, resulting in these two dose-limiting toxicities associated with CDDP treatment[72-74].

Ovarian cancer patients treated with CDDP consistently develop CRCI during and after platinum-based chemotherapy[75]. For example, when Hess et al. examined advanced ovarian cancer patients in comprehensive neurocognitive tests; impairment was detected in two or more cognitive domains in 40% of CDDP chemotherapy recipients[76]. The effects of CDDP on neural *mt*DNA could produce mitochondrial dysfunction and prolonged neurotoxicity after cessation of CDDP treatment, which may play a causal role in the development of CRCI[77,78]. We previously reported that at doses lower than those found in chemotherapy patients, CDDP could potentially induce both severe hippocampal synaptic damage and neural cell loss[59]. *In-vitro,* low-doses of CDDP (2 µM) kill 50% of human NSCs, while a dose five times higher (10 µM) is required to kill 50% of patient-derived malignant glioma stem-like cells[60]. To uncover the potential mechanisms underlying CDDP-induced brain dysfunction, we evaluated the effects of acute and chronic CDDP treatment at clinically relevant doses. We assessed cognitive changes using behavioral paradigms that engage the hippocampus. To evaluate the hypothesis that hippocampal mitochondrial dysfunction and oxidative stress may play a role in the development of CRCI, we examined the *in-vivo* effects of CDDP treatment on hippocampal neuronal dendritic complexity, mitochondrial integrity, and cellular death at

several time-points after the cessation of treatment, as well as the *in-vitro* effects using cultured rat hippocampal neurons and NSCs. We also studied the effects of a clinically-available antioxidant, N-acetylcysteine (NAC) on mitigating CDDP-induced dendritic spine loss, oxidative stress, apoptosis, and cognitive dysfunction.

2.2. Materials and Methods

Animals

Animal studies were performed in accordance with the guidelines established by the Institutional Animal Care and Use Committee (IACUC) of the University of California, Irvine. All the data were generated using Sprague Dawley rats (Charles River Laboratories). Experiments were approved by IACUC and conformed to NIH guidelines.

Drug Treatments

Seventy-nine adult male Sprague Dawley rats weighing 200-250 g at the time of arrival served as subjects. For acute CDDP studies, rats were injected intraperitoneally with CDDP (Teva Pharmaceuticals USA, Inc.) dissolved in 0.9% saline (3 mg/kg/day) for two consecutive days (n = 6). The control animals received 0.9% sterile saline of the same volume (n = 6). For the chronic CDDP + NAC studies, rats received one CDDP (5 mg/kg, i.p.) or saline injection per week for four consecutive weeks. NAC (Cumberland Pharmaceuticals, 250 mg/kg, i.p.) was administered for five days starting two days before each CDDP administration and ending two days after the last dose of CDDP. On days of CDDP administration, NAC was given 4 h after CDDP injection. The rats were divided into four groups: saline-treated controls (Saline, n = 25), N-acetylcysteine-treated (NAC,

n = 18), cisplatin-treated (CDDP, n = 15), and cisplatin + N-acetylcysteine-treated (CDDP + NAC, n = 13). Mannitol (APP Pharmaceuticals, 250 mg/kg, i.p.) was administered to all animals 1 h prior to CDDP, to minimize renal toxicity and increase diuresis. For the *in-vitro* NAC studies, NAC (Sigma) was added to the culture medium 30 min after CDDP treatment.

Golgi-Cox Staining

Brains were harvested and subjected to Golgi-Cox impregnation as specified by the manufacturer's instructions (FD Rapid GolgiStain Kit, FD NeuroTechnologies, Inc). Coronal sections (200 µm) through the hippocampus were processed using Fluoromount G (Southern Biotech) mounting medium. Individual Golgi-impregnated CA3 pyramidal neurons were reconstructed, and the dendritic branching and spines were quantified across the distance from the soma. Sholl analysis used a series of concentric circles (20 µm apart) to calculate the number of dendritic intersections as a function of distance from the soma.

Transmission Electron Microscopy (TEM)

Hippocampi were isolated from Sprague Dawley rats and fixed in glutaraldehyde. Hippocampal sections of the CA3 region were sent to the UC Irvine Health Research Services Core Facility for TEM processing and imaging.

Immunohistochemistry

Coronal sections (30 µm) through the hippocampus were fixed in 4% PFA in PBS, pH 7.4 for 15 min, washed twice with PBS and incubated in blocking buffer (0.1% Triton X, 10% goat serum in PBS, pH 7.4) for 1 h at room temperature. Sections were incubated overnight at 4°C in primary antibody, rabbit anti-Sox2 1:300 in PBS (Abcam). The next day, sections were incubated in secondary antibody goat anti-rabbit conjugated to Alexa 488 (1:3000, Abcam) for 1.5 h. Sections were washed and processed for fluorescent imaging with DAPI Fluoromount G (Southern Biotech) mounting medium.

Terminal deoxynucleotidyl transferase-mediated biotinylated UTP nick end labeling (TUNEL) Assay

Rats were sacrificed, and brains were harvested following 0.9% saline perfusion. Brains were rapidly removed, and flash-frozen in isopentane and stored at -80°C. Coronal sections (30 µm) through the hippocampus were processed for TUNEL assay. The TUNEL assay was performed using the NeuroTACS™ In Situ Apoptosis Detection Kit, according to the manufacturer's instructions (Trevigen Inc).

Cognitive Testing

Fear conditioning (FC), Context Object Discrimination (COD), and Novel Object Recognition (NOR) were done as previously published by JC and JG[79,80]. Cognitive testing was administered 5–6 weeks after the final and fourth CDDP or saline injection. The experiment was repeated three times with three animal cohorts, and data from all

three experiments were combined and shown in the results section. All behavior analysis was conducted by an experimenter blinded to the treatment group of the rats.

Fear Conditioning

A fear-conditioning task was administered five weeks after the final and fourth CDDP or saline injection to characterize chemotherapy effects on cognitive performance. Two similar but distinct chambers, each housed within a sound-attenuating chamber, were used for fear conditioning[79]. The floor of the conditioning chamber consisted of 18 steel rods wired to a shock generator (Coulborn Instruments) for footshock delivery. The fear-conditioning paradigm used was based on previous studies on chemotherapy-treated rodents[30,32].

Rats were placed in a chamber for 5 min (baseline), followed by five-tone (90db, 2000 Hz, 30 s) - shock (1mA, 1s) pairings over 5 min, and left in the conditioning chamber for an additional 5 min (post-training). The following day, rats were returned to the conditioning chamber for 5 min with no tone or shock presentations to assess conditioned freezing to the context (context test). The cue test was administered 1 h later, during which rats were placed in a novel context for 1 min (pre-cue test) followed by a 3 min tone presentation (cue test) and an additional 1 min (post-cue test). For training and testing, freezing behavior was scored as % time spent freezing, defined as complete immobility except for breathing movements.

Context Object Discrimination

COD is a hippocampus-dependent task that tests context discrimination. It requires hippocampal pattern separation[81]. Rats were exposed to two different environments (termed A and B), located in adjacent rooms, for 5 min each per day for two consecutive days and allowed to explore freely[80]. Rats were returned to their home cage for a 20 min interval between training sessions. The order of context presentation was counterbalanced between subjects and across days. Each environment had two identical local objects (unique to each environment). On the third day, rats were tested in environment A for 5 min, in which one of the objects from B replaced one of the objects from A. The amount of time each subject explored each object is recorded using the Limelight2 program (Actimetrics: Coulbourn Instrument). Total exploration time, time spent exploring each object, and the discrimination ratio (time spent exploring the out-of-context object / total exploration time) were quantified.

Novel Object Recognition

Rats were placed in an open Plexiglas box arena (60 x 60 cm) with 60 cm high walls containing two identical objects. Each rat explored the arena for 5 min per day for two consecutive days. The 5 min test trial was given 24 h later, during which the rat was presented with one of the familiar objects paired with a novel object. Total exploration time, time spent exploring each object, and the discrimination ratio (time spent exploring the novel object / total exploration time) were quantified.

Dissociated hippocampal neuron and NSC cultures

NSCs were isolated from the hippocampi of embryonic day 19 (E19) Sprague Dawley rats and cultured as previously described[59]. Passage 6-10 NSCs were used for experiments. Hippocampal neuron cultures were prepared from postnatal day 0 (P0) Sprague Dawley pups, as previously described by our lab and others[59,82]. Neurons were used for experiments on 17-21 days *in-vitro* (17-21 DIV).

MitoTracker Red and Immunocytochemistry

Neurons and NSCs plated on 12 mm coverslips were incubated in culture medium containing 500 nM Mitotracker Red CMXRos (Life Technologies) for 30 min at 37°C and 5% CO_2. After incubation, cells were fixed with ice-cold 4% paraformaldehyde (PFA) in PBS, pH 7.4, for 12 min. NSCs were incubated in blocking buffer (0.2% Triton-X, 10% BSA in PBS, pH 7.4) for 1 h at room temperature. Rabbit anti-Caspase-9 (Cell Signaling) was diluted 1:50 for NSCs, and 1:200 in blocking buffer (0.1% Triton-X, 3% FBS in PBS, pH 7.4) for neurons overnight at 4°C. Mouse anti-PSD95 1:2000 (Thermo Fisher) was used to visualize dendritic spines. The next day, coverslips were washed and incubated in the appropriate secondary antibodies conjugated to Alexa Fluor 488 at 1:200, or Alexa Fluor 594 at 1:400 (Invitrogen); at room temperature for 1.5 h. Cells were processed for imaging with DAPI Fluoromount G (Southern Biotech) mounting medium. Fluorescent images were generated using the Nikon Ti-E inverted microscope with a 20x objective (NA 0.75).

Measurement of Oxidative Stress

Neurons and NSCs plated on 12 mm coverslips were incubated in culture medium containing 5 µM Cell ROX Green Reagent (Life Technologies) for 20 min at 37°C and 5% CO_2. After incubation, cells were fixed with ice-cold 4% PFA in PBS, pH 7.4 for 12 minutes, and washed with PBS before mounting. Cells were processed for imaging with DAPI Fluoromount G mounting medium. Neuronal images were generated using confocal microscopy, Zeiss LSM 700. 10 µm z-series (2 µm steps) images were captured at 20x (NA 0.8) spanning across entire neurons. NSC images were generated with an Olympus Scanner VS110 based on a BX61VS upright microscope with a 20X apochromatic objective (NA 0.75). Relative fluorescence intensity of Cell ROX green probe was quantified by ImageJ. Each experiment was repeated at least twice, with similar results. Each experiment included 3–4 sister coverslips per treatment group. For Cell ROX green fluorescence measurement, five frames were analyzed per coverslip, for a total of 150–200 cells per treatment group.

MtDNA qPCR Assay

Total DNA was purified from cell samples using the Qiagen Genomic Tip and Genomic DNA Buffer Set Kit (Qiagen, Valencia, CA, USA). A mitochondrial fragment (235 bp) was amplified and standardized to a 12.5 Kb fragment from the nuclear-encoded gene, Clusterin (*TRPM-2*). PCR products were normalized to control levels[83]. The sequences for rat *TRPM-2*, *mt*DNA fragment (235 bp) primer sets were:

TRPM-2 forward 5'-AGACGGGTGAGACAGCTGC ACCTTTTC-3',

TRPM-2 reverse 5-CGAGAGCATCAAGTGCAGGCATTAGAG-3'

*mt*DNA fragment forward 5′-CCTCCCATTCATTATCGCCGCCCTTGC-3′

*mt*DNA fragment reverse 5′-GTCTGGGTCTCCT AGTAGGTCTGGGAA-3′

Quantitative RT-PCR Assay

Total RNA was extracted using RNeasy Mini Kit (Qiagen), and cDNA was generated using the iScript™ cDNA Synthesis Kit (Bio-Rad). Quantitative PCR reactions (iQ™ SYBR Green Supermix, Bio-Rad) were conducted using a Bio-Rad CFX96 Real-time System, and the gene expression levels were normalized to those of *18S rRNA*. The sequences for rat *Cytochrome B* and *18sS rRNA* primer sets were:

Cytochrome B forward 5'-CGAAAATCTACCCCCTATT-3'

Cytochrome B reverse 5'-GTGTTCTACTGGTTGGCCTC-3'

18S rRNA forward 5'-TCAATCTCGGGTGGCTGAACG-3'

18S rRNA reverse 5'-GGACCAGAGCGAAAGCATTTG-3'.

All primers were ordered from IDT, Integrated Device Technology, Inc, Coralville, Iowa, USA.

Seahorse XF24 Metabolic Flux Analysis

Mitochondrial respiratory function was assessed using the Seahorse XF24 Extracellular Flux Analyzer. Oxygen consumption rates (OCR) were measured in adherent hippocampal neurons and NSCs using the Cell Mito Stress Kit[84,85] (Seahorse Bioscience). Dissociated hippocampal neurons from P0 pups were plated at a density of $7.5x10^4$ cells/well in poly-D-lysine coated XF24 cell culture microplates. On the day of metabolic flux analysis, the neuronal culture medium was replaced with 500 µl of

bicarbonate-free XF Base Medium (Seahorse Biosciences) supplemented with 17.5 mM glucose, and 0.23 mM sodium pyruvate, pH 7.4. Cells were washed once and incubated at 37ºC in a non-CO_2 incubator for 1 h. Baseline rates were measured at 37ºC three times before the sequential injection of the following mitochondrial inhibitors: oligomycin (2 µM), FCCP (1 µM), and lastly, rotenone (1 µM) and antimycin A (1 µM). NSCs ($6x10^4$ cells/well) were seeded in XF24 cell culture microplates pre-coated with fibronectin. The inhibitor concentrations used were oligomycin (1 µM), FCCP (2 µM), rotenone (1 µM), and antimycin A (1 µM). Three measurements were taken after the addition of each inhibitor. All analyses were normalized to protein content per well using a Qubit 2.0 fluorometer (Invitrogen). Data were analyzed using Student's paired *t*-test. Data were graphed as mean ± SEM, n = 3 per treatment group.

Systematic Analysis and Statistical Considerations

Graphs and statistical analyses were prepared using GraphPad Prism 5.0 Software (GraphPad Software, La Jolla, CA, USA). Results were expressed as mean ± SEM. Comparison between control and treatment cohorts were made by unpaired Student's *t*-test, one-way ANOVA, or two-way repeated measures (RM) ANOVA. Statistical significance levels were set at 0.05. *Post hoc* analysis was made by Bonferroni correction. All imaging and quantification were performed blinded to experimental conditions.

2.3. Results

2.3.1. Acute cisplatin treatment produces a long-term reduction in dendritic branching and spine density of hippocampal pyramidal neurons

Previously, we demonstrated that high-dose (20 mg/kg), acute CDDP exposure produces changes in hippocampal dendritic morphology of Sprague Dawley rats three days after treatment. To study the long term effects of low-dose CDDP on dendritic morphology, adult Sprague Dawley rats were given a 6 mg/kg CDDP regimen administered over two consecutive days (3 mg/kg/day). We assessed dendritic branching (**Figure 2.1A, B**) and spine density (**Figure 2.1C, D**) at 14 and 28 days after treatment. This type of treatment directly translates to 18 mg/m^2/day in humans[86] – which is a lower dose than the lowest regimen administered to cancer patients, which is 50 mg/m^2 every three weeks[87]. Golgi-Cox impregnated neurons in the CA3 region revealed pronounced changes in dendritic morphology at 14 and 28 days after CDDP treatment. At 6 mg/kg, CDDP significantly reduced the dendritic branching of pyramidal neurons ($F_{(24,429)} = 2.958$, $p < 0.0001$) compared to controls (**Figure 2.1B**). Also, CDDP reduced the number of dendritic spines at 28 days after treatment cessation ($p < 0.0001$) (**Figure 2.1D**).

2.3.2. Acute cisplatin treatment disrupts hippocampal mitochondrial morphology

CDDP accumulates in mitochondria and forms adducts with *mt*DNA and proteins[71,72]. To investigate the effect of CDDP on mitochondria of CA3 neurons, we assessed mitochondrial changes at 14 days and 28 days after CDDP administration (6 mg/kg) by TEM (**Figure 2.2**). CA3 neurons from control rats showed intact normal mitochondria (**Figure 2.2A, D**). Mitochondrial degradation and vacuolization were evident

following 14 days (**Figure 2.2B, E**) with more extensive damage seen at 28 days (**Figure 2.2C, F**) after CDDP treatment.

2.3.3. Chronic cisplatin regimen impairs cognitive performance that is mitigated by treatment with N-acetylcysteine

Fear Conditioning

To evaluate the effect of chronic CDDP administration on cognitive performance modeled on the clinical CDDP regimen, rats received one CDDP injection (5 mg/kg, intraperitoneal) per week for four consecutive weeks. NAC (250 mg/kg/day) was administered for five days starting two days before each CDDP cycle and ending two days after the last dose of CDDP. On days of CDDP administration, NAC was given four hours after CDDP. Four hours was considered the optimal time to achieve NAC protection without diminishing-anti-tumor efficacy in pediatric tumor models[88].

Cognitive performance in three tasks, fear conditioning (FC), context-object discrimination (COD), and novel object recognition (NOR) was assessed between five and six weeks after treatment discontinuation (**Figure 2.3A**). Five weeks after the last CDDP injection, animals were tested on the FC task (**Figure 2.3B**). Two-way RM ANOVA revealed a main effect of testing phase ($F_{(4,252)} = 550.6$, $p < 0.0001$) and treatment group by phase interaction ($F_{(12,252)} = 3.016$, $p = 0.0006$), and a main effect for treatment group ($F_{(3, 252)} = 3.044$, $p = 0.0352$) for the percent time spent freezing during the FC task. During the context-test phase, CDDP animals spent significantly decreased percentages of time freezing compared with the control animals (*post hoc*, $p = 0.0018$). Groups did not differ significantly in the freezing behavior across baseline ($p = 0.984$),

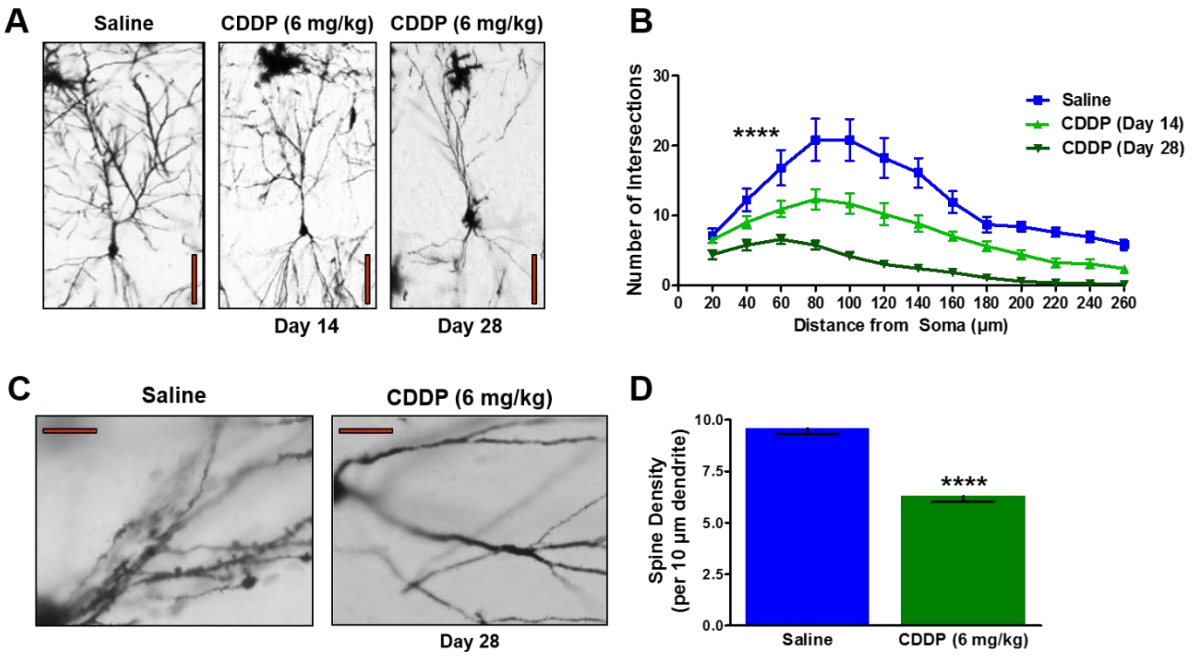

Figure 2.1. Acute CDDP treatment reduces hippocampal dendritic branching and spine density of pyramidal neurons at 14 and 28 days after treatment.
(**A**) Representative Golgi-impregnated CA3 pyramidal neuron images, and (**B**) graph illustrate the time-dependent reduction in dendritic branching caused by low-dose, 6 mg/kg CDDP. Compared to controls, CDDP treated rats have significantly less dendrite branch points from the soma of pyramidal neurons (n = 6 rats per group, 2 neurons per rat). Scale bars, 40 µm. (**C**) Representative images and (**D**) graph of CA3 dendritic spines depicting significant reduction in spine density 28 days after CDDP exposure (n = 24 dendritic branches per group). Data represented as mean ± SEM, **** p <0.0001. Scale bars, 10 µm.

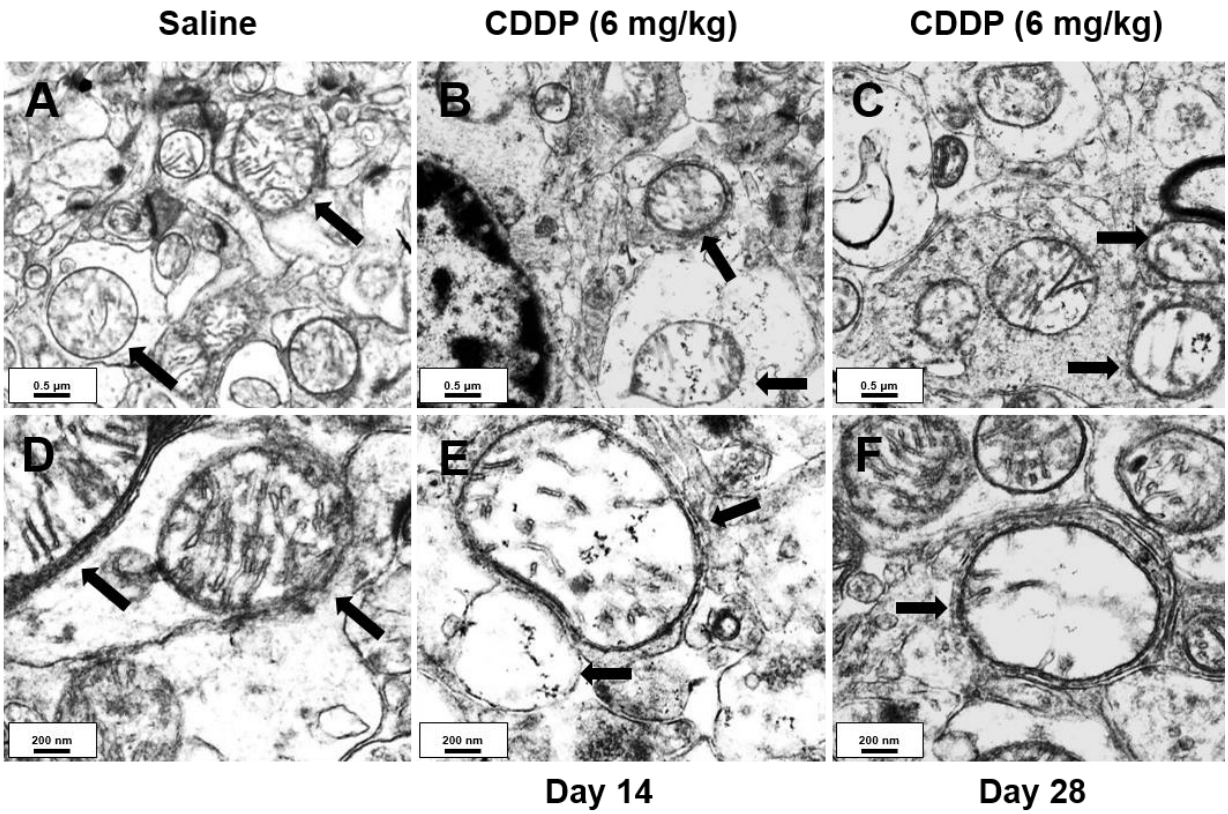

Figure 2.2. Acute CDDP treatment induces mitochondrial degradation and vacuolization in the rat hippocampus.
Adult Sprague-Dawley rats were treated with CDDP (6 mg/kg), and hippocampal mitochondrial morphology was assessed at 14 and 28 days after treatment. (**A, D**) Representative EM images of CA3 neuronal mitochondria, with arrows showing intact normal mitochondria in control CA3 neurons. CDDP (6 mg/kg) induced mitochondrial vacuolization and degradation (arrows) (**B, E**) 14 days after treatment, with more extensive damage at (**C, F**) 28 days.

post-training (p = 0.6827), pre-cue (p = 0.690), and cue test (p = 0.320), indicating a selective deficit on the hippocampus-dependent contextual memory phase of the task. Administration of NAC prevented this CDDP-induced deficit. The CDDP group spent significantly less time freezing during the context test than the CDDP + NAC group (p = 0.0005), whereas the Saline and CDDP + NAC groups did not differ (p = 0.3213). All groups showed significant increases in freezing behavior after the tone-shock pairings (post-training phase) indicating that CDDP did not impair sensory perception. CDDP + NAC animals spent more time freezing during the cue-test compared with controls (p = 0.0032). Cued-memory was intact in all groups; groups froze in response to 5 tone-shock pairings, which indicates that the CDDP-induced deficit was specific to the memory of the context in which the pairing was learned.

Context Object Discrimination

After FC testing, animals were habituated and subjected to the COD task. There were no group differences in total time spent exploring objects (**Suppl. Figure 2.1A**), indicating that CDDP did not impair locomotor activity or exploratory motivation. While saline controls spent significantly more time exploring the out-of-context object compared to the in-context object (p = 0.0002), the CDDP-treated rats displayed no preference in exploring either object (p = 0.8445) (**Suppl. Figure 2.1B**). A one-way ANOVA revealed a significant overall group effect for the discrimination ratio to differ between the groups ($F_{(3,67)}$ = 4.558, p = 0.0058). The discrimination ratio was calculated as [(time spent exploring out-of-context object) / (total exploration time)] for each subject, with 1 being

the maximum time spent exploring the out-of-context object and 0 being maximum time exploring the in-context object (**Figure 2.3C**). The discrimination ratios significantly differed between the saline and CDDP groups ($p = 0.0012$); with a discrimination ratio of 0.45 for CDDP-treated rats, indicating no discrimination between the in-context and out-of-context objects. CDDP treatment diminished the ability to distinguish a previously experienced object, which was placed in a different context. NAC administration partially mitigated the CDDP-induced deficit, the discrimination ratios between the saline and CDDP + NAC groups were not significantly different ($p > 0.05$).

Novel Object Recognition

Following COD, rats were tested on the NOR task. There was no difference in total exploration time between saline and CDDP-treated animals (**Suppl. Figure 2.1C**). While saline controls spent significantly more time exploring the novel object compared to the familiar object ($p < 0.0001$), the CDDP-treated rats showed no preference in exploring either object ($p = 0.2241$) (**Suppl. Figure 2.1D**). A one-way ANOVA did not reveal a significant overall group effect for the discrimination ratio to differ between the groups ($F_{(3,67)} = 2.207$, $p = 0.089$) (**Fig. 3D**). The discrimination ratios differed significantly between saline and CDDP subjects ($p = 0.01$). The CDDP-treated group had a discrimination ratio of 0.503, which indicates no preference between the familiar and novel objects. CDDP treatment impaired the ability to recognize a novel object from a previously experienced familiar object. NAC administration partially mitigated the CDDP-induced deficit, the discrimination ratios between the saline and CDDP+NAC groups were not significantly different ($p = 0.371$). Together, these data suggest that chronic CDDP

treatment results in cognitive deficits, which can be lessened by NAC.

2.3.4. Chronic cisplatin treatment increases apoptotic cell death in the hippocampal regions CA3, CA1, and subgranular zone (SGZ) of the dentate gyrus and decreases neurogenesis, NAC administration reduces cisplatin-induced cell death in these regions

To examine the effect of chronic CDDP treatment on neural apoptosis in the hippocampus, TUNEL was performed to detect apoptotic cells in the CA3, CA1, and SGZ of the dentate gyrus after behavioral testing, six weeks after treatment completion (**Figure 2.4A**). One-way ANOVA analysis revealed a main effect for treatment group in CA3 ($F_{(3,32)}$ = 12.67, p < 0.0001), CA1 ($F_{(3,32)}$ = 5.747, p = 0.0033), and SGZ ($F_{(3,32)}$ = 12.54, p < 0.0001). CDDP-treatment increased the number of TUNEL(+) (apoptotic) nuclei in the CA3 (p < 0.001), CA1 (p < 0.01), and SGZ (p < 0.001*)* as compared with the saline group. NAC administration significantly reduced the CDDP-induced apoptotic cell death in the CA3 (p < 0.01), CA1 (p < 0.05), and SGZ (p < 0.001) as compared to CDDP treatment alone (Bonferroni's Multiple Comparison Test). There were no significant differences in the amount of TUNEL(+) cells in all three regions between the CDDP + NAC group, saline, and NAC groups (p > 0.05) (**Figure 2.4B**), suggesting NAC prevented CDDP-induced neural death in the hippocampus.

To examine the effect of acute CDDP (6 mg/kg) treatment on hippocampal neurogenesis, quantification of Sox2(+) cells in the SGZ of CDDP-treated rats revealed a decrease in the number of NSCs 14 days after treatment (p = 0.0306), with a greater decrease 28 days after treatment (p = 0.0097*)* (**Suppl. Figure 2.2**)**.** This data suggests that at concentrations lower than the therapeutic doses, CDDP can induce NSC damage, which may impair neurogenesis long after exposure.

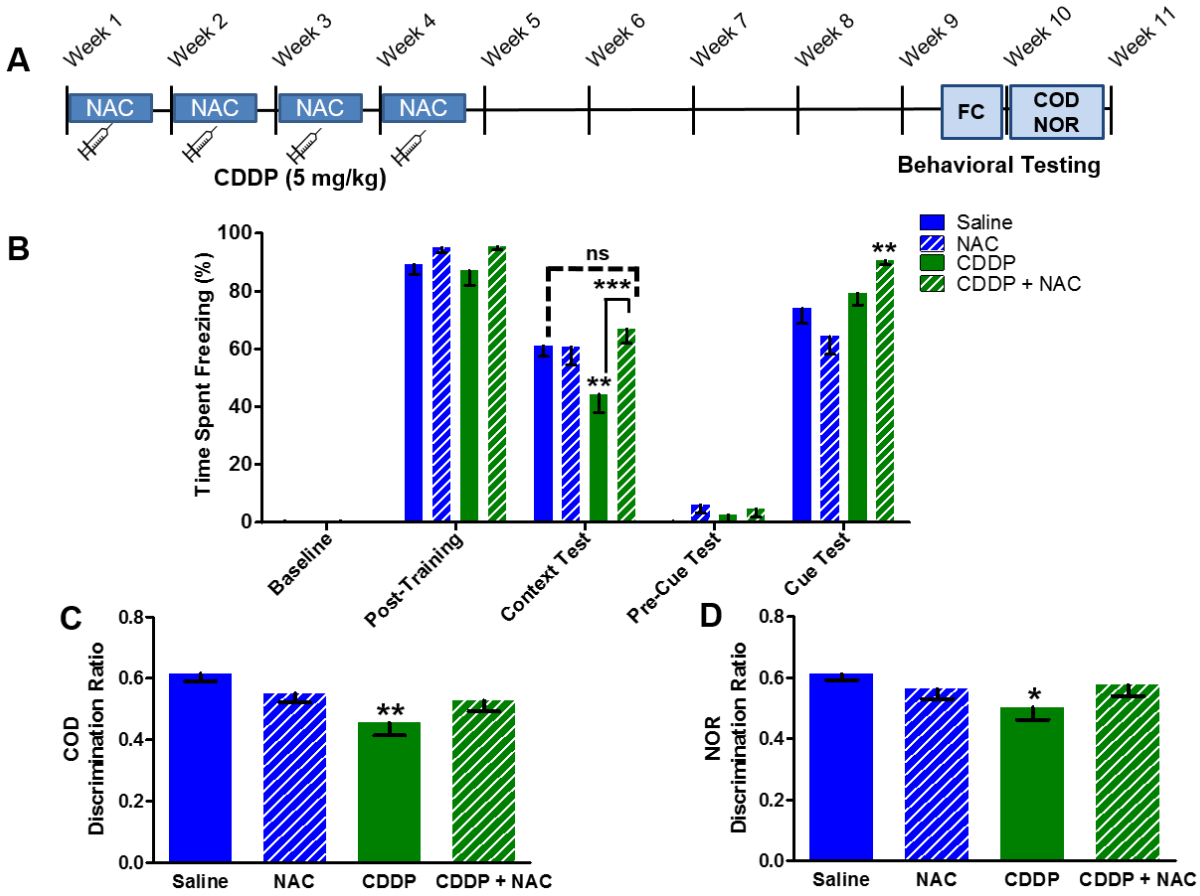
A
Week 1
Week 2
Week 3
Week 4
Week 5
Week 6
Week 7
Week 8
Week 9
Week 10
Week 11
NAC
NAC
NAC
NAC
FC
COD
NOR
CDDP (5 mg/kg)
Behavioral Testing
B
Saline
NAC
CDDP
CDDP + NAC
Time Spent Freezing (%)
100
80
60
40
20
0
ns
***
**
**
Baseline
Post-Training
Context Test
Pre-Cue Test
Cue Test
C
COD
Discrimination Ratio
0.8
0.6
0.4
0.2
0.0
**
Saline
NAC
CDDP
CDDP + NAC
D
NOR
Discrimination Ratio
0.8
0.6
0.4
0.2
0.0
*
Saline
NAC
CDDP
CDDP + NAC

Figure 2.3. Chronic CDDP exposure impairs context discrimination memory and object recognition, which can be mitigated by NAC.
(**A**) Study timeline. To recapitulate the clinical regimen, rats received one CDDP injection (5 mg/kg) per week for four consecutive weeks with or without NAC (250 mg/kg/day, i.p.). Rats were subjected to Fear Conditioning (FC) testing five weeks after the last CDDP injection, followed one week later by Context-Object Discrimination (COD) and Novel Object Recognition (NOR) Task. (**B**) CDDP significantly impaired performance on a contextual fear conditioning task. Baseline freezing levels were equivalent across all groups, and all groups showed increased freezing behavior, as expected, in response to a series of 5 tone-shock pairings ("Post-Training"). The context test was administered 24 h later, and CDDP-treated animals showed decreased freezing compared with the controls. NAC administration prevented the CDDP-induced deficit in the context test. The rats were placed in a novel context 1 h later for the cue test. There was no difference in freezing during the baseline or tone presentations, which indicated that CDDP did not disrupt the CS-US association. (**C**) The CDDP-treated rats had diminished ability to discriminate the out-of-context from the in-context object on the COD task. (**D**) Cisplatin-treated rats had reduced ability to discriminate between the novel and familiar objects on the NOR task. NAC administration partially ameliorated the CDDP-induced deficit in the COD and NOR tasks. Graphs represent mean ± SEM, Saline: n = 25, NAC: n = 18, CDDP: n = 15, CDDP + NAC: n = 13. * p <0.05, ** p <0.01, *** p < 0.001, ns = not significant.

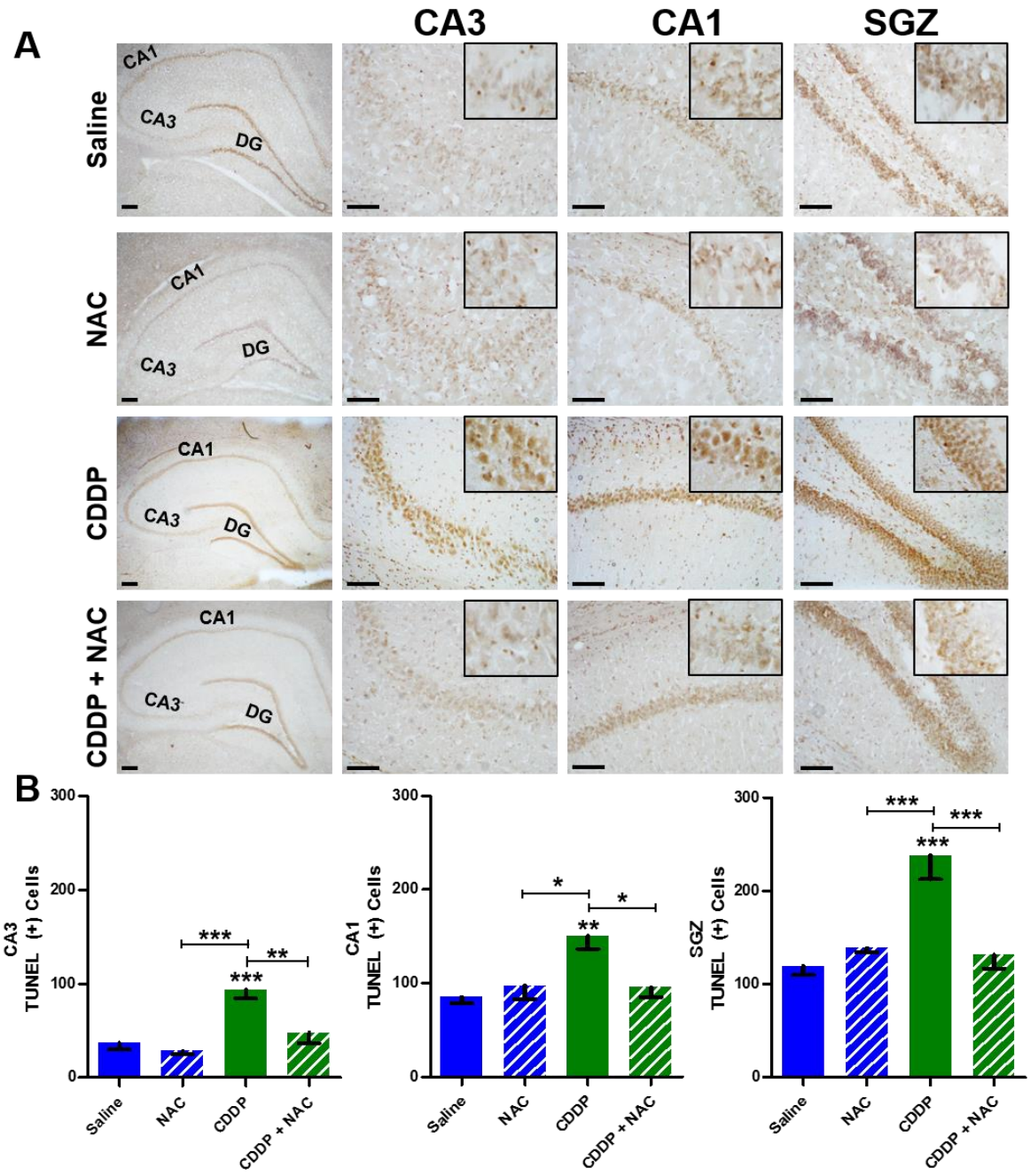
A
CA3
CA1
SGZ
Saline
NAC
CDDP
CDDP + NAC
CA1
CA3
DG
B
CA3 TUNEL (+) Cells
CA1 TUNEL (+) Cells
SGZ TUNEL (+) Cells
300
200
100
0
***
**
*
Saline
NAC
CDDP
CDDP + NAC

Figure 2.4. Chronic CDDP treatment increases TUNEL(+) cells in the rat hippocampus, NAC treatment attenuates apoptotic cell death.
Adult Sprague-Dawley rats were treated with chronic CDDP regimen, and neural apoptosis was assessed in the hippocampus after cognitive testing. **(A)** Representative images of hippocampal coronal sections show an increase in TUNEL(+) cells in the CA3, CA1, and SGZ of the DG after CDDP treatment, NAC significantly reduced CDDP-induced apoptotic cell death. Magnification used is 4x for the whole hippocampus, 20x for the other panels and 40x for the inserts. Scale bars: 4x, 200 μm; 20x, 100 μm. (**B**) Quantification of TUNEL(+) cells situated in the CA3 and CA1, and SGZ areas. Graphs represent mean ± SEM, n = 2 subjects per treatment group, 4 replicates per subject. * $p < 0.05$, ** $p < 0.01$, *** $p < 0.001$.

2.3.5. Cisplatin inhibits mtDNA synthesis in cultured hippocampal neurons and NSCs

We previously identified hippocampal neurons as being more sensitive to CDDP treatment than NSCs. Schematic (**Figure 2.5A**) depicts our findings on the sensitivities of hippocampal neurons and NSCs to CDDP. A sub-lethal (0.1 μM) dose of CDDP destroys synapses located on neuronal dendritic spines, whereas 1 μM CDDP induces measurable alterations on neuronal morphology and cell death. In contrast, 2 μM is the minimum dose that induces measurable apoptosis in NSCs, with 6 μM reducing cell survival to approximately 40%. Based on these studies, we selected these doses to assess mitochondrial function in cultured hippocampal neurons and NSCs.

Previous studies have shown that CDDP binds to *mt*DNA in mouse liver[89] and dorsal root ganglion neurons[72]. However, the effects of CDDP on hippocampal neuron and NSC *mt*DNA have not been investigated. *Mt*DNA is a 16.3 Kb circular piece of DNA that encodes for 13 proteins that are essential components of the electron transport chain. To investigate if CDDP affects *mt*DNA in hippocampal neurons and NSCs, we examined the direct effect of CDDP on *mt*DNA replication in these cells. We used a PCR based assay to amplify a *mt*DNA fragment, in which many DNA lesions block the Taq DNA polymerase progression, resulting in decreased amplification of the damaged DNA template. CDDP produced a time-dependent preferential decrease in amplification of neuronal *mt*DNA as compared with a nuclear gene (Clusterin) (**Figure 2.5B**). CDDP (1 μM) significantly reduced *mt*DNA amplification as early as 4 h post-treatment compared to control (p = 0.0077). Further decreases in neuronal *mt*DNA amplification were observed at 24 h (p = 0.0007) and 48 h post-treatment (p = 0.0002) compared to control.

CDDP produced a dose and time-dependent decrease in amplification of NSC

*mt*DNA (**Figure 2.5C**). CDDP (6 µM) significantly reduced *mt*DNA amplification at 4 h (p = 0.0176) and 48 h (p = 0.0232) post-treatment compared to control. CDDP (2 µM) produced a slight decrease in *mt*DNA amplification at 48 h, although not significant (p = 0.2416).

2.3.6. Cisplatin inhibits mtRNA transcription in NSCs

To examine whether CDDP-induced *mt*DNA damage could affect the transcription of mitochondrial genes, we assessed the transcription of Cytochrome B (CytB) in NSCs following CDDP treatment. CytB is a major subunit of complex III of the mitochondrial electron transport chain and is *mt*DNA encoded[90,91]. We assessed CytB transcription following CDDP treatment (2 µM, 6 µM) at 0 h, 2 h, 4 h, 48 h post-treatment (**Figure 2.5D**). CDDP treatment resulted in a significant decrease in CytB RNA levels at 2 µM (p < 0.0001) and 6 µM (p < 0.0001) as early as 2 h post-treatment. This finding suggests that CDDP-induced *mt*DNA damage may result in changes in mitochondrial respiratory function.

2.3.7. Cisplatin reduces mitochondrial respiratory rates in cultured hippocampal neurons and NSCs

To investigate if CDDP affects mitochondrial respiratory activity in hippocampal neurons and NSCs, we measured oxygen consumption rates (OCR) in these cells following CDDP treatment using the Seahorse XF24 extracellular flux analyzer. OCR is a measurement of oxidative phosphorylation. We examined the effect of 0.1 µM CDDP on hippocampal neurons following 24 h, 48 h, and 7 days of treatment (**Figure 2.5E, F**).

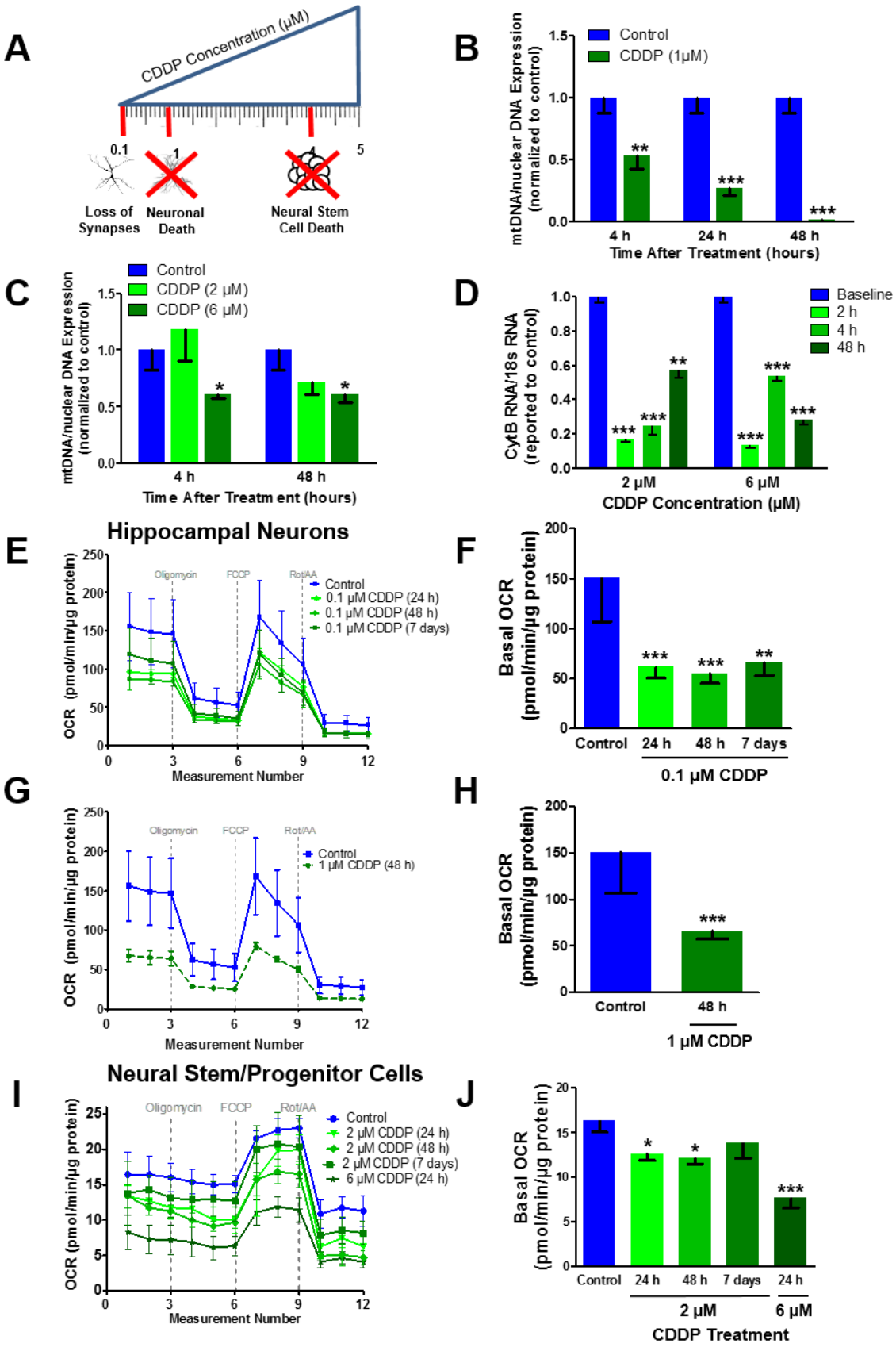
A
CDDP Concentration (μM)
0.1
1
5
Loss of Synapses
Neuronal Death
Neural Stem Cell Death
B
Control
CDDP (1μM)
mtDNA/nuclear DNA Expression (normalized to control)
4 h
24 h
48 h
Time After Treatment (hours)
C
Control
CDDP (2 μM)
CDDP (6 μM)
mtDNA/nuclear DNA Expression (normalized to control)
4 h
48 h
Time After Treatment (hours)
D
Baseline
2 h
4 h
48 h
CytB RNA/18s RNA (reported to control)
2 μM
6 μM
CDDP Concentration (μM)
E
Hippocampal Neurons
Oligomycin
FCCP
Rot/AA
Control
0.1 μM CDDP (24 h)
0.1 μM CDDP (48 h)
0.1 μM CDDP (7 days)
OCR (pmol/min/μg protein)
Measurement Number
F
Basal OCR (pmol/min/μg protein)
Control
24 h
48 h
7 days
0.1 μM CDDP
G
Oligomycin
FCCP
Rot/AA
Control
1 μM CDDP (48 h)
OCR (pmol/min/μg protein)
Measurement Number
H
Basal OCR (pmol/min/μg protein)
Control
48 h
1 μM CDDP
I
Neural Stem/Progenitor Cells
Oligomycin
FCCP
Rot/AA
Control
2 μM CDDP (24 h)
2 μM CDDP (48 h)
2 μM CDDP (7 days)
6 μM CDDP (24 h)
OCR (pmol/min/μg protein)
Measurement Number
J
Basal OCR (pmol/min/μg protein)
Control
24 h
48 h
7 days
24 h
2 μM
6 μM
CDDP Treatment

Figure 2.5. CDDP induces *mt*DNA breakage and mitochondrial respiratory dysfunction in cultured hippocampal neurons and NSCs.
(**A**) Schematic representation of neuronal and NSC sensitivities to CDDP. Low-dose CDDP (0.1 µM) causes loss of synapses, while higher doses cause neuronal death (1 µM), followed by NSC death (4 µM). CDDP causes a severe decrease in (**B**) neuronal and (**C**) NSC *mt*DNA levels. qPCR demonstrates a selective reduction in amplification of a *mt*DNA fragment (235 bp) compared to a nuclear gene (Clusterin) after CDDP treatment. (**D**) Decreased expression of mitochondrial encoded CytB after CDDP administration in NSC. The ratio of CytB RNA and 18S rRNA was quantified by PCR and normalized to baseline levels. The Seahorse Bioscience XF24 was used to measure the Oxygen Consumption Rate (OCR). OCR is significantly decreased in cultured hippocampal neurons treated with CDDP at (**E,F**) 0.1 µM and (**G,H**) 1 µM. (**F,H**) Quantification of neuronal basal OCR levels. (**I,J**) CDDP treatment (2 µM, 6 µM) reduced mitochondrial respiratory rates. (**J**) Quantification of NSC basal OCR levels. Graphs represent mean ± SEM of three biological replicates. * $p < 0.05$, ** $p < 0.01$, *** $p < 0.001$.

Basal OCR was significantly reduced at 24 h ($p < 0.0001$) and 48 h ($p < 0.0001$) compared to untreated. Basal OCR levels 7 days after treatment remained significantly lower compared to untreated levels ($p = 0.0012$). We also examined the effect of CDDP on hippocampal neurons at a higher dose, 1 µM, which significantly reduced basal OCR levels at 48 h ($p < 0.0001$) compared to untreated (**Figure 2.5G, H**).

NSC mitochondrial respiratory rates were also affected by CDDP treatment. We examined the effect of 2 µM CDDP on NSCs following 24 h, 48 h, and 7 days of treatment (**Figure 2.5I, J**). Basal OCR was significantly reduced at 24 h ($p = 0.0266$) and 48 h ($p = 0.0127$). Basal OCR levels increased 7 days after treatment back to control levels ($p = 0.2452$). A pronounced decrease in basal OCR was observed following 24 h of CDDP (6 µM, $p = 0.0075$). These results indicate that CDDP impairs mitochondrial respiratory function in hippocampal neurons and NSCs, which may be long-lasting.

2.3.8. Cisplatin-induced oxidative stress is attenuated by N-acetylcysteine in cultured hippocampal neurons and NSCs

Mitochondria are the main sources of cellular reactive oxygen species (ROS) production. Oxidative stress is involved in the pathogenesis of CDDP-induced dose-limiting toxicities, including nephrotoxicity[92], ototoxicity[93], and peripheral neuropathy[94]. We examined oxidative stress production in hippocampal neurons and NSCs following CDDP treatment (**Figure 2.6**). Cultured hippocampal neurons were treated with CDDP (0.1 µM, 1 µM) for 48 h. The neurons were then incubated with CellROX fluorescent probe for 20 min, and ROS production was measured by fluorescence intensity analysis of confocal images (**Figure 2.6A**). CDDP treatment significantly increased oxidative stress

levels as quantified by relative fluorescence intensity at 0.1 µM ($p < 0.0117$) and 1 µM ($p < 0.0062$) compared to control (**Figure 2.6B**). To further examine CDDP increases in mitochondria-generated ROS, we examined the effect of NAC on oxidative stress levels following CDDP treatment. Addition of NAC (2.5 mM) significantly reduced oxidative stress levels in neurons treated with 0.1 µM ($p < 0.0001$) and 1 µM ($p < 0.0001$).

CDDP treatment significantly increased oxidative stress in NSCs at 2 µM ($p < 0.0001$) and 6 µM ($p < 0.001$) compared to control (**Figure 2.6C,D**). NAC (5 mM) significantly mitigated oxidative stress levels in NSCs treated with 2 µM ($p < 0.001$) and 6 µM ($p < 0.001$).

2.3.9. N-acetylcysteine treatment mitigates cisplatin-induced neuronal dendritic spine loss

The effects of CDDP on neuronal respiratory dysfunction and increased oxidative stress suggested that mitochondrial damage might contribute to CDDP-induced spine loss. Previously, we showed that CDDP reduces postsynaptic density-95 (PSD95) puncta and dendritic spine density in a time- and dose-dependent manner[59]. To test this idea, neurons were treated with CDDP (1 µM) in the presence or absence of NAC (2.5 mM) (**Figure 2.7A**), and PSD95 immuno-labeled puncta were quantified 48 h after treatment (**Figure 2.7B**). CDDP reduced the number of PSD95 puncta as compared with controls ($F_{(3,80)} = 11.71$, $p = 0.001$, n = 12), and *post hoc* comparisons showed that NAC partially restored dendritic spine density at 40–100 µm. These results suggest that CDDP-induced dendritic spine loss involves mitochondrial dysfunction, although other mechanisms could also play a role.

2.3.10. N-acetylcysteine treatment ameliorates cisplatin-induced apoptosis in hippocampal neurons and NSCs

Next, we sought to examine whether CDDP induced mitochondrially-mediated apoptosis in cultured hippocampal neurons and NSCs through caspase-9 activation and if NAC could protect against caspase-9 activation. Caspase-9 is a member of the cysteine-aspartic acid protease (caspase) family. Upon apoptotic stimulation, cytochrome c is released from the mitochondria and associates with procaspase/Apaf-1[95]. Apaf-1 activates caspase-9 by cleaving it at Asp315. Cleaved caspase-9 further activates other caspase proteins to initiate a caspase cascade that culminates in apoptosis[96]. Hippocampal neurons were treated with CDDP (1 μM) in the presence or absence of NAC, and cleaved caspase-9 expression was quantified by fluorescence microscopy (**Figure 2.7C, D**)**.** CDDP (1 μM) increased the percentage of cleaved caspase-9 expressing neurons ($p < 0.0001$) compared to control levels. NAC decreased cleaved caspase-9 expression in CDDP+NAC treated neurons ($p < 0.0001$) as compared with CDDP treatment alone. Notably, the percentage of cleaved caspase-9 expressing neurons was not different between the control and CDDP+NAC treatment groups ($p = 0.7570$).

CDDP (6 μM) increased the percentage of cleaved caspase-9 expression in NSCs ($p < 0.0001$) compared to control (**Figure 2.7E, F**)**.** Mitotracker probe was used to label mitochondria in NSCs. NAC decreased cleaved caspase-9 expression in CDDP+NAC treated NSCs ($p < 0.0001$) as compared with CDDP treatment alone.

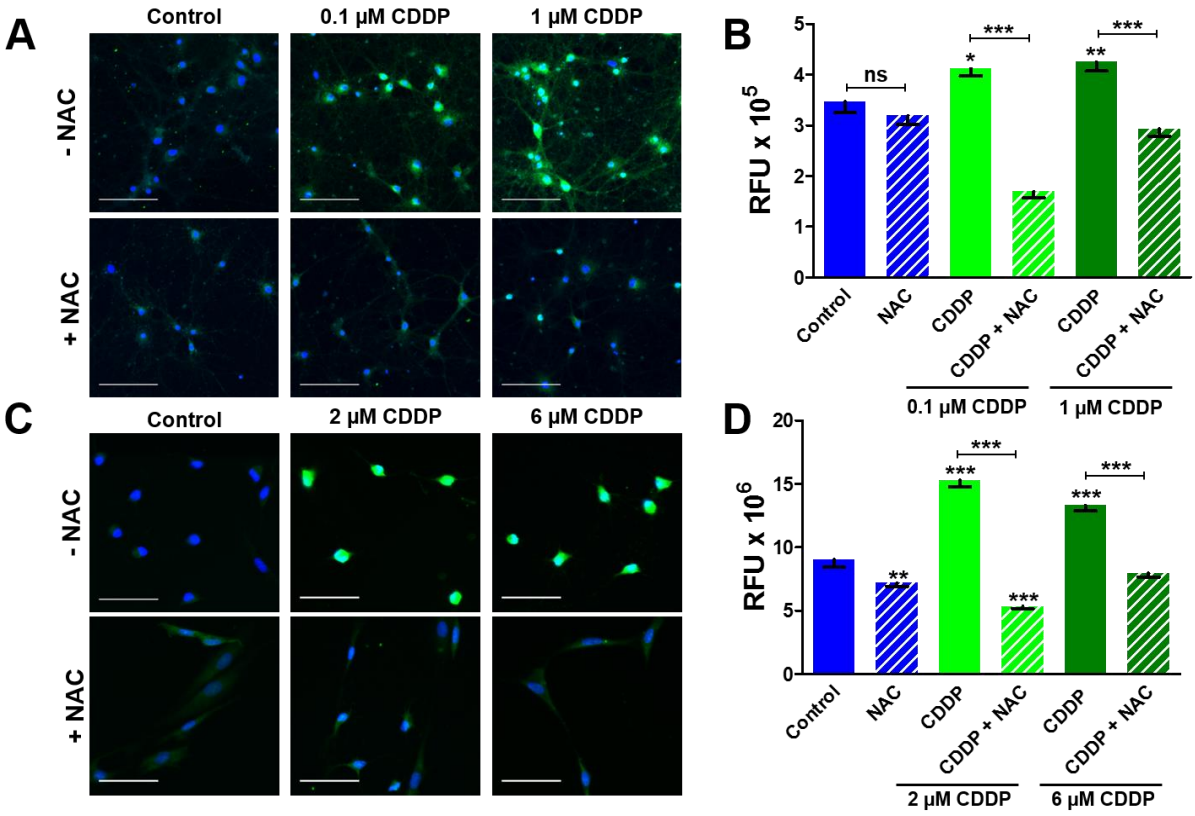

Figure 2.6. *In-vitro*, CDDP treatment increases oxidative stress in hippocampal neurons and NSCs, which can be attenuated by NAC treatment.
(**A**) Rat hippocampal neurons (17 DIV) were exposed to 0.1 µM and 1 µM CDDP in the presence or absence of NAC (2.5 mM) for 48 h. (**B**) Quantification of oxidative stress in CDDP and CDDP+NAC treated hippocampal neurons. (**C**) NSC were exposed to 2 µM and 6 µM CDDP with or without NAC (5 mM) for 48 h. (**D**) Quantification of oxidative stress in CDDP and CDDP+NAC treated NSCs. Graphs represent mean ± SEM, three sister coverslips per treatment. 5 frames/coverslip. Scale bars, 100 µm. * $p < 0.05$, ** $p < 0.01$, *** $p < 0.001$, ns = not significant. (Blue, DAPI; Green, CellROX Oxidative Stress).

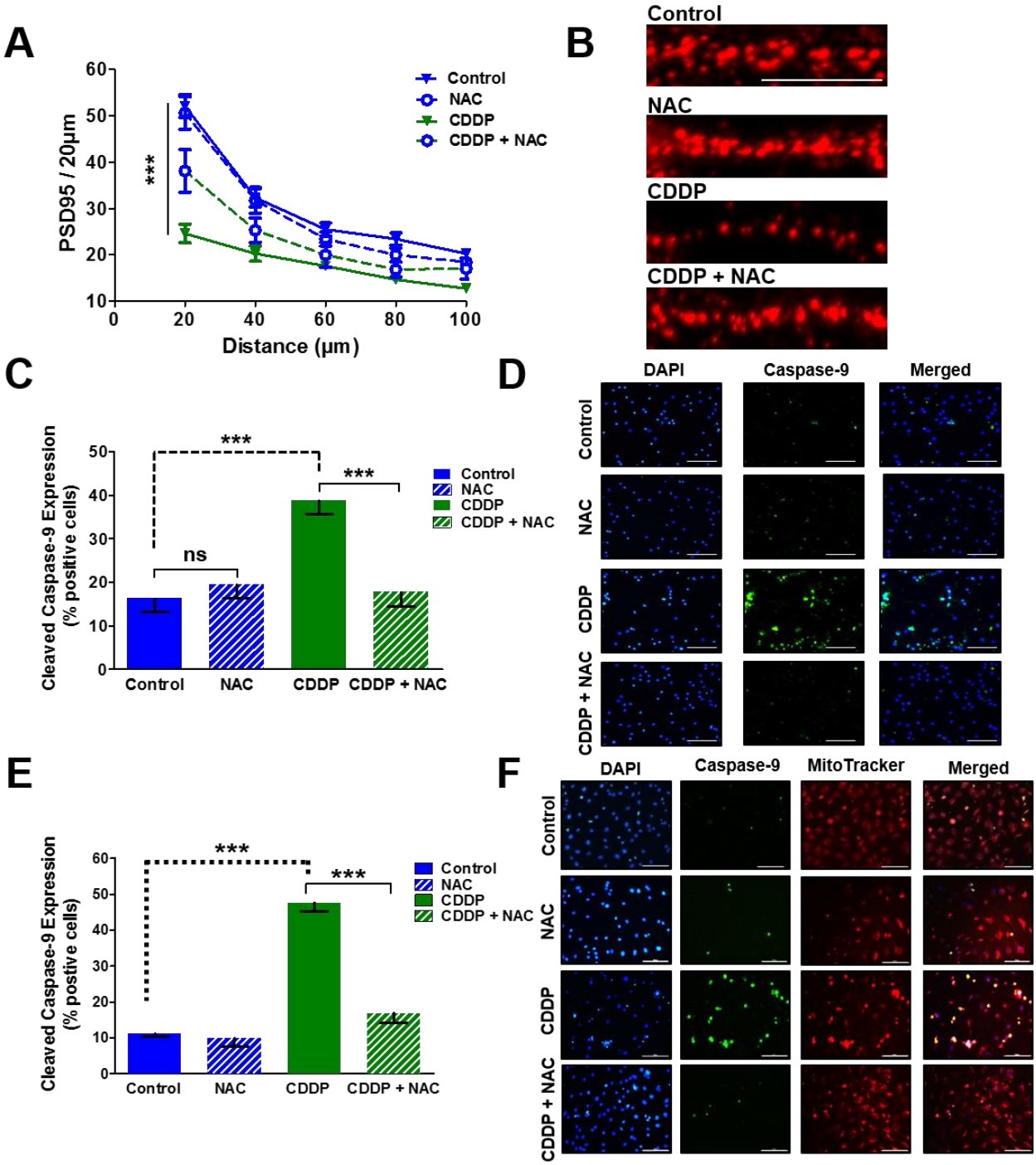
A
PSD95 / 20μm
Distance (μm)
***
Control
NAC
CDDP
CDDP + NAC
B
Control
NAC
CDDP
CDDP + NAC
C
Cleaved Caspase-9 Expression (% positive cells)
***
***
ns
Control
NAC
CDDP
CDDP + NAC
D
DAPI
Caspase-9
Merged
Control
NAC
CDDP
CDDP + NAC
E
Cleaved Caspase-9 Expression (% postive cells)
***
***
Control
NAC
CDDP
CDDP + NAC
F
DAPI
Caspase-9
MitoTracker
Merged
Control
NAC
CDDP
CDDP + NAC

Figure 2.7. *In-vitro*, CDDP induces dendritic spine loss and apoptosis in hippocampal neurons and NSCs, which can be mitigated by NAC treatment.
Rat hippocampal neurons (17 DIV) were exposed to 1 µM CDDP in the presence or absence of NAC (2.5 mM) for 48 h. (**A**) Graph and (**B**) representative images of dendrites immuno-labeled for PSD95 depicting reduction in spine density after exposure to 1 µM CDDP. NAC treatment significantly reduced CDDP-induced spine-loss. Scale bars, 20 µm (**C**) Graph and **(D**) representative images of caspase-9 activation in hippocampal neurons following CDDP Treatment. NAC significantly ameliorated CDDP-induced caspase-9 activation. Rat NSCs were exposed to 6 µM CDDP with or without NAC (5 mM) for 48 h. (**E**) Graph and (**F)** representative images of caspase-9 activation in NSCs following CDDP treatment. NAC significantly reduced caspase-9 activation in CDDP-treated NSCs. Blue, DAPI; green, caspase-9; red, PSD95 (neurons); red, Mitotracker (NSCs). Graphs represent mean ± SEM of three sister coverslips per treatment. 5 frames per coverslip. Scale bars, 100 µm (ns = not significant, * $p < 0.05$, ** $p < 0.01$, *** $p < 0.001$).

Cleaved caspase-9 expression was not significantly different between the CDDP+NAC and control groups (p = 0.0606).

2.4. Discussion

CDDP is the first platinum anti-cancer agent to be widely used in the treatment of several malignancies including lung, ovarian, testicular, and head and neck cancer[97-99]. CDDP interacts with DNA causing DNA-Pt adducts, which result in DNA crosslinking and apoptosis. A neurological complication of CDDP chemotherapy is cognitive impairment; however, the underlying mechanisms are not well understood. Here, we examine the mechanisms of CDDP-induced neurotoxicity by utilizing a rodent model to evaluate the effects of acute and chronic CDDP regimens on neuronal integrity and cognitive function. In addition, we used cultured rat hippocampal neurons and NSCs to elucidate the mitochondria-mediated mechanisms underlying the sensitivity of these cell populations to CDDP. We report that acute CDDP (6 mg/kg) treatment reduced hippocampal dendritic branching and spine density of CA3 pyramidal neurons. When examining the mitochondria of CA3 hippocampal neurons by TEM, we found that acute CDDP induced mitochondrial degradation and vacuolization with loss of cristae. Extensive apoptosis was also observed in the CA1, CA3, and SGZ of the dentate gyrus in the hippocampus of rats treated with the chronic CDDP regimen, as quantified by TUNEL. Notably, the CDDP-induced apoptosis and cognitive impairments were attenuated by NAC administration, suggesting that oxidative stress may be involved in the mechanism of CDDP-induced cognitive impairments. CDDP may produce changes in the hippocampus that persists after the completion of chemotherapy treatment. CDDP kills vulnerable NSCs and

neuronal populations, and those that do survive suffer extensive damage, including mitochondrial dysfunction and oxidative stress.

Neuroimaging studies have reported structural and functional changes in the brain associated with chemotherapy[9]. Most of these studies focus on the breast cancer population, as this group commonly reports cognitive problems after chemotherapy. Magnetic resonance imaging (MRI) studies of breast cancer patients have found reduced hippocampal volume[26,100] and grey and white matter abnormalities[101,102]. Notably, McDonald et al. report prominent reductions in grey matter density in multiple brain regions, including the hippocampus of breast cancer patients as early as one month after completion of chemotherapy with a partial recovery one year later. These structural changes correlate with decreased episodic memory, working memory, and attention deficits – all symptoms of CRCI[103,104]. In addition, a prospective study examining the effects of CDDP in testicular cancer patients found widespread reductions in grey matter in multiple brain regions as well as a reduction in performance in neurocognitive testing six months after the completion of CDDP treatment[105].

Additional imaging and functional studies examining the neurological changes associated with CDDP chemotherapy in the cancer population are warranted. However, studies examining platinum concentrations in the brains of patients that received CDDP chemotherapy for CNS[106] and non-CNS tumors[107] detected platinum (Pt) levels ranging between 0.33 and 2.9 µg/g. More recent studies have detected Pt in the brains of rodents following chronic CDDP administration ranging between 0.1 and 2.4 µg/g[67,68]. Köppen et al. detected high concentrations of Pt (0.6 – 1.9 µg/g) in the hippocampus. Based on these studies, it is plausible that CDDP results in structural CNS changes that correlate

with the cognitive deficits observed in CDDP-treated patients[75,76].

The decrease in the NSC population caused by NSC death and reduced hippocampal neurogenesis following chemotherapy treatment may prolong the regeneration of hippocampal neurons - which are critical for learning and memory processes. Impairment of hippocampal neurogenesis, as well as NSC death following chemotherapy, is linked to the cognitive and mood-based deficits observed in patients and animal models undergoing cancer therapies[10,108,109].

Due to the CDDP-induced damage to dendritic branching and spines, as well as apoptosis of neurons and NSCs within the hippocampal formation at the cellular level, it follows that cognitive tasks that require the hippocampus would be particularly vulnerable to CDDP at the behavioral level. To recapitulate the clinical regimen, rats received one weekly CDDP injection (5 mg/kg) or saline for four consecutive weeks, and performance on FC, COD, and NOR was assessed five to six weeks post-treatment. This five-week interlude allowed animals to rest following chemotherapy to minimize sickness behavior affecting performance in testing and allowed us to examine long-term effects of CDDP on cognitive performance. The CDDP group was impaired in the context but not cued FC; they spent significantly less time engaged in freezing behavior than saline controls during the context test of FC. No difference was observed in freezing behavior between CDDP and control groups during the cue-test, suggesting that CDDP selectively disrupted the memory for the context-shock association, which requires intact hippocampal function, and not the CS-US association, which does not require the hippocampus. Moreover, CDDP-treated rats spent significantly less time exploring the out-of-context object during the COD task. As the hippocampus is critical for both context fear conditioning and COD,

these results suggest that CDDP disrupts hippocampal function, which impairs context memory. Consistent with the notion, clinically, reduced hippocampal volume and neurogenesis loss have been found in chemotherapy-treated colon cancer patients[110] and brain tumor patients[58]. However, CDDP-treated rats also failed to discriminate between the novel and familiar objects during NOR; the NOR task engages the medial prefrontal cortex and perirhinal cortex in addition to the hippocampus. This suggests that although CDDP impairs hippocampal function, additional regions may be affected.

In our search for mechanisms involving CDDP-induced cognitive decrements and neurotoxicity observed *in-vivo,* we found that CDDP induces *mt*DNA damage and impairs respiratory activity in cultured rat hippocampal neurons and NSCs. Mitochondrial dysfunction increases oxidative stress, which provokes free radical production, resulting in dendritic spine loss. Severe mitochondrial dysfunction promotes caspase-9 activation and apoptosis. We found that delayed NAC treatment prevented increases in free radical production; ameliorated caspase-9 activation in CDDP treated hippocampal neurons and NSCs, and partially mitigated neuronal dendritic spine loss. NAC administration during chronic CDDP regimen reduced the CDDP-induced cognitive deficits and ameliorated CDDP-induced apoptotic cell death in the hippocampus. These findings suggest that mitochondrial dysfunction is a strong candidate mechanism for CDDP related cognitive impairments and neurotoxicity.

Oxidative stress and mitochondrial dysfunction in the brain have been associated with other chemotherapeutic agents that induce cognitive impairments, such as doxorubicin and cyclophosphamide[40,41,45], and antioxidant intervention has shown to be a promising therapy in preventing CRCI[41,46,111]. NAC is a precursor of glutathione, the

most abundant intracellular antioxidant[112]. NAC can cross the blood-brain barrier[113] and has proven efficacy in both human[114,115] and rodent models of neurodegenerative disorders[116]. In cancer patients, glutathione levels are severely reduced by CDDP treatment, while glutathione supplementation prevents the oxidative damage caused by mitochondrial dysfunction[117]. Oral NAC was studied in multiple clinical trials in combination with CDDP and has shown some promising results in preventing CDDP-induced ototoxicity[93] and peripheral neuropathy[94]. NAC prevents cancer recurrence in colon cancer patients[118,] and its addition to chemotherapy does not decrease the anti-cancer effect of other drugs[119,120]. Our data suggest that NAC prevents free radical production, ameliorates the apoptotic cellular death, and partially mitigates the dendritic spine loss in cultured hippocampal neurons.

By assessing the effects of CDDP administration on both cognition and neural damage, this study advances the understanding of mechanisms underlying CRCI.

Acknowledgments

We thank Dr. Kevin Kong of the University of California, Irvine Chao Family Comprehensive Cancer Center for advice and providing the pharmaceutical grade drugs used in our studies. We also thank Xing Gong for technical help with immunohistochemistry.

Funding

This work was supported by the National Institute for Neurological Diseases and Stroke Award (NINDS/NIH) [NS072234], the National Center for Advancing Translational

Sciences, NIH [UL1 TR001414], and the UCI Cancer Center Award [P30CA062203] from the National Cancer Institute. The NIH MBRS-IMSD training grant [GM055246] and the NINDS/NIH pre-doctoral fellowship [NS082174] provided support for N. Lomeli.

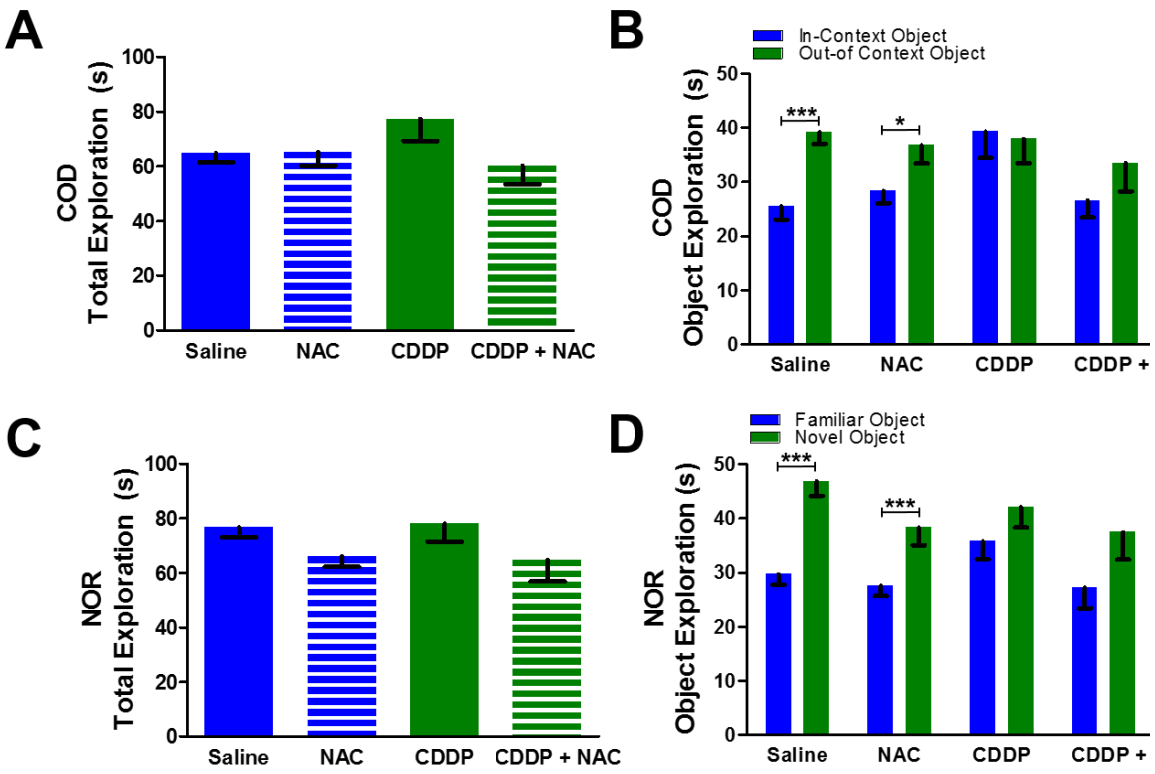

Supplementary Figure 2.1. Total exploration and object exploration in context object discrimination and novel object recognition tasks.
(**A**) No significant difference between groups in total exploration in the COD task. (**B**) The CDDP-treated rats had diminished ability to discriminate the out-of-context from the in-context object on the COD task. NAC treatment lessened the CDDP-induced deficit. (**C**) No significant difference between groups in total exploration in the NOR task. (**D**) CDDP-treated rats had reduced ability to discriminate between the novel and familiar objects on the NOR tasks. NAC treatment improved object recognition in CDDP + NAC group. Graphs represent mean ± SEM, Saline: n = 25, NAC: n = 18, CDDP: n = 15, CDDP + NAC: n = 13. * p <0.05, ** p <0.01, *** p < 0.001

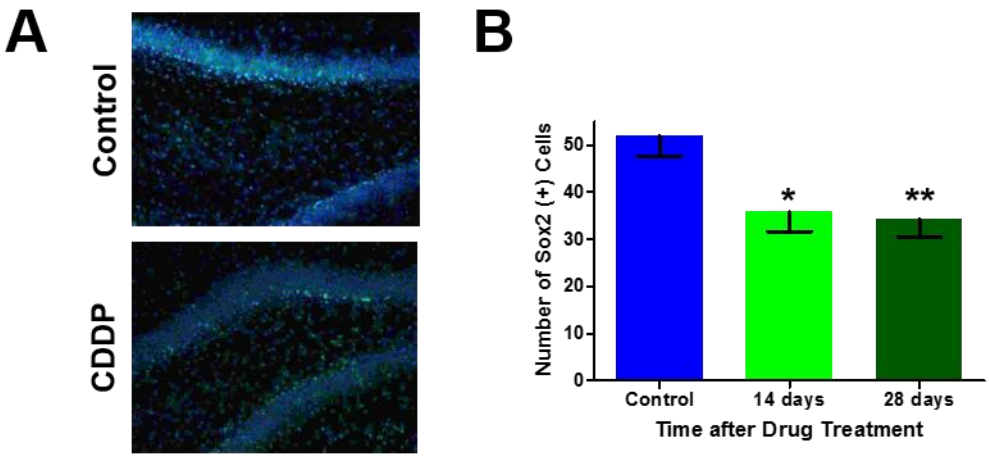

Supplementary Figure 2.2. *In-vivo,* low-dose CDDP treatment (6 mg/kg) leads to a decrease in the number of Sox2(+) cells in the dentate gyrus as early as 14 days after the treatment.
(**A**) Coronal sections through hippocampus from control and CDDP treated animals show that CDDP mildly decreased the number of neural progenitor cells after four weeks of treatment. (**B**) Quantification of Sox2(+) cells in control and CDDP treated animals 14 and 28 days after CDDP treatment (n = 6 rats per group). Data are presented as mean ± SEM, * $p < 0.05$, ** $p < 0.01$.

CHAPTER 3

Systemic Cisplatin Exposure During Infancy and Adolescence Causes Impaired Cognitive Function in Adulthood

Abstract

Cancer survivors diagnosed during infancy and adolescence may be at risk for chemotherapy-related cognitive impairments (CRCI); however, the effects of pediatric chemotherapy treatment on adulthood cognitive function are not well understood. Impairments in memory, attention, and executive function affect 15–50% of childhood leukemia survivors related to methotrexate exposure. Systemic cisplatin is used to treat a variety of childhood and adult cancers, yet the risk and extent of cognitive impairment due to platinum-based chemotherapy in pediatric patients is unknown. Systemic cisplatin penetrates the CNS, induces hippocampal synaptic damage, and leads to neuronal and neural stem/progenitor cell (NSC) loss. Survivors of non-leukemic cancers may be at risk for significant cognitive impairment related to cisplatin driven neurotoxicity. We sought to examine the long-term effects of systemic cisplatin administration on cognitive function when administered during infancy and adolescence in a rat model.

We performed cognitive testing in adult rats exposed to systemic cisplatin during either infancy or adolescence. Rats treated as adolescents showed significantly poor retrieval of a novel object as compared to controls. Further, cisplatin-treated infants and adolescents showed poor contextual discrimination as compared to controls, and an impaired response to cued fear conditioning. Ultimately, systemic cisplatin exposure

resulted in more profound impairments in cognitive function in rats treated during adolescence than in those treated during infancy. Further, exposure to cisplatin during adolescence affected both hippocampus and amygdala-dependent cognitive function, suggesting a more global cognitive dysfunction at this age.

3.1. Introduction

Cognitive impairment is a well-described consequence of cancer treatment, with 17-75% of cancer survivors reporting persistent memory problems years after completion of therapy[29,121]. Cognitive abnormalities observed in cancer survivors typically include impairments in memory, attention, processing speed and executive function[10,11,122,123]. A variety of causes including direct chemotherapy neurotoxicity as well as indirect toxicity related to hormonal abnormalities, oxidative stress, treatment-associated metabolic changes, inflammatory activation, cancer-related symptoms (pain, fatigue) and medical co-morbidities (anemia, renal dysfunction, cardiotoxicity) have been implicated in the pathogenesis of cancer-related cognitive impairment (CRCI)[16,124]. CNS-penetrating chemotherapy, particularly high doses of systemic and intrathecal methotrexate used in pediatric acute lymphoblastic leukemia treatment regimens, can cause chronic leukoencephalopathy and have been most strongly implicated in CRCI[125-127]. The clinical impact of other non-antimetabolite chemotherapeutic agents on cognition in children and adolescents is not known[128-130].

Cisplatin (CDDP) is a CNS penetrating chemotherapeutic agent used to treat a number of malignancies including common pediatric and young adult cancers such as neuroblastoma, hepatoblastoma, germ cell tumors, and primary central nervous system

neoplasms[131,132]. Recent National Cancer Institute Surveillance, Epidemiology, and End Results (SEER) data confirm that the peak incidences of the above-mentioned cancers occur during infancy and/or adolescence, thereby making these patient populations at particular risk of developing side effects attributable to CDDP[133].

To examine, the effects of early-life CDDP exposure on cognition function in young adulthood, we developed an infant and adolescent rodent model of CRCI. Rats have a brief and accelerated childhood compared to humans[134]. The most common method to assess infancy in rats is based on weaning age. Rat pups are weaned at post-natal day 21 (P21), and the average weaning age for humans is approximately 6 months. Rats reach peak adolescence at approximately 38 days (P38), and transition into adulthood at approximately P63. In contrast, humans reach adolescence at approximately 11.5 years and enter adulthood at 18 years of age. Based on these developmental stages, we administered CDDP (2 mg/kg/day) to Sprague Dawley rats at P25–P29 or P35–P39 and examined cognitive function in young adulthood (P65). These rat developmental stages correlate with human infancy (0–2 years) and adolescence (11–18 years), respectively[134,135].

The neurotoxic effects of a variety of chemotherapeutic agents (cisplatin, methotrexate, cyclophosphamide, carmustine, 5-fluorouracil, cytarabine) have been examined in the pre-clinical setting and are associated with neurotoxicity and cognitive impairment[10,11,36,59,136,137]. Specifically, we have previously reported that low-dose *in-vitro* CDDP exposure induces apoptosis in cultured rat hippocampal neurons and neural stem/progenitor cells (NSCs)[59]. Further, we showed that acute *in-vivo* CDDP (6 mg/kg, 10 mg/kg) exposure causes a time-dependent loss of hippocampal dendritic branching

and dendritic spine density in adult rats[59]. When treated with a chronic CDDP regimen (5 mg/kg/week for 4 consecutive weeks), adult male rats exhibited significant impairments in three cognitive tasks[38]. Additional behavioral studies in the adult rodent population have yielded data showing the development of hippocampal-dependent cognitive impairment. One reported pre-clinical model had explored the development of cognitive deficits in pre-weanling rodents exposed to chemotherapy (methotrexate and cytarabine mimicking childhood acute lymphoblastic leukemia treatment); however, a lack of models exploring the late cognitive effects of non-antimetabolite chemotherapy, specifically with a pediatric focus during infancy and adolescence, exists[138]. Given the common use of CDDP to treat a variety of pediatric cancers and the known effect of CDDP on neural structures, we sought to develop a pre-clinical pediatric model examining the long-term cognitive function of infant and adolescent rodents treated with CDDP.

3.2. Methods

Animals

Animal studies were performed in accordance with the guidelines established by the Institutional Animal Care and Use Committee (IACUC) of the University of California, Irvine. All experiments were approved by the IACUC and conformed to National Institutes of Health standards.

Chemotherapy application in-vivo

Thirty-nine male Sprague-Dawley rats (Charles River, San Diego, CA, USA) were obtained weaned from their mother at post-natal day 21 (P21). Treated rats received

intraperitoneal CDDP dissolved in 0.9% saline (Fresenius Kabi USA, LLC) dosed at 2 mg/kg/day for5 consecutive days beginning at post-natal day 25 (P25, infancy) or post-natal day 35 (P35, adolescence). Age-matched controls received 0.9% saline of a similar volume. Mannitol (APP Pharmaceuticals, 125 mg/kg, intraperitoneal) was administered 1 h prior to CDDP, to minimize renal toxicity and increase diuresis. Additional intraperitoneal injections of 0.9% saline were given as needed for supportive care.

Behavioral testing

Cognitive testing was completed during adulthood (post-natal day > 65) including a novel object recognition task (NOR), context object discrimination (COD) task, and fear conditioning (FC) (**Figure 3.1**)[30,32,80,81,139]. Each cognitive task was performed in different rooms and arenas, and the objects used for NOR were distinct from those used for COD. All behavior analysis was conducted by an experimenter blinded to the treatment group of the rats. A pilot experiment included 3 rats in each group (n = 9) treated as above and tested via the NOR task at post-natal day 65–70. A second experiment included 5 rats per treatment group (n = 15). Three rats in the adolescent group (CDDP–P35) died of complications of chemotherapy exposure (renal toxicity). The remainder of the rats completed the NOR task at post-natal days 65–68 (P65–P68), COD task at post-natal days 75–78 (P75–P78) and FC task at post-natal day 93–94 (P93–P94). A third experimental group was added to this study, including 5 control, 5 infant, and 8 adolescent rats treated and tested using the same conditions as the second cohort. Three control rats were excluded from the FC analysis due to lack of response to conditioning; they failed to freeze in response to the foot-shocks administered during training, and as a result

did not exhibit to freeing behavior during the post-training session, context test, nor cue-test.

Novel Object Recognition (NOR)

First, rats were tested for recognition of a novel object[81,139]. Rats were individually placed in a quiet room in an open Plexiglas square arena (60 cm x 60 cm x 60 cm) lined with black cardboard. After habituation to the arena, each rat was given 5 minutes per day on 2 consecutive days to explore 2 identical objects in the arena. The test trial was performed 24 hours later such that each rat was presented with one familiar object paired with a novel object for 5 minutes.

Context Object Discrimination (COD) Task

Individual rats were exposed to 2 different environmental arenas (Arena A and Arena B) located in adjacent rooms. Each rat was given 5 minutes in each arena per day on 2 consecutive days to explore freely. Between training sessions, each rat was returned to the home cage for a 20 min interval[80]. Each environment had 2 identical objects unique to the environment. The order of context presentation was counterbalanced between subjects and across days. On day three each rat was tested for 5 minutes in a modified environment (Arena A') where one of the objects from Arena B replaced one of the objects from Arena A. The total time each rat explored each object was recorded.

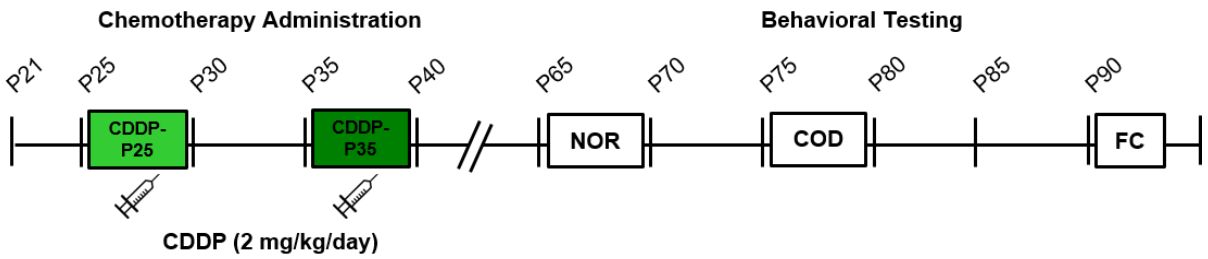

Figure 3.1. Experimental design of a pediatric CRCI model.
Rats received CDDP (2 mg/kg/day) for five consecutive days at P25–P29 (infancy), or P35–P39 (adolescence). Age-matched controls received 0.9% saline of similar volume. Cognitive testing was completed during adulthood, including novel object recognition (NOR) at P65–P70, context object discrimination (COD) at P75–P78, and fear conditioning (FC) at P93–P94.

Fear Conditioning (FC)

The fear conditioning task was administered at approximately post-natal day 90-95 (P90–P95). Two similar but distinct chambers, each housed within a sound-attenuating chamber, were used for fear conditioning[79]. The floor of the conditioning chamber consisted of 18 steel rods wired to a shock generator (Coulborn Instruments) for foot-shock delivery. The fear-conditioning paradigm used was based on previous studies on chemotherapy-treated rodents[30,32]. Specifically, the fear-conditioning task consisted of three distinct phases: a training phase, a context test phase, and a cue test phase. During fear conditioning rats were individually placed in a chamber for 5 minutes (baseline), exposed to 5 tone pairings (90db, 2000 Hz-shock, [1mA, 1s]) for 5 minutes and then left in the conditioning chamber for an additional 5 minutes (post-training). The following day the rats were returned to the conditioning chamber for 5 min to assess conditioned freezing to the context (context test). No tone or shock was administered during the context test. When memory for the context-shock conditioned association is intact, rats spend a significant portion of the context test freezing. The cue test was then administered 1 hour after the context test. For cue testing, rats were placed in a novel context for 1 minute (pre-cue test) followed by a 3-minute tone presentation (cue test) and an additional 1-minute (post-cue test). Freezing behavior was defined as complete immobility with the exception of breathing movements and scored as a percent of the overall time for each phase.

Statistical Analysis

Graphs and statistical analyses were prepared using GraphPad Prism 5.0 Software (GraphPad Software, La Jolla, CA, USA). Results are expressed as mean ± SEM. Comparisons between treatment groups were made by unpaired Student's *t*-test, or two-way repeated measures (RM) ANOVA. Statistical significance levels were set at 0.05. *Post hoc* analysis was made by Bonferroni correction.

3.3. Results

3.3.1. Cisplatin treatment during adolescence causes impaired novel object recognition

The NOR task utilizes the natural tendency of animals to explore novel objects relative to familiar objects[140]. During NOR testing, all groups showed similar total object exploration times, indicating similar engagement and activity level (**Figure 3.2A**). Controls and rats exposed to CDDP during infancy spent significantly more time exploring the novel object compared to the familiar object ($p = 0.0015$ and $p = 0.0141$); however, rats exposed to CDDP during adolescence displayed no preference in exploring either object ($p = 0.4341$). A two-way RM ANOVA revealed a significant difference in object exploration ($F_{(1,72)} = 5.574$, $p = 0.0209$), but no significant difference between treatment groups ($F_{(2,72)} = 0.9079$, $p = 0.4079$), nor interaction between treatment groups and object exploration ($F_{(2,72)} = 2.718$, $p = 0.0728$) (**Figure 3.2B**). CDDP treatment during adolescence but not infancy impaired the ability to recognize a novel object from a previously experienced familiar object. Together these data suggest that CDDP treatment may have an age-dependent effect on cognitive function.

3.3.2. Cisplatin treatment during infancy and adolescence causes diminished contextual discrimination

The COD task tests for context discrimination, which requires hippocampal-dependent pattern separation skill[81]. During the COD testing, all groups showed similar total object exploration times (**Figure 3.3A**). The control group explored the out-of-context object more than the in-context object (p = 0.0009); however, rats exposed to CDDP during infancy and adolescence showed no bias between objects (infants: p = 0.7142, adolescents: p = 0.6867). A two-way ANOVA revealed a significant difference between treatment groups ($F_{(1,54)}$ = 8.822, p = 0.0044), but no significant difference between object exploration ($F_{(2,54)}$ = 0.1681, p = 0.8457), nor interaction between treatment group and object exploration ($F_{(2,54)}$ = 2.004, p = 0.1447) (**Figure 3.3B**). CDDP treatment diminished the ability to distinguish a previously experienced object, placed in a different context. This effect was most prominent in the subjects treated during adolescence.

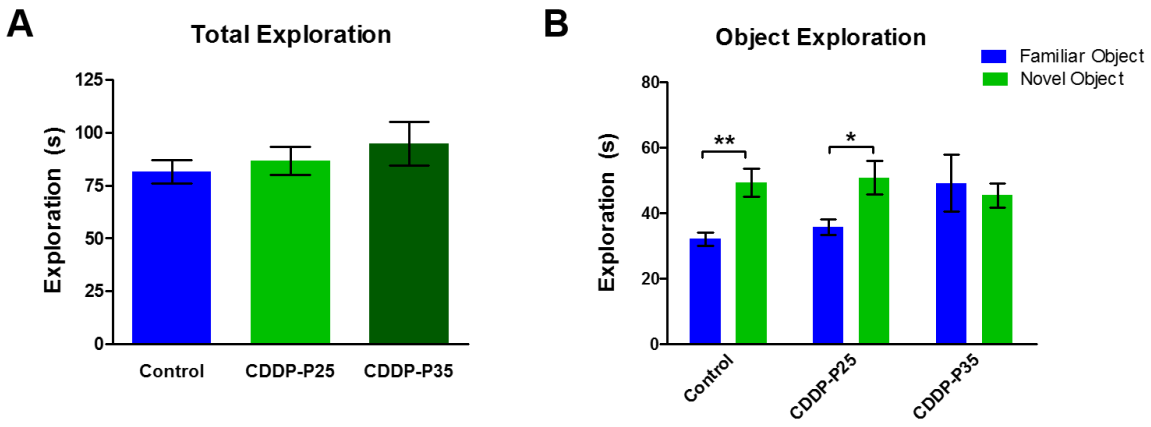

Figure 3.2. Impaired novel object recognition following CDDP exposure in adolescence but not infancy.
During novel object recognition testing, all groups showed similar total exploration times. (**A**) As expected, control (n = 13) and CDDP-P25 (n = 13) rats explored a novel object (NO) significantly more than a familiar object (** $p < 0.005$ and * $p < 0.02$; however, exploration between objects for the CDDP-P35 (n = 13) rats was not different. (**B**) Error bars are SEM.

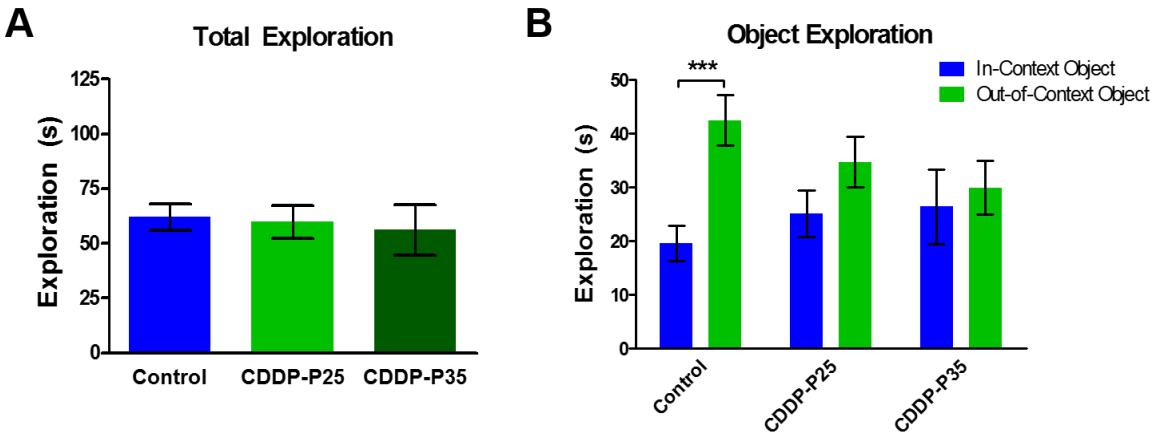

Figure 3.3. Impaired contextual discrimination following cisplatin exposure during infancy and adolescence.
During context object discrimination testing, all groups showed similar total exploration times. (**A**) As expected, control (n = 10) rats explored an out-of-context object significantly more than a familiar object; (*** $p = 0.001$); however, exploration between objects for the CDDP-P25 (n = 10) and CDDP-P35 (n = 10) rats was not different. (**B**) Error bars are SEM.

3.3.3. Cisplatin treatment during infancy and adolescence causes decreased response to a conditioned cued stimulus

Fear conditioning assesses the ability of rodents to learn and remember an association between environmental cues and aversive experiences via evaluation of freezing behavior in response to a conditioned context or cue[141]. After being tested on novel object recognition and context-object discrimination; the animals were tested on the fear conditioning task (**Figure 3.4A**). While contextual fear conditioning requires an intact hippocampus, cued fear conditioning relies on the amygdala[142,143]. A two-way RM ANOVA revealed a main effect of testing phase ($F_{(5,120)} = 74.61$, $p < 0.0001$), treatment group ($F_{(2,120)} = 6.120$, $p = 0.0071$), and treatment group by phase interaction ($F_{(10,120)} = 4.678$, $p < 0.0001$) for the percent time spent freezing during the fear conditioning task. During the context-test phase, CDDP-treated infant and adolescence rats spent decreased percentages of time freezing compared with the control animals, although not significant (infants: $p = 0.1405$; adolescents: $p = 0.1737$). Surprisingly, CDDP treatment affected cued-memory such that both CDDP-treated infants and adolescents spent significantly decreased percentages of time freezing in response to 5 tone-shock pairings, as compared to the control subjects (infants: $p = 0.0003$; adolescents: $p = 0.0412$).

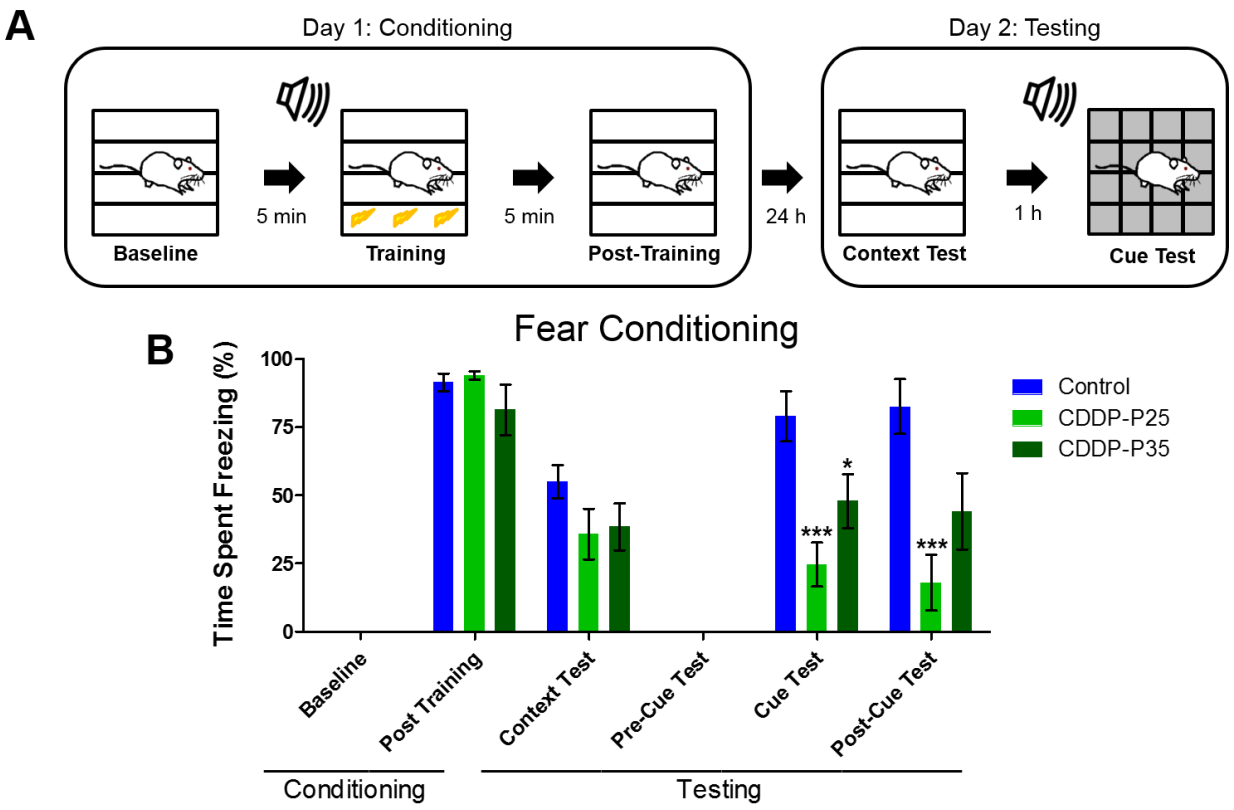

Figure 3.4. Cisplatin decreases response to a conditioned cued stimulus in fear conditioning following exposure during infancy and adolescence.
Schematic of the fear conditioning paradigm. (**A**) During context and cued fear conditioning both CDDP-P25 (n = 10) and CDDP-P35 (n = 10) rats showed a trend toward decreasing freezing response during the context test ($p = 0.14$ and $p = 0.17$) as compared to controls (n = 7). During the Cue and post-Cue Test, CDDP-P25 rats showed a significant decrease in freezing (*** $p < 0.001$). During the Cue Test, CDDP-P35 rats showed significant decreased freezing response (* $p < 0.05$), which persisted to a lesser degree Post–Cue Test ($p = 0.06$). (**B**) Error bars are SEM.

The groups did not differ significantly in the freezing behavior across baseline, post-training, context-test, and pre-cue, suggesting that the deficits may be selective to the amygdala-dependent cue memory phase of the task – the tone to which the foot-shock was paired.

3.4. Discussion

As most of the current preclinical studies on CRCI have been performed on adult rodents, we recognized a need to develop a model exploring the effects of chemotherapy on the developing brain. We have previously shown that when administered chronically to adult male Sprague Dawley rats, CDDP (20 mg/kg) impaired performance in novel object recognition, context object discrimination, and contextual but not cued fear conditioning[38]. In the adult population, ovarian cancer patients treated with CDDP consistently develop CRCI during and after platinum-based chemotherapy[75]. A study that examined advanced ovarian cancer patients in comprehensive neurocognitive tests detected impairments in two or more cognitive domains in 40% of CDDP chemotherapy recipients[76]. However, studies examining the effects of platinum-chemotherapy in pediatric rodent models and in the adolescent and young adult (AYA) cancer survivor population are lacking.

Childhood and adolescence are distinct yet similarly robust periods of brain development and maturation of cognitive skills, which are vulnerable to harmful environmental influences such as illicit drug exposure[144]. Similarly, the developing rodent brain has been shown to be more vulnerable to toxins or stress as compared to the matured rodent brain[145]. These differences in vulnerability highlight the need for the

development of pediatric pre-clinical models of CRCI to parallel those for adults. Here we developed a model of CRCI for examining CDDP-induced cognitive impairments in an infant (P25) and adolescent (P35) rat model. Our current data shows that CDDP, when administered during infancy and adolescence, causes long-term cognitive impairment; however, the degree and type of impairment appears to differ with age at the time of CDDP exposure. Understanding the age-dependent and agent-specific differences in CRCI will be important in developing effective supportive and preventative strategies to preserve cognitive function in growing cancer survivor populations.

Given that CDDP exposure reduces dendritic branching and spine density, and induces apoptosis of neurons and NSCs within the hippocampal formation[38,59], it follows that cognitive tasks that require the hippocampus would be highly susceptible to CDDP, and the effects of CDDP on cognitive function should be explored. The hippocampus is required for spatial and contextual memory[141]. Specifically in rodents, the hippocampus participates in the recollection of where and in what context an object is encountered[141]. Further, the hippocampus is crucial for forming an association between an aversive experience (foot-shock) and the context in which it occurred[142]. COD and context fear conditioning tasks evaluate for intact hippocampus function. In addition to hippocampal specific behavior testing, we utilized other tasks involving cortical brain regions and the amygdala to evaluate cognition function more globally (**Table 3.1**). The amygdala participates in memory processing and emotional reaction and plays a critical role in the formation of an association between an unconditioned stimulus and a cued stimulus[142,143]. Contextual fear conditioning requires an intact hippocampus; however, the cued fear conditioning component of the task requires intact amygdala function. The NOR task

Novel Object Recognition	Context Object Discrimination	Fear Conditioning
▪ Hippocampus ▪ Frontal Cortex ▪ Perirhinal, entorhinal, and inferior temporal cortices	▪ Hippocampus	▪ Hippocampus ▪ Amygdala ▪ Frontal/Ventromedial/Cingulate Cortex

Table 3.1. Neural systems involved in behavioral tasks.

differs from all previous tests in that it assesses general memory function, which requires an intact temporal lobe including hippocampus as well as adjacent cortical structures[140].

3.5. Conclusions

Our data indicate that rats exposed to systemic CDDP during infancy and adolescence experience impairment of cognitive function. The degree and type of cognitive dysfunction may depend on age at the time of CDDP exposure. Rodents treated during adolescence may develop greater impairment in cognitive tasks than those treated during infancy, as evidenced by impaired performance on the NOR and COD; however, neither group showed significant impairment on the contextual FC (**Table 3.1**). A more strongly powered follow-up study may help confirm these conclusions and define the subtle cognitive changes caused by CDDP exposure at various ages. While CDDP-associated cognitive impairment may involve the hippocampus, rats treated with CDDP during adolescence appear to experience more global cognitive deficits. Amygdala functions are diminished after CDDP exposure in infancy and adolescence. Previous data have shown that activation of neural circuitry pathways involving the nucleus of the amygdala contributes to CDDP-induced malaise and energy balance dysregulation[146]. Changes in pathway activation or direct neural toxicity in the amygdala may explain the impairment in amygdala-dependent cognitive tasks in the pediatric rodents. Further, adolescent rats showed a significant lack of discrimination of a novel object in the NOR testing indicating more global disruption of neural circuitry involving cortical brain regions. This was not seen in the population exposed during infancy that exhibited comparable discrimination for a novel object to controls.

The differences in cognitive performance between the subjects exposed to CDDP during infancy and adolescence may be attributed to neurodevelopmental changes that occur at these distinct stages[147]. Infancy is a critical period of robust neurodevelopment. Key developmental processes that occur in infancy in humans, as well as rodents, include: brain reaches 90-95% of adult weight[148], peak in synaptic density[149] and myelination rate, and neurotransmitter and receptor changes. In rodents, the critical period of synaptogenesis occurs during the first three postnatal weeks of life, peaking by P25. In addition, NMDA subunit expression peaks by P20 in the rat hippocampus and cortex[150]. During adolescence, there is specialization and strengthening of neural networks, reduced synaptic density, which reaches adult levels, and refinement of cognitive-dependent circuitry[151]. The robust neurodevelopment that occurs during infancy may facilitate the recovery of cognitive function following chemotherapy treatment, whereas during adolescence, chemotherapy treatment may result in cognitive impairments, which persist long into adulthood.

In our evaluation of young rats exposed to CDDP, we were able to detect an effect of CDDP on long-term cognitive function after rats entered adulthood. In addition to detection of hippocampal-dependent changes, we also identified a potentially more global effect of CDDP on cognition, which may be age-dependent and includes the amygdala and cortical circuitry. Further exploration of CRCI, specifically regarding the impact of CDDP exposure on the developing brain, is imperative not only in developing a more comprehensive understanding of CRCI but also in devising targetable mechanisms for treatment and prevention.

Funding

This work was supported by (1) National Institute for Neurological Diseases and Stroke Award (NINDS/NIH) number NS072234 (2) National Cancer Institute UCI Cancer Center Award Number P30CA062203.

CHAPTER 4

A Novel Ovarian Cancer Rat Model to Examine Cisplatin-Related Cognitive Impairments

Abstract

Gynecologic cancer survivors treated with platinum-based chemotherapy agents, such as cisplatin, report experiencing long-lasting chemotherapy-related cognitive impairments (CRCI), or chemobrain. Using a rat model of CRCI, we had shown that cisplatin-induced cognitive impairments are associated with oxidative stress, which was prevented by the administration of the antioxidant N-acetylcysteine. Currently, there are no FDA-approved medical interventions for the prevention of CRCI. CRCI preclinical studies for therapeutic interventions have focused mainly on healthy, non-tumor bearing rodents. In this study, we developed an ovarian cancer xenograft rat model of CRCI to examine whether N-acetylcysteine administration could prevent cisplatin-induced CRCI without interfering with its anti-cancer efficacy. *In-vitro,* delayed NAC (10 h) following cisplatin treatment in human ovarian cancer cell lines SKOV3.ip1 and OVCAR8 did not decrease cisplatin efficacy, while reducing neural cell death, and hippocampal dendritic damage. In our tumor-bearing CRCI model, female nude rats received subcutaneous and intraperitoneal implantation of human SKOV3.ip1 cells. Rats received one cisplatin (5 mg/kg) injection every two weeks, for a total of 4 cycles, with or without NAC (250 mg/kg/day) administered for five consecutive days during cisplatin treatment. NAC was delayed by 10 h on days of cisplatin administration, based on our *in-vitro* data. Cognitive

testing and whole blood glutathione measurements were performed six to seven weeks after treatment cessation. *In-vivo*, cognitive impairments were observed in tumor-bearing rats in the vehicle and cisplatin-treatment groups, while delayed NAC prevented cognitive impairments, and decreased oxidized glutathione (GSSG) levels in the blood. Delayed NAC administration did not affect cisplatin-induced tumor volume reduction nor rat survival. These data support the use of delayed NAC to mitigate cisplatin-induced CRCI without interfering with cisplatin's anti-cancer efficacy.

4.1. Introduction

Chemotherapy has revolutionized cancer treatment, leading to an increasing number of survivors. In gynecologic malignancies such as ovarian cancer, chemotherapy has led to a significant increase in five-year survival rates, which now over 45%[133]. However, for many chemotherapeutic agents that are able to cross the blood-brain barrier, destroying cancer cells comes with the cost of both acute and long-term detrimental effects on neural structures leading to chemotherapy-related cognitive impairment (CRCI, chemobrain). CRCI refers to a clinical entity encompassing significant impairments in information processing speed, memory, executive functioning, and clarity of thought, which affect the patient's perceived quality of life. While CRCI is a recognized clinical entity, there are no FDA-approved preventative therapies for it.

Platinum-based chemotherapeutic agents, such as cisplatin (CDDP), are widely used to treat ovarian malignancies, and over 70% of women report experiencing CRCI during or after treatment completion[152,153]. Platinum-based chemotherapy is typically delivered in the frontline setting at high doses with curative intent and for the 75% of

ovarian cancer patients who recur it is subsequently used again for platinum-sensitive recurrences. Therefore, it is of utmost importance to develop a strategy to prevent CRCI, an unwanted, under-recognized long-term side effect that seriously affects quality of life.

We recently reported that CDDP induces cognitive impairments in pediatric and adult rat models of CRCI[38,154]. Although the mechanisms through which CDDP causes cognitive impairments are multiple, we identified a strong candidate pathway: mitochondrial dysfunction, causing abnormalities in cellular respiration and neuronal morphology, in addition to increased free radical production in NSCs and hippocampal neurons. Importantly, this process can be potentially prevented or reduced with the administration of clinically available treatments, such as the antioxidant N-acetylcysteine (NAC)[38].

NAC is used in clinical practice as a mucolytic agent for acetaminophen overdose. NAC is the most abundant non-protein thiol (sulfhydryl-containing compound) found in cells and is a precursor of L-cysteine, which is the rate-limiting substrate in glutathione (GSH) production[155]. NAC is also a scavenger of free radicals as it interacts with reactive oxygen species (ROS) such as superoxide (OH^-) and hydrogen peroxide (H_2O_2). NAC has been shown to protect against cisplatin-related toxicities, including nephrotoxicity[156-158], ototoxicity[158], in animal models.

Concerns that N-acetylcysteine and other antioxidants may interfere with the mechanism of action of chemotherapeutic agents and decrease their efficacy has hindered their clinical use for the treatment of chemotherapy-related toxicities[159]. Muldoon et al. have shown that delayed administration of NAC four hours after CDDP in models of neuroblastoma and medulloblastoma does not reduce CDDP efficacy, and in separate

studies, this regimen has been shown to reduced CDDP-associated nephrotoxicity and ototoxicity[88,160].

The aim of this study was to investigate the hypothesis that delayed N-acetylcysteine administration can prevent CDDP-induced cognitive impairments in a rat model of ovarian cancer, without decreasing CDDP's anti-tumor efficacy. Our rationale for choosing an ovarian cancer model was influenced by the fact that platinum-based chemotherapy for gynecologic cancers is routinely used as a mainstay in both the primary and recurrent setting for most ovarian malignancies. With over 40% of ovarian cancer patients experiencing long-term impairments in two or more cognitive domains after completion of chemotherapy[75,76], this patient population can primarily benefit from therapeutic interventions to improve cognitive function and chemotherapy-associated sequelae.

4.2. Materials and Methods

Cell culture

The human epithelial ovarian carcinoma cell lines SKOV3.ip1 and OVCAR8 were cultured in RPMI 1640 (Corning) supplemented with 10% FBS (Sigma Aldrich) and maintained in 5% CO_2 at 37°C. SKOV3.ip1 is a SKOV3 subline established from ascites by i.p. passage of SKOV3[161] in *nu/nu* mice.

NSCs were isolated from the hippocampi of embryonic day 19 (E19) Sprague Dawley rats and cultured as previously described[59]. Passage 7 NSCs were used for experiments. Hippocampal neuron cultures were prepared from postnatal day 0 (P0)

Sprague Dawley pups, as previously described[38]. Neurons were used for experiments on 17-21 days *in-vitro* (17-21 DIV).

Glutathione quantification in hippocampal neurons and NSCs

Hippocampal neuron and NSC intracellular total glutathione (GSH) levels were assayed using the OxiSelect™ Total Glutathione (GSSG/GSH) Assay kit according to the manufacturer's protocol. Briefly, hippocampal neurons and NSCs were cultured in 6-well plates. Cells were washed twice with 500 µl of ice-cold PBS. 125 µl of ice-cold 5% (w/v) metaphosphoric acid (MPA, Sigma Aldrich) was added to each well to deproteinate the samples. Cells were harvested using a cell scraper, and the cell suspension was homogenized and placed on ice for 15 min. The cell suspension was then centrifuged at 14,000 rpm for 15 min at 4°C.The supernatant was collected and stored at -80°C. An equal volume (125 µl) of RIPA buffer was added to neighboring well that received the same experimental treatment for protein quantification.

Immunocytochemistry (ICC)

Neurons plated on 12 mm coverslips were incubated in culture medium in 24-well plates. After incubation, cells were fixed with ice-cold 4% paraformaldehyde (PFA) in PBS, pH 7.4, for 12 min. Rabbit anti-Caspase-9 (Cell Signaling) was diluted 1:100 in blocking buffer (5% donkey serum, 0.3% Triton-100x in PBS, pH 7.4) overnight at 4°C. Mouse anti-PSD95 1:2000 (Thermo Fisher) was diluted 1:2000 in blocking buffer (3% FBS, 0.1% Triton-100x in PBS, pH 7.4). The next day, coverslips were washed and incubated in the appropriate secondary antibodies conjugated to Alexa Fluor 488 at

1:200, or Alexa Fluor 594 at 1:400 (Invitrogen); at room temperature for 1.5 hr. Cells were processed for imaging with DAPI Fluoromount G (Southern Biotech) mounting medium.

Image analysis of dendritic branches and spines and caspase-9 expression

Confocal microscopy, Zeiss LSM700, was used to generate neuronal images. For PSD95 quantification, 3 µm z-series (0.5 µm steps) images were captured at 63X (NA 1.4) spanning across entire neurons. Each individual puncta was considered a separate spine, and counts were not adjusted for puncta size. PSD95 puncta density was quantified as the number of PSD95 puncta per 20 µm of dendrite length, comparing dendrites of the same order using ImageJ[59]. Twelve dendrites from six neurons (two dendrites per neuron) per treatment group were analyzed. Each experimental group included three sister coverslips, and two neurons were imaged per coverslip.

For caspase-9 analysis, images were captured at 20X (NA 0.8). Each experiment included three sister coverslips per group, with five images analyzed per coverslip, for a total of 800-1200 cells per treatment group.

Animals

Animal studies were performed in accordance with the guidelines established by the Institutional Animal Care and Use Committee (IACUC) of the University of California, Irvine. All the animal data were generated using female athymic nude rats (Cr:NIH-RNU, Charles River Laboratories). Experiments were approved by IACUC and conformed to NIH guidelines.

Ovarian Cancer Xenograft Model

Forty Cr:NIH-RNU female rats (16 weeks) were inoculated, i.p. and s.q. with SKOV3.ip1 cells. $10x10^6$ SKOV3.ip1 cells suspended in 0.5 mL of RPMI 1640 medium with 10% FBS were injected in the left lower peritoneal quadrant, and subcutaneously in the right flank using a 25-gauge needle. An additional ten rats served as no-tumor controls and were injected i.p. and s.q. with 0.5 ml of RPMI 1640 medium with 10% FBS. Abdominal circumference, s.q. tumor volume, and body weight were measured weekly. A 10 million tumor cell inoculum was determined by previous reports of ovarian cancer models in nude rats to show tumor spread, uptake rate using other cell lines[162,163]. Survival was calculated from the day SKOV3.ip1 cells were implanted to the day when animals were euthanized as established by endpoint criteria under IACUC guidelines (s.q. tumors reached 3.5 cm in diameter, weight loss greater than 20% was detected, emaciation). To our knowledge, ours is the first study to develop an ovarian cancer xenograft model in nude rats using the SKOV3.ip1 cell line.

Drug Treatments

A total of forty adult female NIH:Cr-RNU rats weighing 180-230 g served as subjects. Rats were randomized to experimental groups. On days of CDDP administration, NAC was given 10 h after CDDP injection. The rats were divided into five groups: no tumor saline-treated controls (NT+VEH, n = 10), tumor saline-treated controls (VEH, n = 10), tumor cisplatin-treated (CDDP, n = 10), and tumor cisplatin + N-acetylcysteine-treated (CDDP + NAC, n = 10). Rats received 5 mg/kg CDDP (Teva Pharmaceuticals, USA, Inc.) or saline i.p. injection once every two weeks, for a total of

four cycles. NAC (Cumberland Pharmaceuticals, 250 mg/kg, i.p.) was administered for five days starting two days before each CDDP administration and ending two days after the last dose of CDDP. Mannitol (APP Pharmaceuticals, 125 mg/kg, i.p.) was administered to all animals 1 h prior to CDDP, to minimize renal toxicity and increase diuresis.

Cognitive Testing

Cognitive testing was administered 6 weeks after the final and fourth CDDP or saline injection. The experiment was repeated twice, and data from both experiments were combined and shown in the results section. All behavioral analysis was conducted by an experimenter blinded to the treatment group of the rats.

Novel Object Recognition

Rats were placed in an open Plexiglas box arena (60 x 60 cm) with 60 cm high walls containing two identical objects. Each rat explored the arena for 5 min per day for two consecutive days. The 5 min test trial was given 24 h later, during which the rat was presented with one of the familiar objects paired with a novel object. Total exploration time, time spent exploring each object, and the discrimination ratio (time spent exploring the novel object / total exploration time) were quantified.

Glutathione measurements in whole blood lysate

Whole blood was collected by cardiac puncture in rats under deep terminal anesthesia. Whole blood was diluted 1:5 in 5% (w/v) MPA. Samples were placed on ice

for 15 minutes, then centrifuged at 12,000 rpm for 15 minutes at 4°C. The upernatant was collected and stored at -80°C. Cayman Chemical Glutathione Assay Kit (No. 703002) was used to measure total GSH and oxidized glutathione (GSSG), and samples were processed according to the manufacturer's protocol[164]. For total GSH determination, 10 µl of samples were incubated with 25 µl of 4M triethanolamine in 465 µl of GSH MES Buffer. For GSSG measurement, 1:100 of 1M 1-vinylpyridine was added to the GSSG standards and to a 200 µl aliquot of the samples processed for total GSH measurement. Samples and standards containing 2-vinylypridine were incubated at room temperature for 1 h. Reduced GSH (GSH) was calculated by subtracting the values from total GSH-GSSG. GSH:GSSG ratio was calculated by: reduced GSH / GSSG[165].

Systematic Analysis and Statistical Considerations

Graphs and statistical analyses were prepared using GraphPad Prism 5.0 Software (GraphPad Software, La Jolla, CA, USA). Results were expressed as mean ± SEM. Comparison between control and treatment cohorts were made by unpaired Student's *t*-test, one-way ANOVA, or two-way repeated measures (RM) ANOVA. Statistical significance levels were set at 0.05. *Post hoc* analysis was made by Bonferroni correction. All imaging and quantification were performed blinded to experimental conditions. Figure 4.3. schematic was created with BioRender.com.

4.3. Results

4.3.1. Delay in N-acetylcysteine administration following cisplatin exposure does not

interfere with cytotoxic activity against ovarian cancer cells while protecting NSC viability

We had shown previously that NAC administration 30 minutes following CDDP treatment in cultured hippocampal neurons and NSCs prevented free radical production, reduced apoptotic cell death, and dendritic spine loss[38]. Others have shown that NAC protection against CDDP-induced cell death is time-dependent in human cancer cell lines[166] and rodent tumor models. To determine the optimal timepoint at which NAC could be administered after CDDP and not affect CDDP anti-cancer activity while preserving its neuroprotective effects in neural cells we conducted a cell viability time-course study. Two ovarian cancer cell lines SKOV3.ip1 and OVCAR8 were treated with CDDP, and NAC was added 30 min, 4 h, 8 h, and 10 h after CDDP administration (**Figure 4.1A**). At 10 µM, CDDP reduced SKOV3.ip1 and OVCAR8 cell viability to 36.8% ± 0.8% and 40.4% ± 2.4%, respectively following 72 h exposure. NAC prevented CDDP-induced cell death when added 30 min after CDDP treatment. When NAC was delayed by 10 h after CDDP, SKOV3.ip1 and OVCAR8 cell viability decreased to 38.7% ± 1.2% and 45.9 % ± 3.2% respectively, not significantly different than CDDP treatment alone.

We next examined the effect of delayed NAC administration on NSCs following CDDP treatment. At 2 µM, CDDP reduced NSC viability to 58.8% ± 0.5%, and at a higher dose of 6 µM CDDP, NSC viability was reduced to 39.8% ± 0.3% (**Figure 4.1B**). Delaying NAC administration by 10 h exerted a protective effect in NSCs at both CDDP doses. NSC viability at low dose 2 µM CDDP was 74.6% ± 1.1% and at 6 µM CDDP was 42.8% ± 0 .2%, following a 10 h delay NAC administration (p <0.0001).

4.3.2. Delayed N-acetylcysteine administration prevents cisplatin-induced PSD95 loss and cleaved caspase-9 expression in cultured hippocampal neurons

To examine the effect of delayed NAC administration in CDDP-treated hippocampal neurons, we first quantified PSD95 puncta. Two-way RM ANOVA showed that 1 µM CDDP reduced PSD95 puncta as compared with controls ($F_{(3,80)}$ = 5.812, p = *0.005)* (**Figure 4.1C,D**). CDDP-treated neurons that received 10 h delayed NAC had more PSD95-immunolabeled puncta compared to those treated with CDDP alone (p= 0.022) and was comparable to control PSD95 density (p =*0.37)*. These data suggested that a 10 h delay in NAC addition can prevent CDDP-induced neural damage without interfering with CDDP's anti-cancer killing effect *in-vitro.*

Next, we quantified cleaved caspase-9 expression in hippocampal neurons 48 h after 1 µM CDDP exposure with or without 10 h delayed NAC (**Figure 4.1E,F**). Cleaved caspase-9 expression was quantified by fluorescence microscopy as a measure of apoptosis. CDDP increased active caspase-9 expression compared to control (p =0.0098), which was prevented by the addition of NAC 10 h post CDDP ($F_{(3,7)}$ = 13.01, p = 0.0030).

4.3.3. Delayed N-acetylcysteine prevents cisplatin-induced glutathione depletion in cultured NSCs and hippocampal neurons

Glutathione (GSH) is the most abundant intracellular antioxidant, it plays a critical role in protecting the brain from oxidative stress, acting as a scavenger of reactive oxygen species[164]. Oxidative stress generated by mitochondrial dysfunction has been associated with depletion of glutathione in animal models of cisplatin-induced renal toxicity[167,168] and peripheral neuropathy[169]. NAC is a thiol and a precursor of L-cysteine, which is the rate-limiting substrate in glutathione production (**Figure 4.2A**). Neurons require GSH to sustain dendritic integrity; decreases in brain GSH levels are associated with cognitive

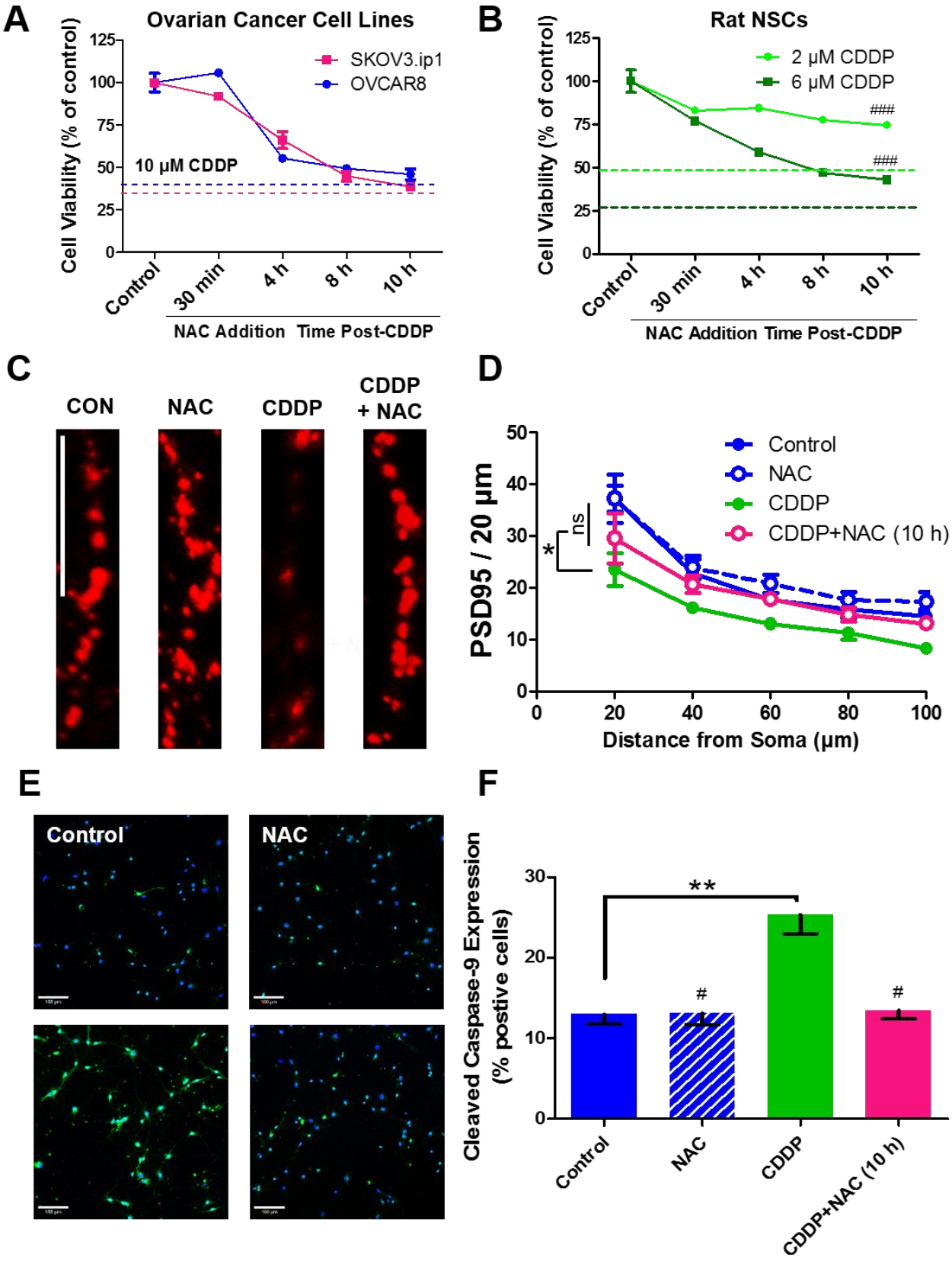
A
Ovarian Cancer Cell Lines
Cell Viability (% of control)
SKOV3.ip1
OVCAR8
10 μM CDDP
Control
30 min
4 h
8 h
10 h
NAC Addition Time Post-CDDP
B
Rat NSCs
2 μM CDDP
6 μM CDDP
###
###
C
CON
NAC
CDDP
CDDP + NAC
D
PSD95 / 20 μm
Control
NAC
CDDP
CDDP+NAC (10 h)
ns
*
Distance from Soma (μm)
E
Control
NAC
F
Cleaved Caspase-9 Expression (% postive cells)
**
#
#
Control
NAC
CDDP
CDDP+NAC (10 h)

Figure 4.1. *In-vitro,* 10 h delayed NAC administration following CDDP reduces CDDP-induced NSC death, PSD95 puncta loss, and hippocampal neuron apoptosis without reducing its anti-cancer efficacy.

(**A**) Human ovarian cancer cell lines SKOV3.ip1 and OVCAR8, were exposed to 10 µM CDDP with or without the addition of 5 mM NAC, at the indicated times. (**B**) Rat NSCs were exposed to 2 µM or 6 µM CDDP, with or without the addition of 5 mM NAC, at the indicated times. Cell viability was determined 72 h after CDDP addition by XTT assay. ### $p < 0.0001$ denotes difference between CDDP and CDDP+NAC (10 h). (**C**) representative images and (**D**) graph of dendrites immuno-labeled for PSD95 depicting reduction in PSD95 puncta density after exposure to 1 µM CDDP. 10 h delayed 2.5 mM NAC administration prevented CDDP-induced reduction in PSD95 density. Scale bars, 20 µm. (**E**) representative images and (**F**) quantification of caspase-9 activation in hippocampal neurons following 1 µM CDDP treatment with or without 2.5 mM NAC. 10 h delayed NAC administration prevented CDDP-induced caspase-9 activation. Cleaved caspase-9 expression was assessed 48 h after CDDP treatment. Scale bars, 100 µm. Blue, DAPI; green, caspase-9; red, PSD95. Graphs represent mean ± SEM of three sister coverslips per treatment. * $p < 0.05$, ** $p < 0.01$.

decline in aging and neurodegenerative disorders[170]; therefore we sought to examine the effect of CDDP on NSC and neuronal GSH levels. CDDP significantly depleted total GSH levels in NSCs, which was restored by delayed NAC administration ($F_{(3,8)}$ = 190.1, p < 0.0001) (**Figure 4.2B**). Total GSH levels in hippocampal neurons were mildly decreased by CDDP, although delayed NAC administration significantly increased total GSH levels compared to CDDP alone ($F_{(3,8)}$ = 21.43, p = 0.0004). Total GSH levels in hippocampal neurons are over 6-fold lower in comparison to NSCs, suggesting that differences in the abundance of GSH may influence the response of these two cell types to oxidative stress, which is may be associated with the sensitivity of neurons to lower doses of CDDP compared to NSCs.

4.3.4. Delayed N-acetylcysteine administration during chronic cisplatin treatment does not promote tumor growth

To examine the effects of CDDP on cognition and the potential for NAC to ameliorate CDDP-induced deficits in a clinically relevant animal model of CRCI[171], we developed an ovarian cancer xenograft rat model (**Suppl. Figure 4.1**) Cr:NIH-RNU female rats were injected with the human ovarian cancer cell line SKOV3.ip1, 10 x 10^6 cells intraperitoneal into the lower-left peritoneal quadrant, and 10 x 10^6 cells subcutaneously into the right flank. Subcutaneous tumors were measurable by 10 days post-implantation. Abdominal inspection at the time of necropsy, 28 days post-implantation, revealed nodules on the peritoneum, omentum, and bowel, which is phenotypically representative of ovarian cancer in humans (**Suppl. Figure 4.1**)[162,163].

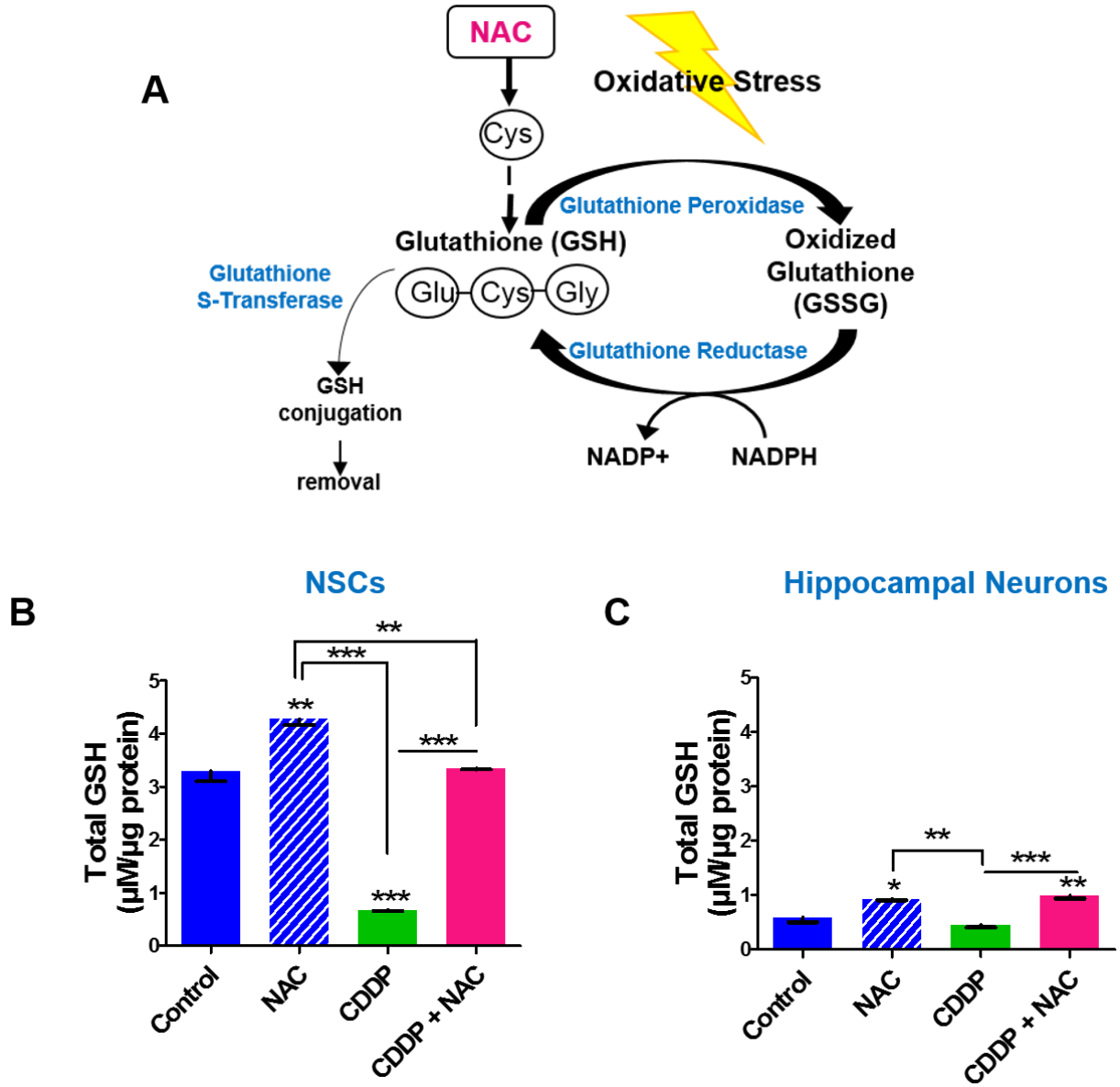

Figure 4.2. *In-vitro*, CDDP depletes total GSH levels in NSCs and hippocampal neurons. NAC prevents CDDP-induced GSH loss.

(**A**) Simplified schematic representation of the GSH pathway. GSH is synthesized from three amino acids: glutamate, cysteine, and glycine. NAC is a precursor of cysteine, which is the main factor limiting GSH synthesis. Upon exposure to pro-oxidants such as reactive oxygen species, GSH is oxidized to form oxidized GSH disulfide (GSSG), which is catalyzed by Glutathione peroxidase. GSSG is reduced to GSH by the enzyme glutathione reductase, which requires NADPH. This then regenerates GSH for cellular antioxidant defense. (**B**) 6 µM CDDP significantly reduced total GSH levels in NSCs. 10 h delayed 5 mM NAC administration following CDDP, prevented GSH depletion. (**C**) Delayed 2.5 mM NAC addition following 1 µM CDDP exposure prevented GSH depletion. GSH levels were assessed 48 h after addition of NAC and were normalized to protein concentration. Graphs represent mean ± SEM of three sister coverslips per treatment. * $p < 0.05$, ** $p < 0.01$, *** $p < 0.001$.

Seventeen days after tumor cell implantation, rats received one CDDP injection (5 mg/kg, i.p.) or saline of equal volume, every two weeks, for a total of four doses. NAC (250 mg/kg, i.p.) or saline of equal volume, was administered for five days starting two days before each CDDP cycle and ending two days after the last dose of CDDP. On days of CDDP administration, NAC was given ten hours after CDDP (**Figure 4.3A**). Weekly measurements of subcutaneous tumor volume were taken using Vernier calipers, and abdominal girth (cm), which is indicative of ascites were also measured. CDDP significantly decreased tumor growth as compared to the VEH group ($p = 0.022$). Delayed 10 h NAC administration following CDDP did not affect tumor growth. Tumor volume in the CDDP+NAC group was significantly lower than the VEH group ($p = 0.029$) and did not differ from CDDP alone ($p = 0.46$) (**Figure 4.3B**). At day 37 post-tumor implantation, the tumors (s.q.) in four of the rats in the VEH group reached 3.5 cm in diameter and were euthanized as established by IACUC endpoint criteria. Abdominal circumference (cm) did not differ between any of the groups, which suggests that our tumor-model does not develop ascites (data not shown).

4.3.5. Delayed N-acetylcysteine prevents cisplatin-induced cognitive impairments

Cognitive performance using the novel object recognition (NOR) task was assessed six weeks after the last dose of cisplatin (**Figure 4.3C**). While the non-tumorigenic control group, NT+VEH, spent significantly more time exploring the novel object compared to the familiar object ($p = 0.0059$), we found that the tumorigenic control group, VEH performed poorly in NOR, as it failed to discriminate between both objects ($p = 0.74$). The CDDP group showed no preference in exploring either object ($p = 0.44$), whereas delayed NAC administration in the CDDP+NAC group prevented the CDDP-

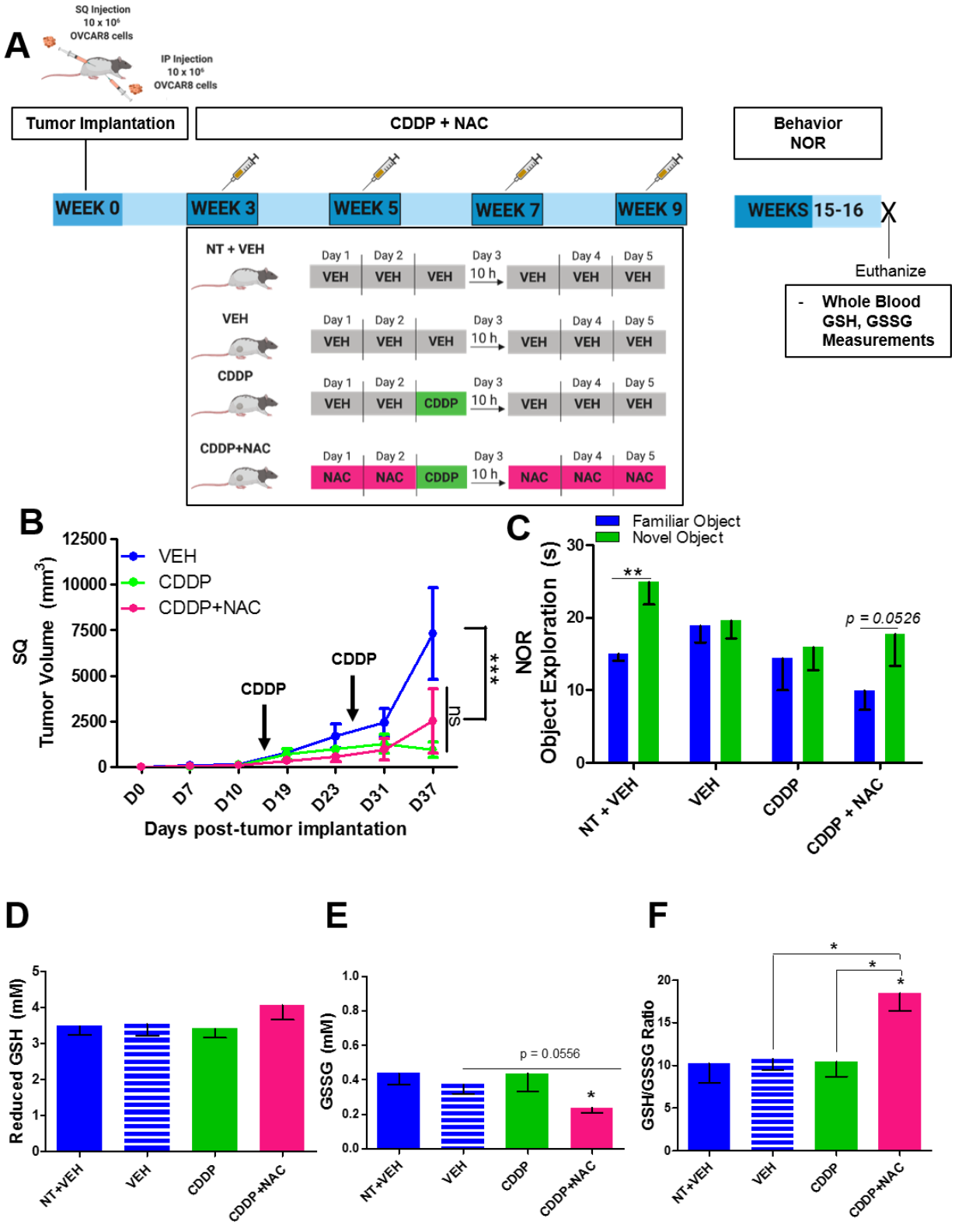
A
SQ Injection
10 x 10⁶
OVCAR8 cells
IP Injection
10 x 10⁶
OVCAR8 cells
Tumor Implantation
CDDP + NAC
Behavior
NOR
WEEK 0
WEEK 3
WEEK 5
WEEK 7
WEEK 9
WEEKS 15-16
Euthanize
- Whole Blood GSH, GSSG Measurements
NT + VEH
VEH
CDDP
CDDP+NAC
Day 1
Day 2
Day 3
Day 4
Day 5
10 h
VEH
CDDP
NAC
B
SQ Tumor Volume (mm³)
VEH
CDDP
CDDP+NAC
CDDP
CDDP
***
ns
D0
D7
D10
D19
D23
D31
D37
Days post-tumor implantation
C
Familiar Object
Novel Object
NOR Object Exploration (s)
**
p = 0.0526
NT + VEH
VEH
CDDP
CDDP + NAC
D
Reduced GSH (mM)
NT+VEH
VEH
CDDP
CDDP+NAC
E
GSSG (mM)
p = 0.0556
*
NT+VEH
VEH
CDDP
CDDP+NAC
F
GSH/GSSG Ratio
*
*
*
NT+VEH
VEH
CDDP
CDDP+NAC

Figure 4.3. Delayed NAC reduces CDDP associated impairments in object recognition, increases GSH/GSSG ratio in whole blood, while not enhancing tumor growth in an ovarian cancer rat model of CRCI.
(**A**) Study timeline. Cr:NIH-RNU female rats were implanted with 10 x 10^6 SKOV3.ip cells i.p. and s.q. Rats received one CDDP (5 mg/kg, i.p.) injection every two weeks, for eight weeks with or without NAC (250 mg/kg, i.p.), starting three weeks after tumor implantation. NAC was administered for five days starting two days before each CDDP cycle and ending two days after the last dose of CDDP. On days of CDDP administration, NAC was given ten hours after CDDP. Cognitive performance was assessed six weeks after the last CDDP injection via the NOR task. (**B**) Subcutaneous tumor volume was measured weekly in tumor-bearing rats. NT+VEH: n = 5, VEH: n = 6, CDDP: n = 5, CDDP+NAC: n = 5. (**C**) The VEH and CDDP-treated rats had diminished ability to discriminate between the familiar object and novel object on the NOR task. NAC administration prevented the CDDP-induced deficit on the NOR task (**D**) Reduced GSH (**E**) GSSG (**F**) GSH/GSSG Ratio measured in whole blood following NOR completion. Graphs represent mean ± SEM. * $p < 0.05$, ** $p < 0.01$, ** $p < 0.001$, ns = not significant. NT+VEH: n = 10, VEH: n = 6, CDDP: n = 7, CDDP+NAC: n = 6.

induced deficit, as this group showed a preference for the novel object (p = 0.052*)*. An interpretation of these results is that tumor development can independently contribute to cognitive impairments, which is consistent with the findings in other preclinical models[172]. Delayed NAC can be safely administered in our tumor model without interfering with CDDP's anti-tumor efficacy, and it prevents CDDP-induced impairments in the NOR task.

4.3.6. Delayed N-acetylcysteine reduces oxidized GSGG levels in whole blood

Next, we examined GSH levels (reduced GSH, and oxidized GSSG, GSH/GSSG ratio) in whole blood, seven weeks after CDDP completion (**Figure 4.3D-F**). We found no difference in reduced GSH levels in any of the groups, however delayed NAC administration following CDDP significantly decreased levels of oxidized GSSG in the tumor-bearing rats compared to the non-tumorigenic vehicle-treated group (p = 0.0175) (**Figure 4.3E**). Under normal conditions, reduced GSH constitutes 98% of the total GSH pool, with a 10:1 ratio of GSH-to-GSSG. GSH/GSSG ratio is used as a marker of antioxidant capacity and under conditions of oxidative stress, this ratio decreases[164]. We found no significant difference in the GSH/GSSG ratio in either the VEH or CDDP group compared to the NT+VEH group seven weeks after treatment completion. Interestingly, the CDDP+NAC group had a higher GSH/GSSG ratio compared to the other groups ($F_{(3,30)}$ = 4.426, p = 0.0108) seven weeks after treatment, suggesting that NAC had long-lasting effects in enhancing antioxidant capacity. Administration of CDDP in a lymphoma mouse model decreased total GSH levels in blood within 48 h after treatment; additionally, tumor-bearing mice had lower GSH blood levels compared to non-tumor bearing controls, suggesting that tumor growth and CDDP may reduce antioxidant capacity[173]. It is

plausible that CDDP may alter the GSH/GSSG ratio in the tumor-bearing rats in our study and at the time of analysis, seven weeks after CDDP completion the GSH levels were restored; however, GSH analysis at earlier time points following CDDP administration are needed.

4.3.7. Delayed N-acetylcysteine administration following cisplatin does not alter survival of tumor-bearing rats

Sixty percent of tumor-bearing rats in the VEH group underwent euthanasia between 23 and 37 days after tumor cell implantation (average survival 37 days) in accordance with IACUC guidelines (**Figure 4.4**). Deaths in the CDDP and CDDP+NAC group between 23 and 37 days after treatment were associated with toxicities following the first CDDP dose, not related to tumor growth. The rats that were treated with CDDP or CDDP+NAC survived significantly longer than the VEH group ($p = 0.041$, log-rank test), and surviving subjects were euthanized 120 days post-tumor implantation following behavioral testing completion. Delayed NAC (10 h) administration following CDDP did not reduce survival compared to CDDP administration alone.

2.4. Discussion

In this study, we show that NAC may be used to prevent CDDP-induced CRCI without affecting CDDP's anti-tumor efficacy using a delayed administration strategy. Concerns about NAC's ability to interfere with the efficacy of chemotherapeutic agents have hindered its concurrent use during chemotherapy regimens as a potential

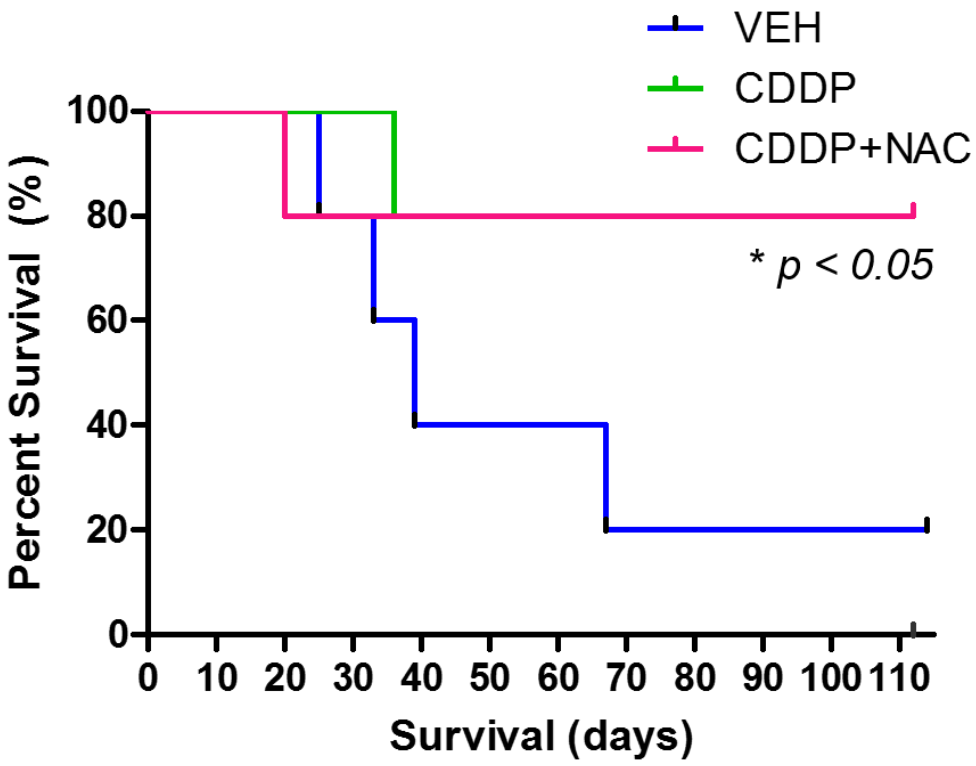

Figure 4.4. Delayed NAC administration following CDDP did not affect survival in an ovarian cancer xenograft model.
Kaplan-Meier survival probability plot of tumor-bearing mice in VEH, CDDP, or CDDP+NAC treatment groups. VEH: n = 6, CDDP: n = 5, CDDP: n = 5. The log-rank method was used to test for a difference in survival between groups.

therapeutic agent to treat sequelae associated with CDDP, including ototoxicity and peripheral neuropathy. There are various mechanisms by which NAC exerts its antioxidant activity. NAC acts as a source of L-cysteine for increased GSH biosynthesis in conditions of severe GSH depletion (for ex. hepatotoxicity associated with acetaminophen overdose)[174]. NAC scavenges oxidants directly through its thiol group. Direct binding of the thiol group on NAC to platinum (Pt), may inactivate CDDP intracellularly, by preventing binding of the Pt to DNA bases[175]. Recent studies have shined light on a novel mechanism that may also contribute to the potent antioxidative property of NAC – intracellularly, NAC is converted to mitochondrial sulfane sulfur species which are more reactive towards oxidants than thiols[176].

We and others have shown that the addition of NAC to CDDP-treated human cancer cell lines loses its protective effect on cell viability when administered in a dose-delayed manner[166]. Here, we found that a 10 h delay in NAC addition following CDDP-treatment in two ovarian cancer cell lines had no significant difference in cell viability compared to CDDP-treatment alone. While the same 10 h delay, reduced NSC death, prevented cleaved-caspase-9 expression and dendritic spine loss in hippocampal neurons *in-vitro*. Additionally, CDDP decreased GSH levels in NSCs and hippocampal neurons, which were restored by the addition of NAC. Mechanistically, delayed NAC administration may maintain cisplatin's DNA-platinum crosslinking activity in rapidly dividing cancer cells, but provide protection against oxidative stress in less rapidly dividing cells such as NSCs, and post-mitotic cells such as neurons[88].

We had previously shown that NAC administration during chronic CDDP treatment prevented cognitive impairments in young adult Sprague Dawley rats[38]. To assess the

effects of NAC on a tumor-bearing model of CRCI that would be consistent with our previous studies using rats, we developed an ovarian cancer xenograft model in athymic female nude rats. The human SKOV3.ip1 cell line was implanted subcutaneously and intraperitoneal at a density of 10 x 10^6 cells per site. SKOV3.ip1 tumor-bearing rats developed quantifiable subcutaneous tumors within 10 days post-implantation, and pathological examination 28 days post-engraftment revealed peritoneal tumors, consistent phenotypically with human ovarian cancer. Ovarian neoplasms commonly metastasize, disseminating throughout the peritoneal cavity[162,163].

Subcutaneous implantation of SKOV3.ip1 allowed us to reliably measure tumor growth and treatment response in our model. Intraperitoneal implantation of SKOV3.ip1 was chosen to accurately depict *in-vivo* ovarian cancer dissemination and its contributions to CRCI, however the disadvantage being that monitoring intraperitoneal ovarian cancer progression noninvasively requires the use of fluorescence tomography and would necessitate putting the rats under isoflurane anesthesia, which is associated with cognitive impairments[177] and may introduce variables in our behavioral studies. Since our initial aim was to assess whether delayed NAC ameliorated CDDP-induced deficits in an ovarian tumor-bearing model, for this pilot study we opted to implant SKOV3.ip1 at two sites. Based on our findings in this study, we will refine our model and experimental design so that we can assess the effects of delayed NAC administration following CDDP on intraperitoneal tumor growth in our model using fluorescence tomography - in a rat cohort that will not undergo neurocognitive testing.

Delayed NAC prevented CDDP-associated impairments in the novel object recognition task. Tumor-bearing rats treated with CDDP failed to discriminate between

the novel and familiar objects during the NOR task. Interestingly, tumor-bearing rats that did not receive CDDP (VEH group) also exhibited impairments in the NOR task. These results are consistent with clinical reports that cancer patients exhibit cognitive impairments at the time of diagnosis, prior to receiving treatment[171,178,179]. Winocur et al. also observed cognitive deficits in tumor-bearing mice that had not received chemotherapy using FVB/N-TG (MMTV-*neu*) 202 Mul/J mice, a transgenic breast cancer model[172]. These results suggest that cancer, independently of chemotherapy, contributes to cognitive impairment. Additional studies to examine if the observed cognitive impairments correlate with structural changes in the brain, and/or cytokine dysregulation in this tumor-bearing model of CRCI will provide new insight into other variables that influence CRCI in cancer patients. Delayed NAC administration following CDDP did not enhance tumor growth compared to CDDP treatment alone, nor did it reduce survival. Therefore, our study supports the use of delayed NAC administration as a preventative therapy for CDDP-induced CRCI.

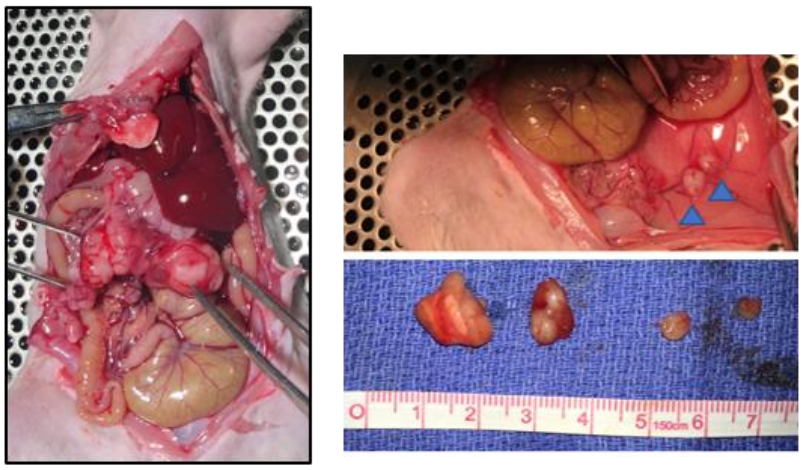

Supplementary Figure 4.1. SKOV3.ip1 tumor-bearing rats develop intraperitoneal tumors.
Representative images of intraperitoneal tumors in Cr:NIH-RNU female rats injected with 10 x 10^6 SKOV3.ip cells i.p., 28 days post-engraftment.

CHAPTER 5

Mitochondrial-associated Impairments of Temozolomide on Neural Stem/Progenitor Cells and Hippocampal Neurons

Abstract

Primary brain tumor patients often experience neurological, cognitive, and depressive symptoms that profoundly affect quality of life. The DNA alkylating agent, temozolomide (TMZ), along with radiation therapy, forms the standard of care for glioblastoma (GBM) - the most common and aggressive of all brain cancers. Numerous studies have reported that TMZ disrupts hippocampal neurogenesis and causes spatial learning deficits in rodents; however, the effect of TMZ on mature hippocampal neurons has not been addressed. In this study, we examined the mitochondrial-mediated mechanisms involving TMZ-induced neural damage in primary rat neural stem/progenitor cells (NSCs) and hippocampal neurons. TMZ inhibited *mt*DNA replication and transcription of mitochondrial genes (ND1 and Cyt b) in NSCs within 2-4 h, whereas the effect of TMZ on neuronal *mt*DNA transcription was less pronounced. Transmission electron microscopy imaging revealed mitochondrial degradation in TMZ-treated NSCs. Acute TMZ exposure (4 h) caused a rapid reduction in dendritic branching and loss of postsynaptic density-95 (PSD95) puncta on dendrites. More prolonged TMZ exposure impaired mitochondrial respiratory activity, increased oxidative stress, and induced apoptosis in hippocampal neurons. The presented findings suggest that NSCs may be more vulnerable to TMZ than hippocampal neurons upon acute exposure; however long-term TMZ exposure results in neuronal mitochondrial dysfunction and dendritic damage, which may be associated with delayed cognitive impairments.

5.1. Introduction

Chemotherapy-related cognitive impairments (CRCI) have been described for various chemotherapeutic agents in patients with CNS (central nervous system) and non-CNS tumors[171,180]. Primary brain tumor patients often experience neurological, cognitive, and depressive symptoms. A meta-analysis of depression in cancer patients revealed that with a prevalence rate of 28%, brain cancer is the subtype most strongly associated with depression[181]. The majority (85%) of patients experience neurological complications, although, for over 30% of long-term GBM survivors, the cognitive impairments persist throughout life[182,183]. The effect of chemotherapy on cognitive sequelae in brain tumor patients is difficult to assess in this patient population due to tumor-specific factors that alter neurocognitive function, such as the tumor location. Additionally, age, genetic background, treatment related-factors such as cranial radiation, surgical resection, adjuvant treatment, duration, and dosing further contribute to the impairment of neurocognitive function[184, 185].

Cranial radiation therapy (RT) for treatment of CNS tumors has been widely shown to suppress long-term potentiation (LTP) in the dentate gyrus of the hippocampus[186], deplete neural stem progenitor/cells (NSCs) and neurons, and provoke morphological damage to surviving neurons[187], which can result in progressive cognitive impairment[188,189]. The DNA alkylating agent Temozolomide (TMZ), along with RT forms the standard of care for GBM following tumor resection. GBM is the most common and aggressive of all high-grade gliomas, accounting for approximately 80% of all malignant primary brain tumors[190]. TMZ targets nuclear DNA (*n*DNA) and generates *n*DNA adducts that induce cell cycle arrest and cell death by apoptosis. Also, it alters *mt*DNA and

respiratory function in glioma[191,192]. However, its effect on NSCs and non-proliferating neural cells such as neurons is not clear.

Reports of TMZ-induced neural toxicity have primarily focused on the loss of neural NSCs in the rodent hippocampus. TMZ is used as an experimental tool to deplete adult neurogenesis; these studies have found its application to be associated with depression[193], anxiety[194], and impaired spatial and contextual discrimination in mice[195,196]. To date, no studies have investigated changes in hippocampal neuronal integrity or neural mitochondrial function after TMZ exposure. NSCs, hippocampal neurons and the excitatory synapses they carry, play a critical role in hippocampal processes including learning and memory[197,198]; therefore it is plausible that neuronal damage may also contribute to the observed deficits following TMZ exposure.

Mitochondrial dysfunction, elevated oxidative stress, and dendritic spine remodeling are hallmarks of neuronal toxicity in a variety of neurodegenerative disorders[52,199,200]. The brain is highly susceptible to oxidative stress as it has a high metabolic demand and low antioxidant capacity compared to other organs[201]. Neuronal dynamic process such as synaptic plasticity, neurotransmission, and membrane ion gradients are highly dependent upon ATP generated by the mitochondrial electron transport chain (ETC)[202]. Mitochondrial respiratory dysfunction and oxidative stress are associated with chemotherapy-related cognitive impairments provoked by various chemotherapeutic agents such as cisplatin[38,64], cyclophosphamide[32,203], doxorubicin[204,205], and methotrexate[206]. Given the known effects of TMZ on mitochondrial function in glioma[191,192] and its association with depression and NSC depletion[60,193], we hypothesized that TMZ induces hippocampal mitochondrial dysfunction and oxidative

stress. We examined the *in-vitro* effects of TMZ on mitochondrial DNA integrity and transcription in NSCs and neurons. Additionally, we examined the effects of TMZ on neuronal mitochondrial respiratory function, oxidative stress, and resulting changes in neuronal morphology and survival.

5.2. Materials and Methods

Standard protocol approvals

All experiments conformed to National Institutes of Health guidelines. Hippocampal neuron and NSC cell cultures were generated using Sprague Dawley rats (Charles River Laboratories) following the guidelines established by the Institutional Animal Care and Use Committee of the University of California, Irvine (UCI). Institutional Review Board (IRB) approval was obtained at the UCI Medical Center and Children's Hospital of Orange County (CHOC) for the isolation and expansion of human-derived NSCs (SC27)[207].

Dissociated hippocampal neuron and NSC cultures

Dissociated hippocampal neuron cultures were prepared from Sprague Dawley pups on postnatal day 0 (P0) of either sex as described previously[59]. Cultures were seeded at a density of 400-600 cells/mm^2 on 12 mm coverslips (Thermo Scientific) pre-coated with 0.2 mg/ml poly-D-lysine (Sigma) and initially maintained in Neurobasal Medium (NBM) with B-27 (Invitrogen) at 37°C and 5% CO_2. On the third day *in-vitro* (3 DIV), cultures were treated with 5 µM arabinoside-cytosine (Sigma) to inhibit glial proliferation and refreshed biweekly with conditioned media (NBM preconditioned for 24

h over 1- to 3-week-old glia cell cultures). Neurons were used for experiments on 17-24 days *in-vitro* (17-21 DIV).

Rat NSCs were isolated from the hippocampi of embryonic day 19 (E19) Sprague Dawley pups and cultured as described[59]. The cells were plated onto T25 flasks pre-coated with 20 µg/ml fibronectin (Invitrogen) and maintained in Knockout™ DMEM/F-12 with 2 mM GlutaMAX-I Supplement, 20 ng/mL bFGF, 20 ng/mL EGF, and 2% StemPro® Neural supplement (Gibco). Passage 6-10 NSCs were used for experiments. Human NSCs (SC27) were derived from brains of premature neonates and cultured as previously described[207]. SC27 cells were cultured on 10 µg/ml fibronectin coated T75 flasks in DMEM/Ham's F-12 medium (Gene Clone), containing 1% BIT9500 (Stem Cell Technologies),10 µg/mL Gentamycin (MP Biomedicals), 10 µg/mL Ciprofloxacin (TEVA), 2.5 µg/ml Amphotericin B (Fisher Scientific), 100 µg/ml Pen/Strep (Gibco), 292 µg/mL L-glutamine (Gibco), 20 ng/mL bFGF, and 20 ng/mL EGF. SC27 cultures were passaged when confluent using Nonenzymatic Cell Dissociation Solution (Sigma Aldrich).

Temozolomide application in-vitro

In-vitro, TMZ (Sigma Aldrich) was made into a 100 mM stock solution by dissolving in DMSO (Sigma Aldrich). TMZ was diluted to a final concentration as specified in the figures in the respective culture medium of each cell type. The control group was exposed to an equal volume of DMSO at the same time-points.

Transmission Electron Microscopy (TEM)

In-vitro, SC27 (passage 9) cultures were treated with TMZ or DMSO of equal volume (control) for 48 h. The cells were washed with PBS, collected, and fixed for TEM in glutaraldehyde at room temperature. The samples were sent to the University of California, Irvine Pathology Services Core Facility for TEM processing and imaging.

MtDNA qPCR assay

The PCR assay was a modification of Santos et al., 2006[83]. Total DNA was purified from cell samples using the Qiagen Genomic Tip and Genomic DNA Buffer Set Kit (Qiagen, Valencia, CA, USA). For SC27 cells, a small mitochondrial fragment (221-bp) was amplified and standardized to a 13.5-kb fragment from the nuclear-encoded gene β-globin. A mitochondrial fragment (235-bp) was amplified and standardized to a 12.5-kb fragment from the nuclear-encoded gene, Clusterin (TRPM-2*)* in rat hippocampal neurons and NSCs. PCR products were normalized to control levels.

The sequences for human β-globin (13.5-kb) and *mt*DNA fragment (221-bp) primer sets:

β-globin forward 5′-CGAGTAAGAGACCATTGTGGCAG-3′

β-globin reverse 5′-GCACTGGCTTTAGGAGTTGGACT-3′

*mt*DNA fragment forward 5′-CCCCACAAACCCCATTACTAAACCCA-3’

*mt*DNA fragment reverse 5’-TTTCATCATGCGGAGATGTTGGA-3’.

The sequences for rat TRPM-2 (12.5-kb) and *mt*DNA fragment (235-bp) primer sets:

TRPM-2 forward 5′-AGACGGGTGAGACAGCTGCACCTTTTC-3′

TRPM-2 reverse 5′-CGAGAGCATCAAGTGCAGGCATTAGAG-3′

*mt*DNA fragment forward 5′-CCTCCCATTCATTATCGCCGCCCTTGC-3′

*mt*DNA fragment reverse 5′-GTCTGGGTCTCCTAGTAGGTCTGGGAA-3′.

Cell viability assay (MTT)

Rat NSCs were seeded in 96-well plates at a concentration of 10^4 cells/well. After 24 h post-seeding, the cells were incubated with 100 µM, 200 µM, or 500 µM TMZ. After 7 days, cell viability was measured by MTT assay (Roche). 20 µl of 5 mg/ml MTT tetrazolium salt dissolved in PBS, pH 7.4, was added to each well, and the plate was incubated for 5 h. The medium was aspirated from each well, and 200 µl of DMSO was added to each well to dissolve the insoluble formazan salts. Absorbance was measured at 570 nm using a BioRad 680 plate reader. Each treatment group contained 5 replicates, in 3 independent experiments. Cell viability was normalized to the control group.

Quantitative RT-PCR assay

The assay was performed as described previously[38]. Total RNA was extracted using RNeasy Mini Kit (Qiagen), and cDNA was generated using the iScript™ cDNA Synthesis Kit (Bio-Rad). The sequences for ND1 gene expression levels were normalized to those of 18S rRNA. The sequences for rat ND1 primer sets were: forward 5'-CACCCCCTTATCAACCTCAA-3'; reverse ATTTGTTTCTGCGAGGGTTG. Cyt b gene expression levels were normalized to those of 18S rRNA. The sequences for rat Cyt b and 18S rRNA primer sets were: Cyt b forward 5′-CGAAAATCTACCCCCTATT-3′, reverse 5′-GTGTTCTACTGGTTGGCCTC-3′; 18S rRNA forward 5′-

TCAATCTCGGGTGGCTGAACG-3′, reverse 5′-GGACCAGAGCGAAAGCATTTG-3′. All primers were ordered from IDT, Integrated Device Technology, Inc, Coralville, Iowa, USA.

Seahorse XF24 Cellular Bioenergetic Analysis

The Seahorse XF24 Extracellular Flux Analyzer (Agilent Technologies) was used to determine the bioenergetic profile of intact neurons[38]. Oxygen consumption rates (OCR) were measured in adherent hippocampal neurons using the Cell Mito Stress Kit (Agilent Technologies). Dissociated hippocampal neurons were plated at a density of 5 x 10^4 cells/well in 0.1 mg/ml poly-D-lysine coated XF24 cell culture microplates. Baseline rates were measured at 37°C three times before the sequential injection of oligomycin (2 µM), FCCP (1 µM), and rotenone (1 µM) plus antimycin A (1 µM). Basal OCR levels were determined by subtracting the non-mitochondrial respiration rate from the last rate measurement before the oligomycin injection. Maximum respiration was calculated by subtracting the non-mitochondrial respiration rate from the maximum rate measurement after FCCP injection. Three OCR measurements were taken after the addition of each inhibitor. All measurements were normalized to protein content per well using the DC protein assay (Bio-Rad). OCR data was collected using the Wave software (Agilent Technologies) and analyzed using the XF Cell Mito Stress Kit Report generator.

Immunocytochemistry (ICC)

The 24 well-plates containing the coverslips with cultured neurons were placed into ice slush. Neurons were fixed with ice-cold 4% paraformaldehyde (PFA, Fisher Scientific) in PBS, pH 7.4, for 12 min. The following antibodies were used: mouse anti-

PSD95 1:4000 (Thermo Fisher MA1-046) and rabbit anti-cleaved Caspase-9 (Cell Signaling 9507) 1:100. Anti-PSD95 was diluted in blocking buffer (3% bovine serum albumin, 0.1% Triton-X in PBS, pH 7.4) and anti-cleaved caspase-9 was diluted in blocking buffer (5% donkey serum and 0.3% Triton-X in PBS, pH 7.4) overnight at 4°C. The next day coverslips were washed with PBS and incubated in the appropriate secondary antibodies conjugated to Alexa Fluor 488 at 1:500 or Alexa Fluor 568 at 1:400 (Invitrogen) at room temperature for 1.5 h.

Image analysis of dendritic branches and spines

Dendritic spines were visualized by using ICC for PSD95, a reliable marker of mature synapses[82]. Dendritic branching was evaluated using Sholl analysis. Total dendritic length was measured, and the number of intersections between branches and the concentric circles at increasing 20 µm segments from the soma was quantified. For PSD95 quantification, each individual puncta was considered a separate spine, and counts were not adjusted for puncta size. PSD95 puncta density was quantified as the number of PSD95 puncta per 20 µm of dendrite length, comparing dendrites of the same order[59]. Severe dendritic injury such as beading was identified in the 500 µM TMZ (24 h) group which prevented analysis.

CellROX Oxidative Stress Quantification

Neurons plated on 12 mm coverslips were incubated in culture medium containing 5 µM CellROX Green Reagent (Life Technologies) for 20 min at 37°C and 5% CO_2 [38]. After incubation, cells were fixed as described above and washed with PBS before

mounting. Cells were processed for imaging with DAPI Fluoromount G (Southern Biotech) mounting medium. Confocal microscopy, Zeiss LSM700, was used to generate neuronal images. 10 µm z-series (2.5 µm steps) images were captured at 20X (NA 0.8) spanning across entire neurons. Relative fluorescence intensity of the CellROX green probe was quantified by ImageJ. The experiment was repeated twice, with similar results. Each experiment included 3 sister coverslips per treatment group. 5 images were analyzed per coverslip, for a total of 800-1200 cells per treatment group.

Terminal deoxynucleotidyl transferase-mediated biotinylated UTP nick end labeling (TUNEL assay)

The TUNEL assay was performed using the NeuroTACS™ *In Situ* Apoptosis Detection Kit (Trevigen, Inc. Gaithersburg MD). Following 12 minute fixation with 4% PFA in PBS, pH 7.4, neurons were incubated in NeuroPore™ for 2 h at 4°C. The assay was performed as described in the manufacturer's protocol. Neurons were imaged by light microscopy using an Olympus BX43 light microscope at 10X magnification.

Systematic analysis and statistical considerations

Each experiment included 2-3 replicates per treatment group. In the imaging experiments, neurons were sampled equally from each coverslip. For PSD95 puncta quantification, 4 dendrites from 2 separate neurons were sampled per coverslip for each treatment group. Images for PSD95 puncta analysis and Sholl analyses were generated using confocal microscopy, Zeiss LSM 510 (Oberkochen, Germany). 3 µm z-series (0.5 µm step) images were captured from distinct non-overlapping dendrites and extended at

least 100 µm from the soma at 63X (NA 1.4) using an oil-immersion objective. All imaging and quantification were performed blinded to experimental conditions. Analysis of all treatment groups was performed using two-way repeated-measures (RM)-ANOVA, followed by Bonferroni's *post-hoc* multiple comparisons test. Significance levels were set at 0.05, and data are presented as mean ± SEM. Data were analyzed using GraphPad Prism 5.0 Software.

5.3. Results

5.3.1. Temozolomide alters human NSC morphology in-vitro

NSCs (SC27) are sensitive to TMZ as single-dose treatment with 200 µM TMZ kills 50% of cells after 7 days. In contrast, this treatment has minimal effect on low-grade and high-grade derived glioma stem-like cells (GSCs)[60]. To investigate the effect of TMZ on mitochondria in NSCs, NSCs were exposed to 500 µM TMZ for 48 h, and morphology was examined by transmission electron microscopy (TEM) (**Figure 5.1**). Normal mitochondria were observed in the control (**Figure 5.1A, B**). After 48 h TMZ exposure, mitochondrial degradation and vacuolization were observed (**Figure 5.1C, D**).

5.3.2. Temozolomide inhibits mtDNA synthesis in NSCs

Temozolomide (TMZ) targets genomic DNA by its addition of methyl groups to purine residues. The most common lesions produced are methylation at the N^7 and O^6 sites on guanine, and O^3 on adenine[208]. We hypothesized that NSC *mt*DNA might be vulnerable to damage by TMZ due to its lack of histones and proximity to the ETC, which make it susceptible to oxidative damage. Also, *mt*DNA lesions may be less efficiently

repaired compared to those of *n*DNA due to the absence of the nucleotide excision repair pathway in mitochondria[209]. To explore the effect of TMZ on NSC mitochondria, we examined the effect of TMZ on SC27 *mt*DNA replication. To compare *mt*DNA integrity, a 13.4-kb *mt*DNA fragment from control and TMZ-treated SC27 cells was amplified by qPCR. The PCR products were resolved by agarose gel electrophoresis (**Figure 5.2A**). TMZ decreased the amount of full-length 13.4-kb mtDNA product amplified compared to control cells. We next used a quantitative PCR-based assay to compare the amplification of a *mt*DNA fragment to amplification of a *n*DNA fragment[38,83]. TMZ produced a preferential decrease in amplification of NSC *mt*DNA as compared with a nuclear gene (β-Globin) (**Figure 5.2B**). TMZ (200 μM) significantly reduced *mt*DNA amplification in SC27 cells to 62.6% ± 2.1%, 2 h post-treatment compared to control ($p < 0.0001$), which further decreased by 85.5% ± 2.4% 48 h post-treatment ($p < 0.001$).

Human NSCs (SC27) are sensitive to TMZ, and provide a relevant *in-vitro* model to examine the effects of chemotherapy on neural populations, however to compare the effect of TMZ on the hippocampus (NSCs and neurons), we sought to examine whether rat hippocampal NSC derived from the dentate gyrus (DG) would have comparable sensitivity to TMZ as human NSCs. Rat NSCs were exposed to clinically-relevant doses of TMZ for 7 days, and cell survival was as assessed by XTT assay. TMZ induced a dose-dependent decrease in cell viability (**Figure 5.2C**). The TMZ IC_{50} in rat NSCs is 366 μM, which is comparable to the IC50 (200 μM TMZ) in human NSCs, 7 days after TMZ exposure[60]. We continued our subsequent studies using cultured rat NSCs and hippocampal neurons, which we have used to examine the effects cisplatin in a rat

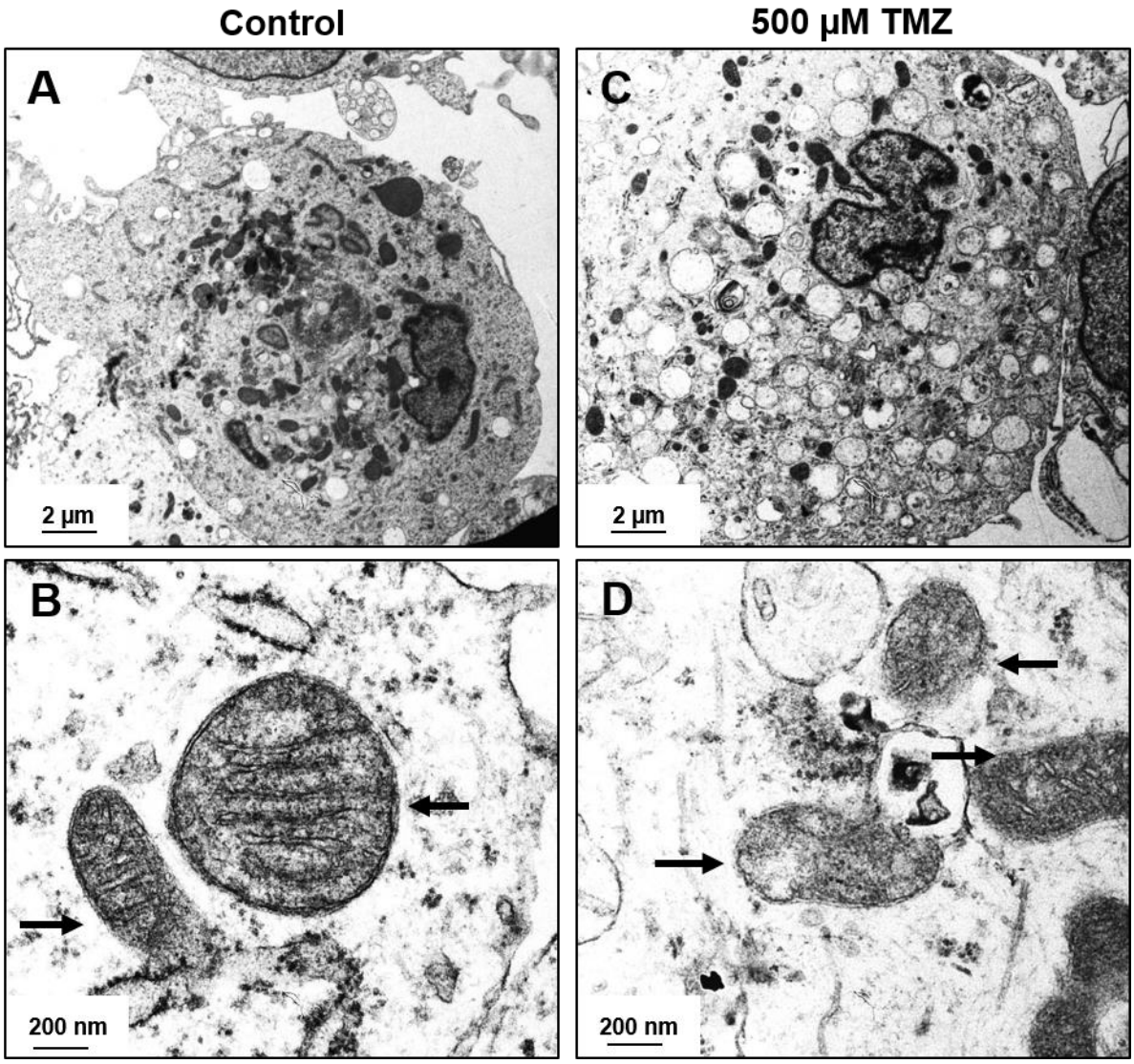

Figure 5.1. TMZ induced mitochondrial degradation in cultured NSCs.
(**A**) Transmission electron microscopy (TEM) of control SC27 cells showed (**B**) intact normal mitochondria (arrows). (**C**) SC27 treated with 500 µM TMZ showed (**D**) mitochondrial degradation (arrows) at 48 hours.

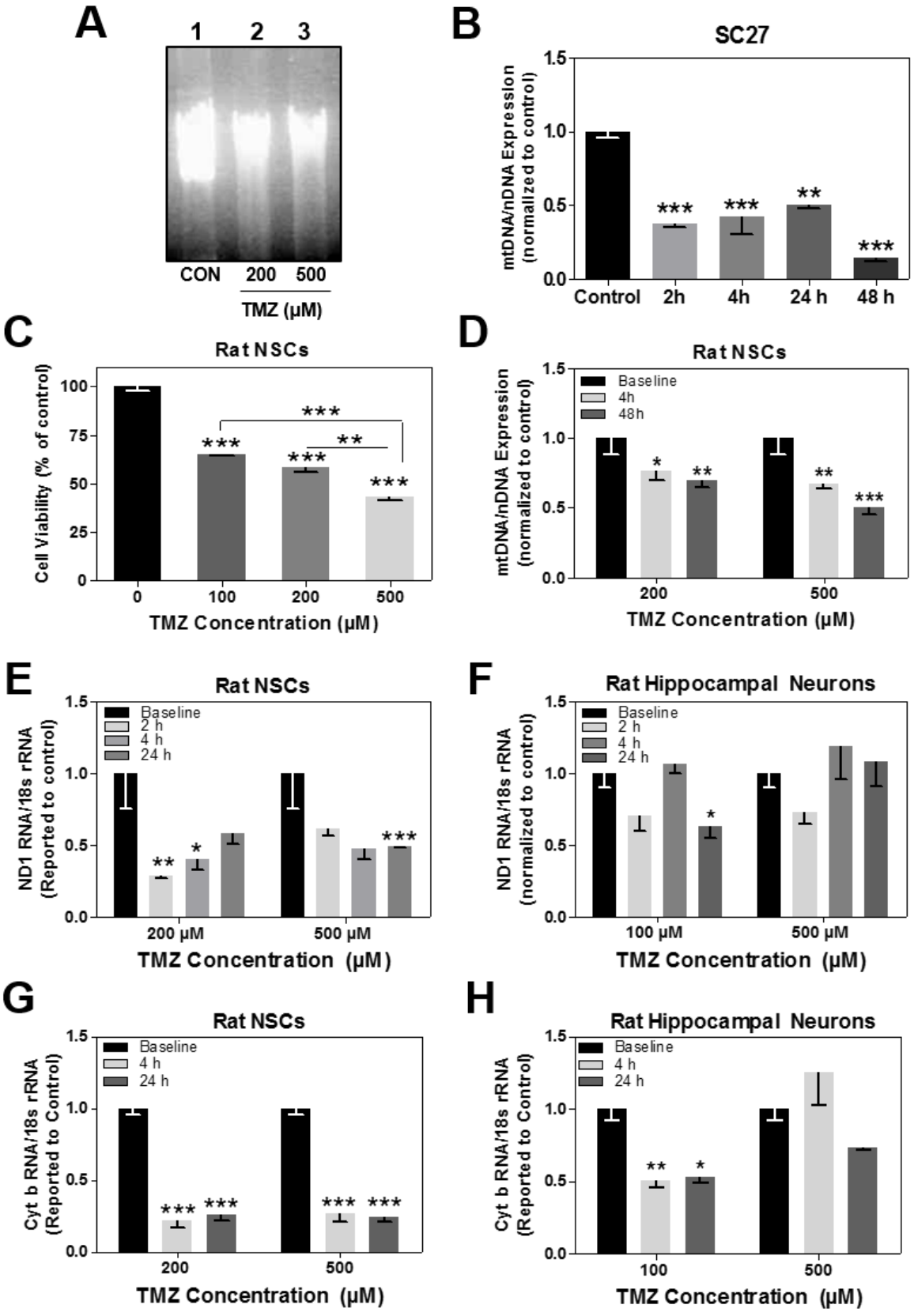
A
1 2 3
CON 200 500
TMZ (μM)
B
SC27
mtDNA/nDNA Expression (normalized to control)
Control 2h 4h 24 h 48 h
C
Rat NSCs
Cell Viability (% of control)
TMZ Concentration (μM)
D
Rat NSCs
Baseline
4h
48h
mtDNA/nDNA Expression (normalized to control)
TMZ Concentration (μM)
E
Rat NSCs
Baseline
2 h
4 h
24 h
ND1 RNA/18s rRNA (Reported to control)
200 μM 500 μM
TMZ Concentration (μM)
F
Rat Hippocampal Neurons
Baseline
2 h
4 h
24 h
ND1 RNA/18s rRNA (normalized to control)
100 μM 500 μM
TMZ Concentration (μM)
G
Rat NSCs
Baseline
4 h
24 h
Cyt b RNA/18s rRNA (Reported to Control)
200 500
TMZ Concentration (μM)
H
Rat Hippocampal Neurons
Baseline
4 h
24 h
Cyt b RNA/18s rRNA (Reported to Control)
100 500
TMZ Concentration (μM)

Figure 5.2. TMZ affects *mt*DNA integrity and impairs transcription of NADH dehydrogenase 1 and Cytochrome b in NSCs and cultured hippocampal neurons. (**A**) A representative agarose gel of a 13.4-kb *mt*DNA fragment amplified by quantitative PCR from genomic DNA of SC27 cells treated with 200 μM TMZ (lane 2), and 500 μM TMZ (lane 3) for 72 hours. Lane 1 is control. (**B**) TMZ (500 μM) caused a marked decrease in SC27 *mt*DNA levels. qPCR demonstrates a selective reduction in amplification of a 221-bp *mt*DNA fragment compared to a nuclear gene (β-globin). (**C**) TMZ causes a dose-dependent decrease in viability of cultured rat NSCs after 72 hours as measured by XTT assay. (**D**) The decrease in amplification of intact rat 235-bp *mt*DNA fragment compared to a nuclear gene (Clusterin). Quantification of NADH dehydrogenase 1 mRNA levels (ND1) in (**E**) rat NSCs and (**F**) primary hippocampal neurons. Decreased transcription of mitochondrial encoded Cytochrome b (Cyt b) in (**G**) rat NSCs and (**H**) primary hippocampal neurons treated with TMZ. Graphs represent mean ± SEM of 2-3 replicates. * $p < 0.05$, ** $p < 0.01$, *** $p < 0.001$.

model[38,59]. TMZ reduced amplification of rat NSC *mt*DNA compared to a *n*DNA fragment (Clusterin) (**Figure 5.2D**). 200 µM TMZ reduced amplification of rat NSC *mt*DNA at 4 h by 23.8% ± 3.5% ($p < 0.05$) and at 48 h by 30.1% ± 2.9% ($p < 0.05$). High-dose TMZ (500 µM) caused a further reduction in *mt*DNA amplification at 4 h by 32.3% ± 2.4% ($p < 0.05$) and even further at 48 h by 49.8% ± 2.9% ($p < 0.01$).

5.3.3. Temozolomide inhibits transcription of mitochondrial genes in NSCs and hippocampal neurons

We next examined the effect of TMZ on the transcription of NADH dehydrogenase subunit 1 (ND1) and Cytochrome b (Cyt b), two mitochondrial-encoded genes associated with the mitochondrial ETC, in rat NSCs and hippocampal neurons. ND1 is a mitochondrial-encoded protein subunit of complex I, the largest of the five complexes of the ETC. Defects involving complex I and III of the ETC have been associated with mutations in Cyt b[210,211]. Studies in human and mouse cell lines harboring deleterious mutations in Cyt b have shown that an intact complex III is required for the assembly and respiratory activity of complex I, suggesting a structural association between these two complexes[212]. We examined whether TMZ impaired transcription of ND1. 200 µM TMZ markedly reduced ND1 transcription levels in rat NSCs 2 h after treatment by 71.2% ± 1.3% ($p = 0.0054$), and 4 h by 59.7% ± 7.1% ($p < 0.05$) (**Figure 5.2E**). High-dose 500 µM TMZ decreased ND1 levels by 50.8% ± 0.3% ($p = 0.0003$), at 24 h. Strikingly, TMZ had a minimal effect on ND1 levels in hippocampal neurons (**Figure 5.2F**). 100 µM TMZ reduced ND1 levels by 36.9% ± 7.8% ($p = 0.043$) 24 h post-treatment, and 500 µM TMZ by 27.3% ± 7.4%, 2 h post-treatment although not significantly.

Cyt b is a major subunit of the catalytic core of complex III of the ETC and is the only component of complex III that is *mt*DNA encoded [213]. We assessed Cyt b transcription in rat NSCs following TMZ treatment (200 µM, 500 µM) at 0 h, 4 h, and 24 h post-treatment (**Figure 5.2G**). 200 µM TMZ resulted in a pronounced decrease in Cyt b mRNA at 4 h (78.1% ± 5.1% reduction), and 24 h (74.1% ± 3.7% reduction) post-treatment ($p < 0.001$). High-dose TMZ (500 µM) had a comparable reduction in Cyt b RNA levels at 4 h (73.3% ± 5.7%) and 24 h (75.9% ± 2.8%) post-treatment ($p < 0.001$). Low-dose TMZ (100 µM) significantly reduced hippocampal neuron Cyt b levels by 49.7% ± 4.7% at 4 h ($p = 0.0094$), and 46.6% ± 4.6% at 24 h ($p = 0.0347$) post-treatment (**Figure 5.2H**). High-dose TMZ (500 µM) had a modest 26.9% ± 1.5% decrease in Cyt b levels at 24 h post-treatment, although not significant ($p = 0.0736$). These results suggest that the NSC mitochondrial genome might be more sensitive to TMZ than that of hippocampal neurons.

5.3.4. Temozolomide reduces mitochondrial respiratory rates in cultured hippocampal neurons

To investigate if the *mt*DNA damage and a decrease in transcription levels of mitochondrial-encoded genes ND1 and Cyt b observed following TMZ treatment may be associated with impairment of mitochondrial respiratory activity, we measured oxygen consumption rates (OCR) in hippocampal neurons following TMZ treatment using the Seahorse XF24 extracellular flux analyzer. OCR is a measure of oxidative phosphorylation. We examined the effect of 200 µM TMZ (**Figure 5.3A,C, D**) and 500 µM TMZ (**Figure 5.3B, E, F**) on neuronal mitochondrial respiration after 24 h and 48 h of treatment. 200 µM TMZ decreased basal OCR levels at 24 h and 48 h, although not

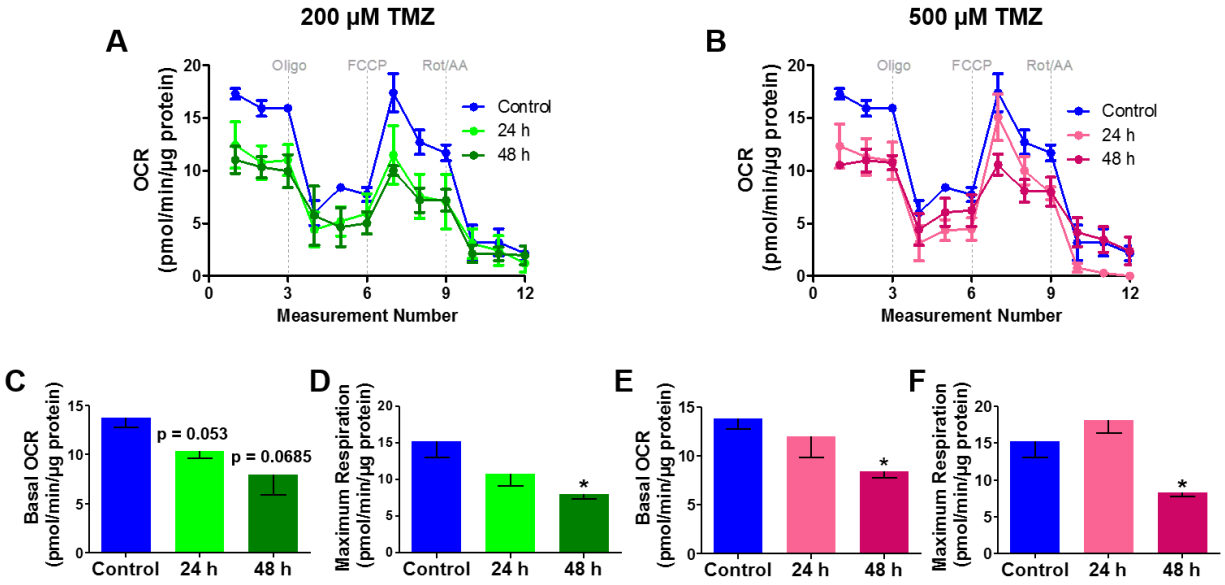

Figure 5.3. TMZ decreases mitochondrial respiration in cultured hippocampal neurons.
The Seahorse X24 Flux Analyzer was used to measure neuronal Oxygen Consumption Rate (OCR) using the Cell Mito Stress Kit. Mitochondrial bioenergetic profile of cultured hippocampal neurons treated with (**A**) 200 µM TMZ and (**B**) 500 µM TMZ for 24 and 48 hours. Quantitative analysis of neuronal basal OCR levels treated with (**C**) 200 µM TMZ and (**E**) 500 µM TMZ reveals a decrease in basal oxygen consumption. Temozolomide decreased the neuronal maximum respiratory rate at (**D**) 200 µM TMZ and (**F**) 500 µM TMZ after 48 hours of treatment. Maximum respiration was calculated by subtracting the non-mitochondrial respiration rate from the maximum rate measurement after FCCP injection. Graphs represent ± SEM, n = 3 replicates per group. * $p < 0.05$.

significantly (**Figure 5.3C**). At the higher dose of 500 µM, TMZ significantly reduced basal OCR levels 48 h post-treatment (p = 0.0125) (**Figure 5.3E**). TMZ decreased neuronal mitochondrial maximum respiration 48 h post-treatment at 200 µM µM (p = 0.0374) and 500 (p = 0.0386) compared to control levels by 47.1% ± 6.7% and 45.8% ± 5.0% respectively (**Figure 5.3D,F**). The decrease in maximum respiration suggests that TMZ may impair the capacity of neurons to increase oxidative phosphorylation to meet the ATP demand under stressful energetically demanding conditions.

5.3.5. Temozolomide alters neuronal dendritic structures

Exposure to radiation and various chemotherapeutic agents has been shown to damage neuronal morphology[32,59,187,214-217]. To examine the effect of TMZ on dendritic structures, we measured the number of dendritic branch points from the soma in hippocampal neurons treated with graded doses of TMZ (100 µM, 250 µM, and 500 µM) for 4 h and 24 h and immunolabeled for postsynaptic density-95 (PSD95) (**Figure 5.4A**). TMZ exposure reduced neuronal dendritic branch points 4 h after treatment (**Figure 5.4B**), with a more pronounced reduction in dendritic complexity evident at the highest TMZ dose (500 µM), and after 24 h (**Figure 5.4C**). Two-way RM ANOVA revealed an effect of interaction between TMZ dose and distance from soma for 4 h ($F_{(33,220)}$ = 3.599, p < 0.0001) and 24 h ($F_{(33,220)}$ = 2.629, p < 0.0001). Notably, 500 µM TMZ induced a rapid reduction in dendritic branching at 4 h post-treatment. However, the effects on *mt*DNA-encoded genes (**Figure 5.2F, H**) and mitochondrial respiratory function (**Figure 5.3B, E, F**) are slower, only becoming apparent 48 h after treatment, suggesting that neuronal

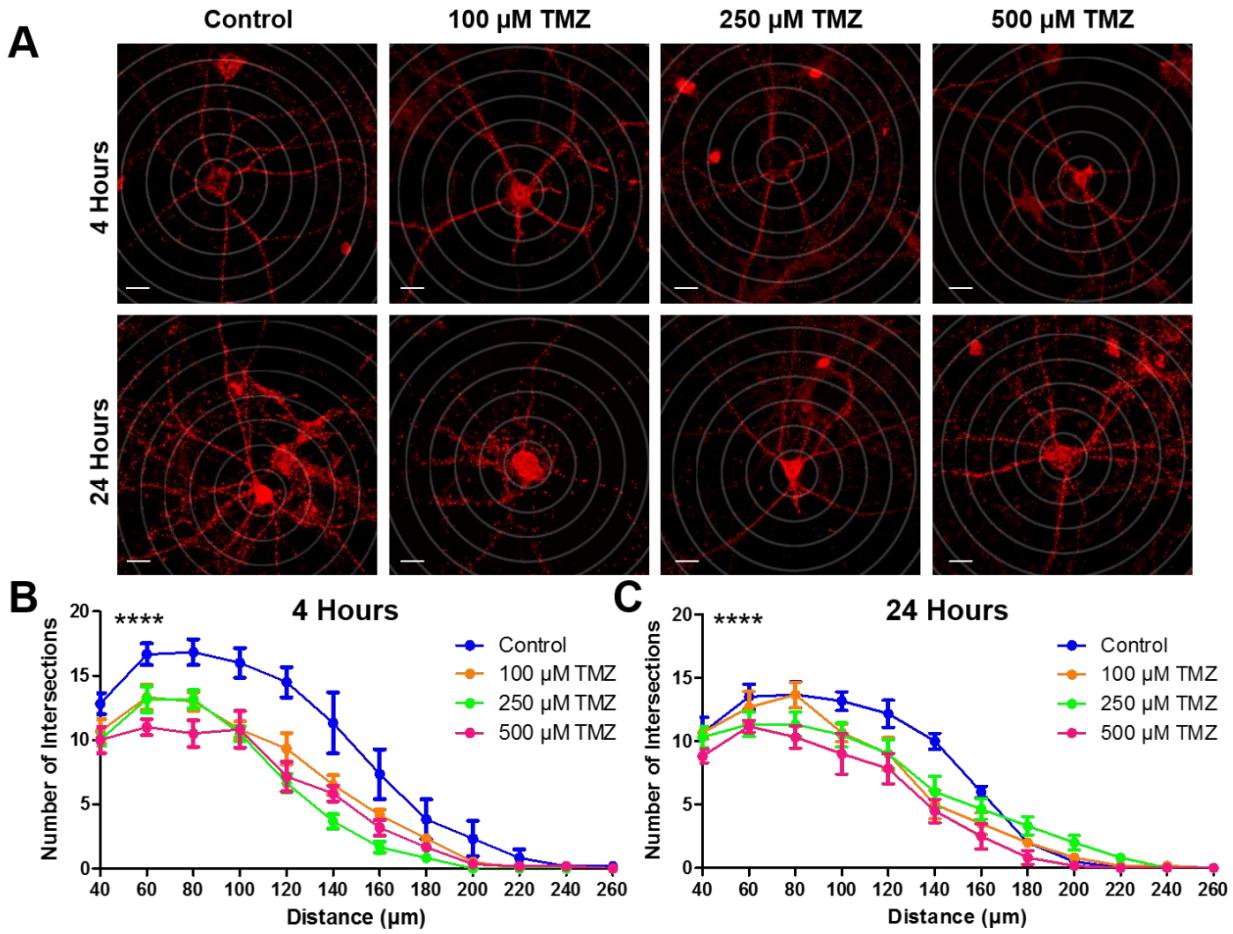

Figure 5.4. *In-vitro* treatment with graded doses of TMZ reduces dendritic branching of cultured hippocampal neurons.
(**A**) Representative images of hippocampal neurons treated with TMZ and immunolabeled for postsynaptic density-95 (PSD95). Neurons are superimposed over concentric Sholl circles (20 µm increments). (**B,C**) Quantification of dendritic branches at intersecting points with Sholl circles at increasing distance from the soma after (**B**) 4 hours and (**C**) 24 hours of treatment shows that TMZ reduces dendritic complexity at both time-points. Data are presented as mean ± SEM, **** $p < 0.0001$, (n = 6 neurons per group). Scale bars, 20 µm. Red, PSD95.

damage provoked by TMZ is slow, but progressive and morphological damage may precede mitochondrial dysfunction.

5.3.6. Temozolomide induces a loss of postsynaptic density-95 (PSD95) puncta in a dose- and time-dependent fashion

After assessing TMZ-induced changes in dendritic arborization, we sought to examine whether TMZ alters the number of PSD95 puncta found on dendritic branches, as a correlate measure of dendritic spine density[59,82]. PSD95 is a scaffolding protein found at excitatory synapses; it anchors synaptic proteins including NMDA and AMPA receptors, and potassium channels[218,219]. TMZ had an early (4 h) reduction in PSD95 puncta ($F_{(3,48)}$ = 23.30, p < 0.0001) (**Figure 5.5A**). 100 µM TMZ did not reduce PSD95 puncta compared to control (p > 0.05) at 4 h, but at 24 h this dose significantly reduced PSD95 compared to control (p < 0.001) and had a comparable effect to 250 µM at 24 h (**Figure 5.5A, B**). TMZ induced more extensive damage at 24 h, as loss of PSD95 was more pronounced (100 µM and 250 µM) and resulted in dendritic beading at the highest dose, 500 µM, which prevented PSD95 quantification in this treatment group ($F_{(2,32)}$ = 67.02, p < 0.0001) (**Figure 5.5B**). This loss of PSD95 occurs concurrently with a reduction in dendritic branching.

5.3.7. Temozolomide induces oxidative stress in hippocampal neurons

TMZ-induced DNA damage increases ROS production, which contributes to apoptosis in glioma[220,221]. We examined oxidative stress production in hippocampal neurons treated with TMZ (250 µM, 500 µM) for 7 days. Neurons were incubated with

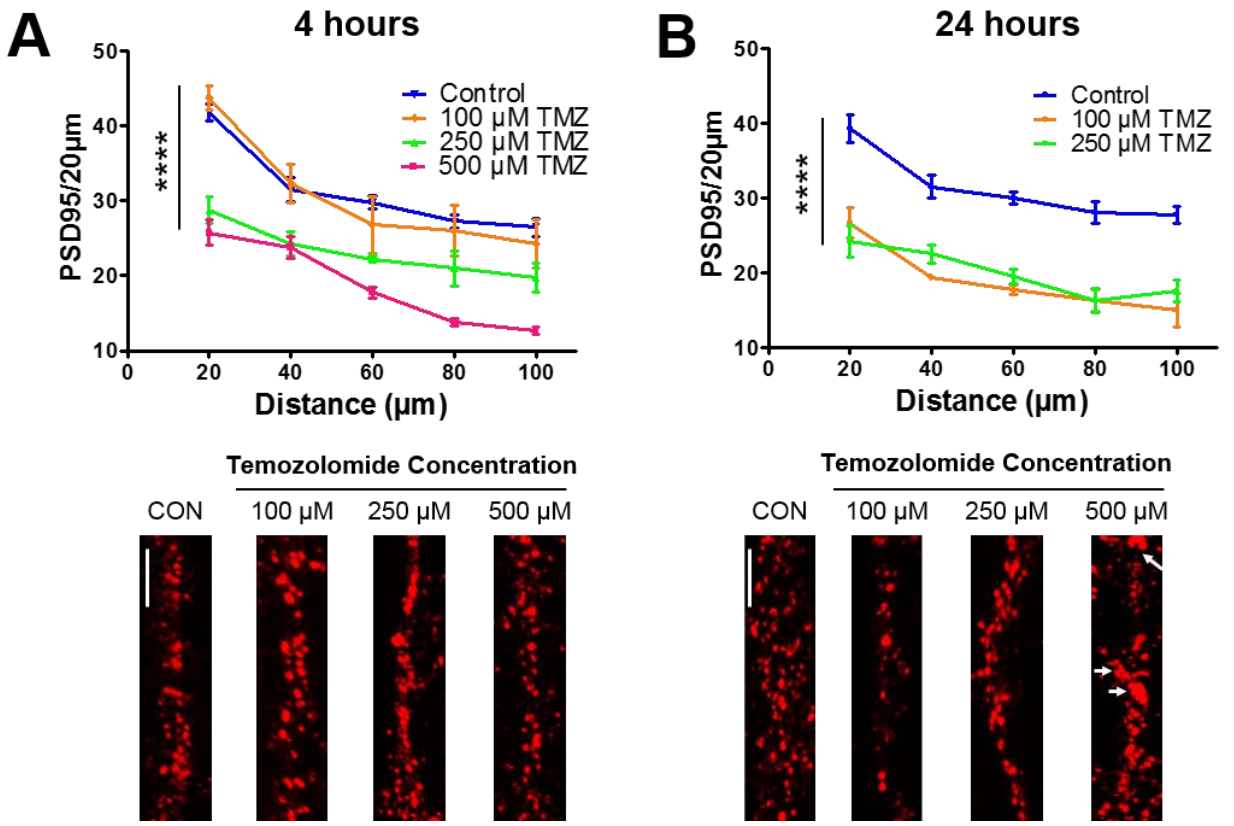

Figure 5.5. TMZ causes a dose- and time-dependent loss of PSD95 puncta in cultured hippocampal neurons.
(**A**) Graph and representative images of dendrites immunolabeled for postsynaptic density-95 (PSD95) depict a dose-dependent reduction in PSD95 puncta after a 4-hour exposure. (**B**) The loss of PSD95 is more prominent after 24-hour exposure. Dendritic beading (arrows) prevented quantification out to 100 µm from the soma for the 500 µM TMZ dose at 24 hours, and therefore was omitted from the analysis. Scale bars, 5 µm. Data are presented as mean ± SEM, **** $p < 0.0001$, (n = 4 neurons per group). Scale bars, 20 µm. Red, PSD95.

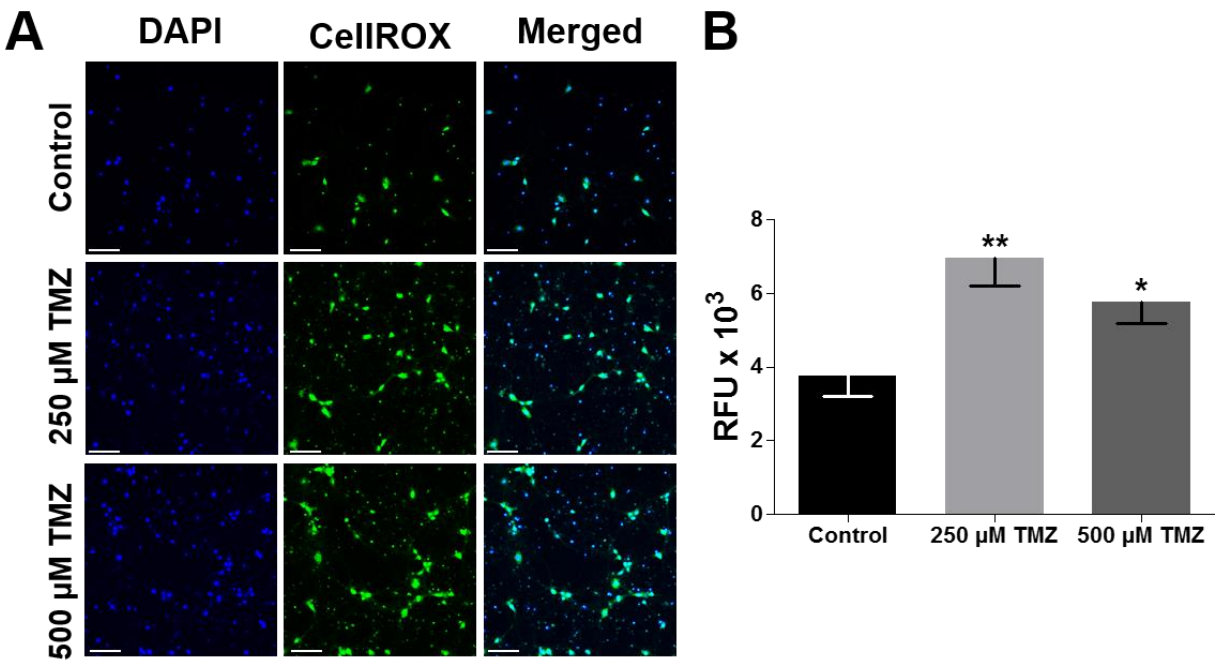

Figure 5.6. TMZ increases oxidative stress in cultured hippocampal neurons. (**A**) Rat hippocampal neurons (21 DIV) were exposed to 250 µM and 500 µM TMZ for 7 days. (**B**) Quantification of relative fluorescence intensity of CellROX probe as a measure of oxidative stress in TMZ treated neurons. Data are presented as mean ± SEM, * $p < 0.05$, ** $p < 0.01$, three sister coverslips per treatment. 5 images per coverslip. Scale bars, 100 µm. Blue, DAPI; Green, CellROX Oxidative Stress.

CellROX fluorescent probe for 20 min, and ROS production was quantified by measuring the fluorescence intensity of confocal images (**Figure 5.6A**). TMZ significantly increased oxidative stress levels by 86% at 250 µM, and 54% at 500 µM compared to control levels ($F_{(2,42)}$ = 6.514, p = 0.0034), there was no statistical difference between low-dose and high-dose TMZ (**Figure 5.6B**). Compared to studies examining TMZ-induced ROS production in glioma using similar doses of TMZ (250 µM), we found that ROS induction in neurons is slower[220,222]. In gliomas, ROS production peaked 72 h post-treatment, whereas, in our neuronal studies, a shorter duration of TMZ exposure did not result in significantly higher ROS levels compared to control (data not shown). These results suggest that TMZ related changes in neural structures may result in delayed complications that are not evident acutely after treatment.

5.3.8. Temozolomide induces active caspase-9 expression and apoptotic cell death in hippocampal neurons

Next, to examine the effect of TMZ on neuronal apoptotic cell death, we quantified cleaved caspase-9 expression in hippocampal neurons 7 days after TMZ exposure (**Figure 5.7A, B**). Upon cleavage, caspase-9 recruits and activates caspase -3 and -7 which culminates in apoptosis via the mitochondrial intrinsic cell death pathway[223]. TMZ exposure resulted in a dose-dependent increase in caspase-9 expression 7 days after treatment ($F_{(2,6)}$ = 11.35, p = 0.0091). High dose TMZ (500 µM TMZ) increased caspase-9 activation compared to control (p = 0.0009).

We also detected apoptosis by TUNEL assay, in neurons treated with TMZ (250 µM, 500 µM) for 5 and 7 days ($F_{(2,10)}$ = 73.04, p < 0.0001) (**Figure 5.7C, D**). At 5 days,

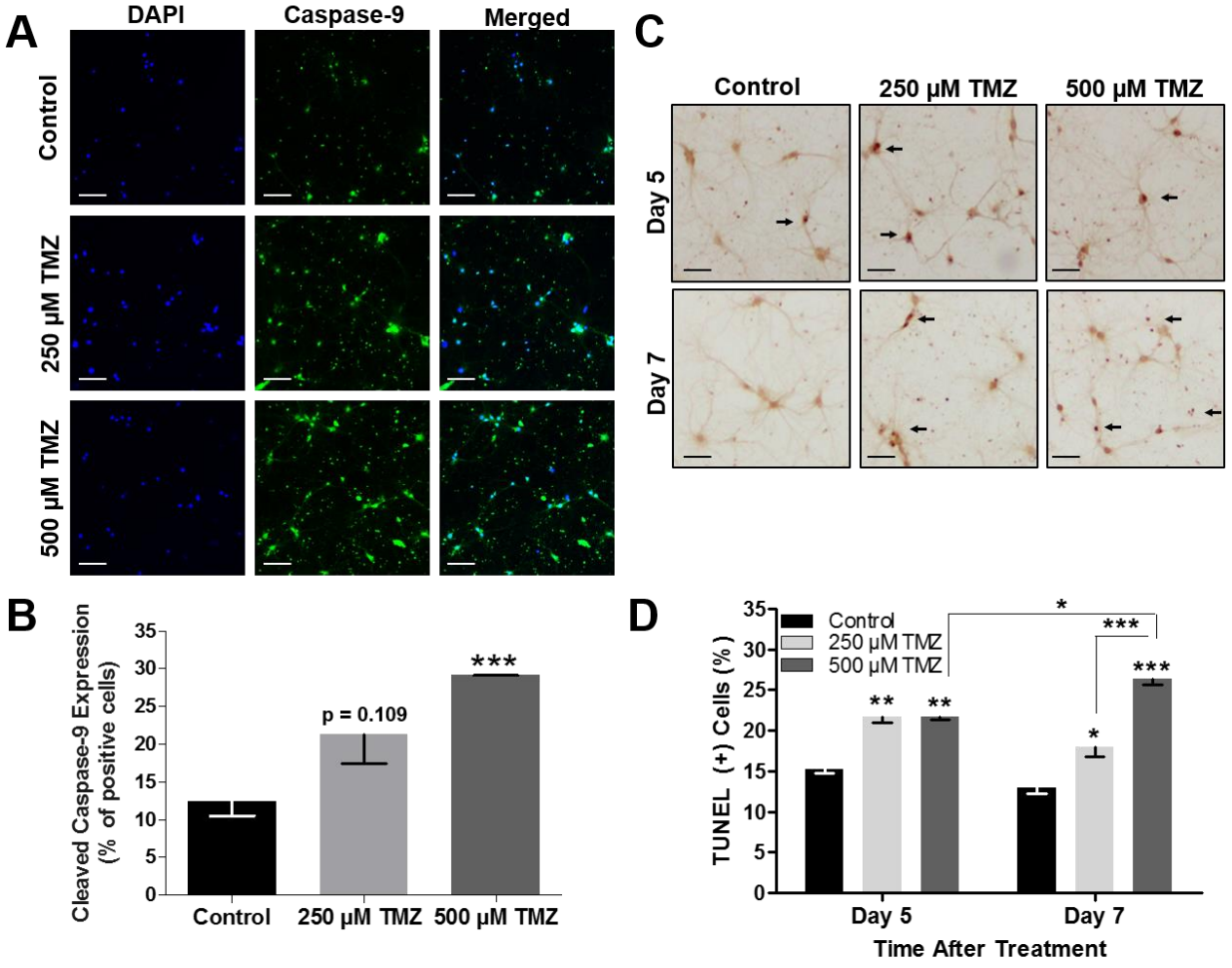

Figure 5.7. TMZ increases apoptosis in cultured hippocampal neurons.
(**A**) Rat primary hippocampal neurons (21 DIV) were exposed to 250 µM and 500 µM TMZ for 7 days. (**B**) TMZ induced a dose-dependent increase in cleaved caspase-9 expression 7 days after treatment. (**C**) Images of TUNEL positive hippocampal neurons (24 DIV) exposed to 250 µM and 500 µM TMZ for 5 days, and 7 days. (**D**) Quantification of TUNEL(+) (nuclear dark brown staining) neurons show that TMZ increased apoptotic neuronal death at both doses and time-points. High dose TMZ (500 µM) further increased apoptotic cell death 7 days after treatment. Scale bars, 100 µm. Data are presented as mean ± SEM, * $p < 0.05$, ** $p < 0.01$, *** $p < 0.001$, n = 2-3 sister coverslips per group, 10 images per coverslip. Blue, DAPI; green, cleaved caspase-9; brown; TUNEL.

both TMZ doses caused a similar induction in apoptosis, 21.7% ± 0.74% and 21.6% ± 0.31%, respectively compared to control, 15.2% ± 0.48% (**Figure 5.7D**). At 7 days, we observed a dose-dependent increase in apoptosis, 17.95% ± 1.09% and 26.42% ± 0.79%, respectively compared to control 12.92% ± 0.79%. There was an increase in apoptotic cell death in neurons exposed to high-dose TMZ, 500 µM for 5 days compared to 7 days ($p < 0.05$), which was not evident at the lower dose. These results suggest that TMZ-induced damage in neurons is dose-dependent, with higher doses resulting in more pronounced mitochondrial respiratory dysfunction, dendritic damage, and cell death.

5.4. Discussion

The cognitive impairments and mood disorders associated with glioma-directed treatment are of grave concern for the increasing number of survivors. As the standard of care treatment for glioblastoma, TMZ is widely used, yet its effects on normal brain structure and function are understudied. Here we identified mitochondrial damage in cultured NSCs and hippocampal neurons as a mechanism underlying TMZ-induced neurotoxicity. We examined mitochondrial morphology by TEM and found that TMZ induced mitochondrial degradation and vacuolization in human NSCs. TMZ exposure reduced amplification of a long, 13.4-kb *mt*DNA fragment and exerted a selective reduction in *mt*DNA amplification compared to *n*DNA in human NSCs. Similarly, TMZ resulted in a comparable decrease in cell viability and decrease in *mt*DNA amplification in rat NSCs. Acute, 4 h TMZ exposure significantly decreased ND1 and Cyt B mRNA transcription, two genes that encode components of complex I and complex III of the ETC respectively, which is indicative of damage to NSC *mt*DNA integrity elicited by TMZ.

Although less sensitive to TMZ than NSCs, neuronal *mt*DNA integrity was modestly damaged by TMZ, which resulted in impaired mitochondrial respiration after 48 h of TMZ exposure. Since excitatory synapses on dendritic spines mediate learning-related plasticity, we examined the effects of TMZ on the morphology of hippocampal neurons. TMZ reduced dendritic complexity and synaptic protein PSD95 puncta density in a time- and dose-dependent manner. These neuronal morphological changes were temporally concurrent with the observed *mt*DNA damage and respiratory dysfunction, which suggests hippocampal toxicity. Chronic exposure of TMZ increased oxidative stress in hippocampal neurons, culminating in neuronal apoptosis seven days after treatment. Alarmingly, NSCs (human and rat) are more sensitive to TMZ than glioma cell lines. In contrast, mature neurons are less vulnerable to TMZ compared to NSCs. 500 μM TMZ resulted in a 26.42% ± 0.79% decrease in neuronal cell viability (**Figure 5.7D**), compared to a 43.47% ± 1.8% decrease in NSC viability seven days after treatment (**Figure 5.2C**).

Similar to other DNA damaging agents such as cisplatin, TMZ induces mitochondrial dysfunction, apoptosis of neural cells, and morphological damage in surviving neurons. Using the same *in-vitro* system, cultured rat NSCs and hippocampal neurons, we found that neurons were much more sensitive to cisplatin at doses lower than those used clinically (0.1 – 1 μM), which induced dendritic damage and apoptosis at earlier time-points compared to TMZ, whereas NSCs were less sensitive[59]. These results highlight the observations that some chemotherapeutic agents have higher neurotoxic potential than others, but also that distinct neural lineages have unique susceptibilities to chemotherapeutic agents[10]. Also, these agents may have varying acute and chronic effects on neural cell populations in distinct microenvironments which can result in

delayed neurological complications observed in patients, including cognitive dysfunction, white and grey matter changes, and progressive myelin disruption.

Clinical studies have shown that TMZ contributes to anxiety, depression, and cognitive impairments in glioma patients as well as those with non-CNS malignancies. A phase 1 dose-escalation study of TMZ for the treatment of metastatic melanoma (excluding patients with CNS metastasis) reported anxiety and depression in 59% and 35% of patients, respectively[224]. Longitudinal MRI to assess structural brain changes in newly diagnosed GBM patients treated with RT plus systemic TMZ revealed significant and progressive decreases in whole brain volume, cortical gray matter loss, and ventricular dilation[225]. Progressive loss of white matter integrity was observed in the subventricular zone (SVZ), a region rich in NSCs. As gray matter loss and ventricular dilation are strongly associated with the neurocognitive decline in neurodegenerative diseases such as Alzheimer's disease[226,227], the incidence of these structural alterations in patients receiving chemoradiation may be indicative of changes in neurocognitive function. Of note, the onset of significant morphologic brain changes coincided with the time of RT completion, six weeks after the combined therapy. Although it is difficult to parse out the individual and synergistic contributions of RT and chemotherapy in these studies, the changes observed followed a delayed time course, resulting in progressive neurodegeneration weeks after the initial exposure[225].

In addition to TMZ, glioma patients may also receive adjuvant therapies, such as bevacizumab, an anti-VEGF monoclonal antibody, which has been associated with neurotoxicity. The FDA approved bevacizumab for recurrent GBM in 2017. In patients with recurrent GBM, treatment with bevacizumab has been shown to induce brain atrophy

compared to control group patients who received the standard of care treatment but did not receive bevacizumab[228]. Bevacizumab has also been linked to neurocognitive decline in newly diagnosed patients[229]. Investigation of the effects of bevacizumab on the morphology and survival of dissociated rat hippocampal cell cultures revealed that long-term exposure to bevacizumab resulted in delayed (20-30 day post-treatment) reductions in dendritic length, without reducing neuronal or glial cell viability. In contrast, cortical neurons and glia are much more sensitive to bevacizumab, as cell viability was reduced 30 days post-treatment. While many commonly used cancer therapies induce cognitive dysfunction, various cells types have distinct sensitives to chemotherapeutic agents, and damage to multiple neural lineages and blood vasculature may contribute to the neurocognitive impairments and mood changes experienced by cancer survivors.

To our knowledge, our study is the first to identify mitochondrial damage as a mechanism associated with TMZ-induced neurotoxicity in NSCs and neuronal cultures. Other studies have examined the neurotoxic effects of TMZ on primary rat cortical microglia[230], organotypic rat corticostriatal[231], and entorhinal-hippocampal slice cultures[232] and found that at clinically relevant doses, 10-500 µM, TMZ does not decrease cell viability following acute 24 h – 72 h exposure. Collectively, these studies show that in agreement with the present study, TMZ may have chronic *delayed* effects on the normal brain, which may augment damage provoked by RT and other anti-cancer agents used during cancer treatment. Additional studies examining the chronic long-term effects of TMZ on neurons, oligodendrocytes, NSCs, and other neural subtypes are warranted.

5.5. Conclusions

In summary, we demonstrated that mitochondrial dysfunction is a mechanism underlying TMZ-induced neurotoxicity in cultured NSCs and hippocampal neurons. TMZ induced *mt*DNA damage in NSCs and neurons. Concomitant with the mitochondrial respiratory dysfunction in neurons was a loss of PSD95 puncta and decrease in dendritic branch length, which is indicative of morphological damage. More extended exposure to TMZ increased oxidative stress and reduced neuronal viability. TMZ induced more pronounced decrements in NSC *mt*DNA integrity and viability compared to neurons, suggesting that NSCs are more vulnerable to TMZ than neurons. TMZ may have various acute and chronic effects on mitochondria that affect neural function and survival, which may contribute to the neurological complications experienced by GBM patients.

Acknowledgments

The authors thank Adrienne Andres for assistance with the PSD95 immunocytochemistry experiments, and Vivek Abraham for technical help with Sholl analysis.

Financial support

This work was supported by the National Institute for Neurological Diseases and Stroke Award (NINDS/NIH) [NS072234], the National Center for Advancing Translational Sciences, NIH [UL1 TR001414], and the UCI Cancer Center Award [P30CA062203] from the National Cancer Institute. The NIH MBRS-IMSD training grant [GM055246] and the NINDS/NIH pre-doctoral fellowship [NS082174] provided support for N. Lomeli. The

National Institute of Environmental Health Sciences of the NIH supported D.C. Pearre with the grant T32CA060396, and its contents of the project described are solely the responsibility of the authors and do not necessarily represent the official views of the NIEHS or NIH.

CHAPTER 6

Conclusion and Future Directions

The underlying biological basis for cisplatin-induced CRCI involves structural changes in the hippocampus, loss of dendritic spines, and NSC and neuronal death. Loss of dendritic spines indicates a loss of excitatory synapses and hippocampal cell death has detrimental consequences for learning and memory. The brain regions and cognitive functions that are affected by cisplatin and the mechanisms involved are probably multiple. Previous studies from our lab and others had shown that mature neurons and NSCs are susceptible to cisplatin, and are killed by cisplatin doses that do not effectively destroy cancer cells, which suggests that at doses used clinically, cisplatin can illicit major damage to neural structures that contributes to CRCI[10,60].

Through the use of *in-vitro* (primary rat NSC and hippocampal neuronal cultures) and *in-vivo* rat models of cisplatin-induced CRCI, we have identified a strong candidate pathway associated with NSC and neuronal damage/death: mitochondrial dysfunction, causing impaired cellular respiration, depletion of the antioxidant glutathione, and increased ROS production. Administration of the antioxidant NAC prevented/reduced free radical production, reduced apoptotic cell death, dendritic spine loss, and reduced the cisplatin-induced cognitive impairments in young adult male Sprague Dawley rats. Given that cisplatin is used to treat testicular cancer, and testicular cancer is the most common cancer affecting young men (18-39 years) and induces long-term lower cognitive performance and white matter changes in testicular cancer survivors 10 years post-treatment, our model is relevant for this patient population[233,234]. In our pediatric and

adolescent rat model of CRCI, we found that cisplatin-treated infants and adolescents showed poor contextual discrimination which requires hippocampal-dependent pattern separation skill. Unlike our cisplatin-induced CRCI model in adult male rats, we found that the cisplatin-treated infants and adolescents had an impaired response to cued fear conditioning, which engages the amygdala. The rats treated at adolescence also showed more global cognitive deficits. In our ovarian cancer cisplatin-induced CRCI model we found that NAC could be administered in a delayed manner, 10 h post-cisplatin treatment, without affecting cisplatin-induced tumor volume reduction nor survival, while preventing cisplatin-induced CRCI. Notably, we found that tumor-bearing rats that did not receive cisplatin or NAC also presented cognitive impairments. This finding correlates with the clinical evidence that cancer patients experience cognitive deficits at baseline before receiving treatment. Yan et al. found that tumor-bearing mice exhibited depressive behavior, and impaired object recognition memory, which was associated with increase in pro-inflammatory cytokines in the hippocampus, reduced levels of hippocampal brain-derived neurotrophic factor (BDNF) mRNA, and decrease in hippocampal neurogenesis[235]. Future studies should examine the mechanisms involved with cancer-induced cognitive impairments.

Although we found that NAC prevented cisplatin-induced ROS production, apoptosis, and GSH depletion in cultured NSCs and hippocampal neurons (**Figure 2.6,2.7,4.2**) we did not assess the effect of cisplatin and/or NAC on mitochondrial biogenesis. Mitochondrial biogenesis is defined as the growth and division of mitochondria, which increases mitochondrial mass. Changes in mitochondrial biogenesis, mitochondrial copy number, and *mt*DNA integrity are associated with mitochondrial

dysfunction and oxidative stress[236]. Quantification of *mt*DNA copy number by RT-PCR, and western blotting for proteins involved in biogenesis: peroxisomal proliferating activating receptor γ coactivator-1alpha (PGC-1α), mitochondrial transcription factor A (TFAM), nuclear respiratory factor-1 and -2 (NRF-1, NRF-2) could reveal whether cisplatin neurotoxicity and/or NAC neuroprotection affects mitochondrial biogenesis[237]. The effects of cisplatin-induced ROS production on mitochondrial biogenesis may depend on the dose and duration of cisplatin exposure, as reports in the literature suggest that acute oxidative stress can induce PGC-1α and mitochondrial biogenesis as a compensatory mechanism, however severe and chronic oxidative stress may decrease mitochondrial transcription factors, including PGC-1α, NRF-1, NRF-2[238]. Additional studies should also examine GSH and GSSG levels, and enzymatic activity and protein levels of GSH pathway enzymes, including glutathione peroxidase, glutathione reductase, and glutathione-S-transferase in the hippocampus to further validate the *in-vitro* data suggesting that cisplatin depletes GSH levels in NSCs and hippocampal neurons (**Figure 4.2**).

*Mt*DNA damage in NSCs has been shown to alter their differentiation fate towards astrocytic differentiation[239,240]. High ROS levels have been shown to suppress proliferation of neural progenitor cells, and direct their differentiation towards the astrocyte lineage at the expense of neuronal differentiation[241]. In contrast, NAC has been shown to enhance neuronal differentiation in mouse embryonic stem cells. Acute cisplatin treatment (10 mg/kg) decreases the number of Sox2+ cells in the dentate gyrus (**Suppl. Figure 2.2**). Future experiments should examine whether cisplatin-induced oxidative stress affects the differentiation fate of hippocampal NSCs and whether NAC prevents

cisplatin-induced changes in NSC differentiation and proliferation. Based on the results of our studies indicating that cisplatin induces *mt*DNA damage and oxidative stress in NSCs, we anticipate that cisplatin may alter the differentiation fate of NSCs towards an astrocytic fate at the expense of neuronal differentiation. Alternatively, it is possible that cisplatin does not alter differentiation fate of NSCs but instead inhibits their proliferation. Both possibilities may explain the loss of neurogenesis induced by cisplatin.

Since NAC is FDA approved for the treatment of acetaminophen-induced liver damage and its use as a mucolytic agent, the pharmacology, formulation, and potential toxicities of NAC are known. Conducting clinical studies to examine if NAC can be repurposed for the treatment of CRCI would reduce the time-frame and costs associated with preclinical and clinical testing of newly developed drugs[242]. Based on the promising data presented in this dissertation demonstrating the potential of NAC to ameliorate cisplatin-induced CRCI, we are now proposing a direct translation of our NAC approach for the prevention of cognitive damage caused by platinum-based therapies (PBT) in ovarian cancer patients. The first planned project is a novel phase I/II clinical trial which will determine if NAC can be used to prevent or alleviate CRCI in ovarian cancer patients treated with PBT. The study would evaluate the safety and tolerability of NAC, as well as the recommended phase 2 dose (RP2D) in ovarian cancer patients receiving PBT using a Phase I, dose-escalating design. Once the RP2D is established, the efficacy of NAC in ameliorating CRCI in this patient population can be assessed using a phase II randomized, double-blinded, placebo-controlled study design. Longitudinal neurocognitive assessments and MRI imaging to assess hippocampal volume at baseline and 6 months post-PBT completion may determine the effect of PBT on cognitive function

and hippocampal volume, and if NAC supplementation prevents PBT-induced changes in both measures. Additionally, this study may determine if there is a correlation between changes in cognitive function and hippocampal volume as has been previously described in this patient population[243]. Lastly, as in the preclinical studies, serum glutathione levels and the related glutathione enzyme pathway will be assayed. The results of this study may provide a strategy for developing a phase III trial that could benefit patients with multiple cancer types also treated with PBT.

However, prior to conducting clinical studies to examine if NAC can prevent cisplatin-induced CRCI, NAC pharmacokinetic data in rats is needed to determine what are the NAC concentrations achieved in the serum of rats and does this correlate with the NAC concentrations achievable in humans. This will require completing a dose-response experiment in our preclinical model to compare if intraperitoneal NAC administration achieves similar concentrations of serum NAC as those following NAC oral administration in humans, and measuring NAC serum levels by high performance liquid chromatography (HPLC). In our preclinical studies, NAC (250mg/kg) is administered by intraperitoneal injection on five consecutive days during cisplatin treatment, and is dose delayed by 10 h on days of cisplatin administration. As NAC is available in an oral formulation, this would be the preferred method of delivery in the clinical studies. If intraperitoneal NAC administration does not achieve similar concentrations of serum NAC as oral NAC administration in humans, we may need to conduct a pharmacokinetic experiment administering NAC by oral gavage in rats.

To build upon the mechanism of cisplatin-induced CRCI proposed in my dissertation and to assess other potential targeted therapies using small molecules with

superior blood-brain barrier (BBB) penetration, future experiments will probe the downstream molecular pathways from cisplatin-generated mitochondrial dysfunction and free radical production. Specifically, two candidate pathways that will be examined are the c-Jun N-terminal kinase (JNK) and p38 mitogen-activated protein kinase (MAPK) pathways (**Figure 6.1**). Mitochondrial dysfunction and oxidative stress are associated with depletion of glutathione in models of cisplatin-induced renal toxicity[167,168] and peripheral neuropathy[169]. NAC is a precursor in the production of glutathione. Mitogen-activated protein kinases (MAPK) are downstream effectors of the glutathione system. By increasing glutathione, NAC has been shown to prevent JNK/p38 MAPK activation[244]. NAC has also been shown to mitigate cisplatin-induced oxidative stress in models of by blocking the activation of the JNK/p38 MAPK pathways[167,245,246]. The JNK and p38 MAPK pathways are activated by cellular stressors, including oxidative stress[166,247]. Cisplatin may increase the levels of phospho-p38 MAPK and phospho-JNK, thereby activating an intracellular signaling cascade that culminates in apoptosis of hippocampal neurons and NSCs. Phosphorylation profiling of MAPK pathway proteins using a MAPK pathway phospho antibody array and western blotting for JNK and p38 MAPK proteins can be used to uncover potential targets altered by cisplatin.

If cisplatin-induced CRCI is associated with JNK and/or p38 MAPK activation, pharmacological inhibition of these pathways using BBB-penetrant small molecules such as the JNK inhibitor SP600125 and the p38 MAPK inhibitor Neflamapimod could provide novel therapeutic interventions for the prevention of cisplatin-induced CRCI. The p38 MAPK inhibitor Neflamapimod and the JNK inhibitor SP600125 are small molecules, with

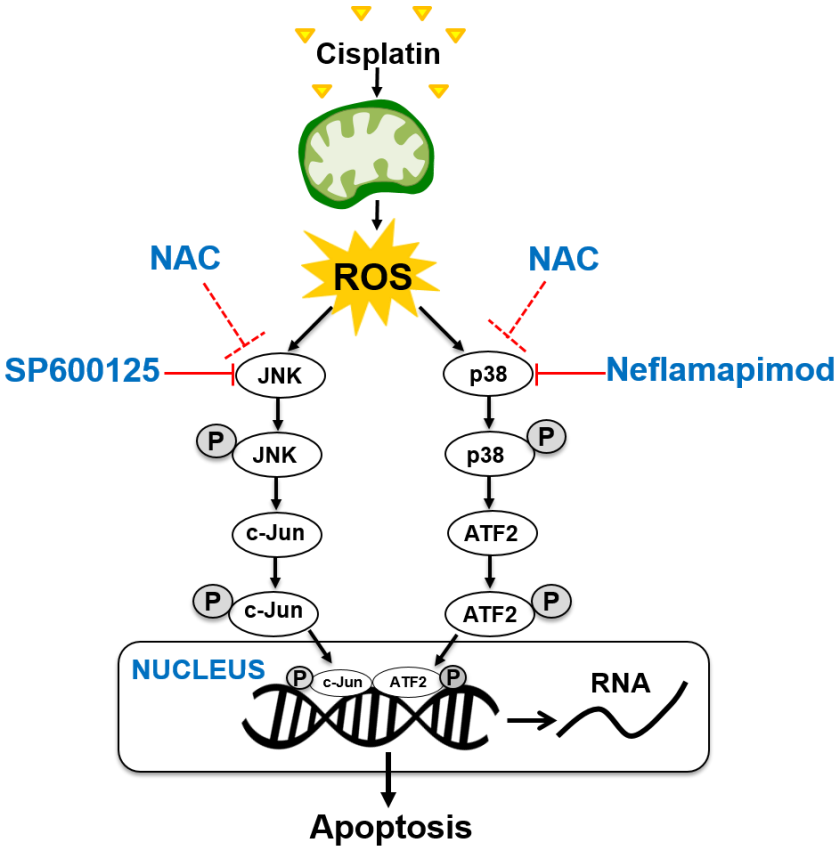

Figure 6.1. Schematic representation of the JNK/p38 MAPK pathways and potential therapeutic targets for cisplatin-induced CRCI.

great brain penetrance. The small molecule JNK inhibitor SP600125 is a potent BBB penetrant selective inhibitor of the JNK1,2, and 3 isoforms, it has been shown to exert neuroprotective properties in multiple rat models of neurodegeneration including Parkinson's disease[248], neuropathic pain[249], and stroke[250,251]. Neflamapimod (VX-745, EIP Pharma, LLC) is a specific BBB penetrant inhibitor of the alpha isoform of p38 MAPK that is currently in a phase 2b clinical trial for Alzheimer's disease (AD) [252]. Neflamapimod acts by targeting synaptic dysfunction and has shown to improve episodic memory in AD patients[253]. In aged rats, Neflamapimod increased hippocampal levels of PSD95, and improved performance in the Morris Water Maze task compared to aged controls[254]. Future studies would examine whether these inhibitors can prevent cisplatin-induced toxicity in cultured NSCs and hippocampal neurons in addition to our rat models, including the tumor-bearing model of cisplatin-induced CRCI.

In summary, my dissertation studies suggest that mitochondrial dysfunction is a strong candidate mechanism for cisplatin-induced CRCI, and NAC supplementation is a viable therapeutic strategy for preventing cisplatin-induced CRCI. In addition, the development of various rat models of cisplatin-induced CRCI described in this dissertation: (1) young adult male Sprague Dawley rats (2) infant and adolescent male Sprague Dawley rats and (3) ovarian tumor-bearing female Cr:NIH-RNU rats indicate that various domains of cognition area affected by cisplatin and the extent of cognitive impairments following cisplatin chemotherapy exposure may be age- and sex-specific. Our results underscore the importance of developing animal models that accurately reflect CRCI in humans – and take into consideration the effect of age, sex, cancer, type

of chemotherapeutic agent, as this is crucial for developing preventive and treatment strategies for CRCI.

REFERENCES

1. Diamond A. Executive functions. *Annu Rev Psychol.* 2013;64:135-168.

2. Craig TJ, Abeloff MD. Psychiatric symptomatology among hospitalized cancer patients. *The American Journal of Psychiatry.* 1974;131(12):1323-1327.

3. Levine PM, Silberfarb PM, Lipowski ZJ. Mental disorders in cancer patients. A study of 100 psychiatric referrals. *Cancer.* 1978;42(3):1385-1391.

4. Schottenfeld D, Robbins GF. Quality of survival among patients who have had radical mastectomy. *Cancer.* 1970;26(3):650-655.

5. Weiss HD, Walker MD, Wiernik PH. Neurotoxicity of commonly used antineoplastic agents (first of two parts). *N Engl J Med.* 1974;291(2):75-81.

6. Weiss HD, Walker MD, Wiernik PH. Neurotoxicity of commonly used antineoplastic agents (second of two parts). *N Engl J Med.* 1974;291(3):127-133.

7. Silberfarb PM, Philibert D, Levine PM. Psychosocial aspects of neoplastic disease: II. Affective and cognitive effects of chemotherapy in cancer patients. *Am J Psychiatry.* 1980;137(5):597-601.

8. Ahles TA, Saykin AJ, Furstenberg CT, Cole B, Mott LA, Skalla K, Whedon MB, Bivens S, Mitchell T, Greenberg ER, Silberfarb PM. Neuropsychologic impact of standard-dose systemic chemotherapy in long-term survivors of breast cancer and lymphoma. *J Clin Oncol.* 2002;20(2):485-493.

9. Saykin AJ, Ahles TA, McDonald BC. Mechanisms of chemotherapy-induced cognitive disorders: neuropsychological, pathophysiological, and neuroimaging perspectives. *Semin Clin Neuropsychiatry.* 2003;8(4):201-216.

10. Dietrich J, Han R, Yang Y, Mayer-Proschel M, Noble M. CNS progenitor cells and oligodendrocytes are targets of chemotherapeutic agents in vitro and in vivo. *Journal of biology.* 2006;5(7):22.

11. Dietrich J, Monje M, Wefel J, Meyers C. Clinical patterns and biological correlates of cognitive dysfunction associated with cancer therapy. *Oncologist.* 2008;13(12):1285-1295.

12. Dietrich J, Prust M, Kaiser J. Chemotherapy, cognitive impairment and hippocampal toxicity. *Neuroscience.* 2015;309:224-232.

13. Kaiser J, Bledowski C, Dietrich J. Neural correlates of chemotherapy-related cognitive impairment. *Cortex.* 2014;54:33-50.

14. Monje M, Dietrich J. Cognitive side effects of cancer therapy demonstrate a functional role for adult neurogenesis. *Behav Brain Res.* 2012;227(2):376-379.

15. Janelsins MC, Kesler SR, Ahles TA, Morrow GR. Prevalence, mechanisms, and management of cancer-related cognitive impairment. *International Review of Psychiatry.* 2014;26(1):102-113.

16. Ahles TA, Saykin AJ. Candidate mechanisms for chemotherapy-induced cognitive changes. *Nat Rev Cancer.* 2007;7(3):192-201.

17. Wefel JS, Saleeba AK, Buzdar AU, Meyers CA. Acute and late onset cognitive dysfunction associated with chemotherapy in women with breast cancer. *Cancer.* 2010;116(14):3348-3356.

18. Horowitz TS, Suls J, Treviño M. A Call for a Neuroscience Approach to Cancer-Related Cognitive Impairment. *Trends in Neurosciences.* 2018;41(8):493-496.

19. Deprez S, Amant F, Smeets A, Peeters R, Leemans A, Van Hecke W, Verhoeven JS, Christiaens MR, Vandenberghe J, Vandenbulcke M, Sunaert S. Longitudinal assessment of chemotherapy-induced structural changes in cerebral white matter and its correlation with impaired cognitive functioning. *J Clin Oncol.* 2012;30(3):274-281.

20. Billiet T, Emsell L, Vandenbulcke M, Peeters R, Christiaens D, Leemans A, Van Hecke W, Smeets A, Amant F, Sunaert S, Deprez S. Recovery from chemotherapy-induced white matter changes in young breast cancer survivors? *Brain Imaging and Behavior.* 2018;12(1):64-77.

21. Schagen SB, Muller MJ, Boogerd W, Rosenbrand RM, van Rhijn D, Rodenhuis S, van Dam FS. Late effects of adjuvant chemotherapy on cognitive function: a follow-up study in breast cancer patients. *Ann Oncol.* 2002;13(9):1387-1397.

22. Ahles TA, Saykin AJ, McDonald BC, Li Y, Furstenberg CT, Hanscom BS, Mulrooney TJ, Schwartz GN, Kaufman PA. Longitudinal assessment of cognitive changes associated with adjuvant treatment for breast cancer: impact of age and cognitive reserve. *J Clin Oncol.* 2010;28(29):4434-4440.

23. Koppelmans V, Breteler MMB, Boogerd W, Seynaeve C, Gundy C, Schagen SB. Neuropsychological Performance in Survivors of Breast Cancer More Than 20 Years After Adjuvant Chemotherapy. *Journal of Clinical Oncology.* 2012;30(10):1080-1086.

24. Apple AC, Ryals AJ, Alpert KI, Wagner LI, Shih PA, Dokucu M, Cella D, Penedo FJ, Voss JL, Wang L. Subtle hippocampal deformities in breast cancer survivors with reduced episodic memory and self-reported cognitive concerns. *Neuroimage Clin.* 2017;14:685-691.

25. Chen X, He X, Tao L, Li J, Wu J, Zhu C, Yu F, Zhang L, Zhang J, Qiu B, Yu Y, Wang K. The Working Memory and Dorsolateral Prefrontal-Hippocampal Functional Connectivity Changes in Long-Term Survival Breast Cancer Patients Treated with Tamoxifen. *Int J Neuropsychopharmacol.* 2017;20(5):374-382.

26. Bergouignan L, Lefranc JP, Chupin M, Morel N, Spano JP, Fossati P. Breast cancer affects both the hippocampus volume and the episodic autobiographical memory retrieval. *PLoS One.* 2011;6(10):e25349.

27. Cheng H, Li W, Gong L, Xuan H, Huang Z, Zhao H, Wang LS, Wang K. Altered resting-state hippocampal functional networks associated with chemotherapy-induced prospective memory impairment in breast cancer survivors. *Scientific Reports.* 2017;7:45135.

28. Feng Y, Tuluhong D, Shi Z, Zheng LJ, Chen T, Lu GM, Wang S, Zhang LJ. Postchemotherapy hippocampal functional connectivity patterns in patients with breast cancer: a longitudinal resting state functional MR imaging study. *Brain Imaging and Behavior.* 2019.

29. Hodgson KD, Hutchinson AD, Wilson CJ, Nettelbeck T. A meta-analysis of the effects of chemotherapy on cognition in patients with cancer. *Cancer treatment reviews.* 2013;39(3):297-304.

30. Christie LA, Acharya MM, Parihar VK, Nguyen A, Martirosian V, Limoli CL. Impaired cognitive function and hippocampal neurogenesis following cancer chemotherapy. *Clin Cancer Res.* 2012;18(7):1954-1965.

31. Salas-Ramirez KY, Bagnall C, Frias L, Abdali SA, Ahles TA, Hubbard K. Doxorubicin and cyclophosphamide induce cognitive dysfunction and activate the ERK and AKT signaling pathways. *Behav Brain Res.* 2015;292:133-141.

32. Acharya MM, Martirosian V, Chmielewski NN, Hanna N, Tran KK, Liao AC, Christie LA, Parihar VK, Limoli CL. Stem Cell Transplantation Reverses Chemotherapy-Induced Cognitive Dysfunction. *Cancer Research.* 2015;75(4):676-686.

33. Gibson EM, Nagaraja S, Ocampo A, Tam LT, Wood LS, Pallegar PN, Greene JJ, Geraghty AC, Goldstein AK, Ni L, Woo PJ, Barres BA, Liddelow S, Vogel H, Monje M. Methotrexate Chemotherapy Induces Persistent Tri-glial Dysregulation that Underlies Chemotherapy-Related Cognitive Impairment. *Cell.* 2019;176(1-2):43-55 e13.

34. Geraghty AC, Gibson EM, Ghanem RA, Greene JJ, Ocampo A, Goldstein AK, Ni L, Yang T, Marton RM, Pasca SP, Greenberg ME, Longo FM, Monje M. Loss of Adaptive Myelination Contributes to Methotrexate Chemotherapy-Related Cognitive Impairment. *Neuron.* 2019;103(2):250-265.e258.

35. Mustafa S, Walker A, Bennett G, Wigmore PM. 5-Fluorouracil chemotherapy affects spatial working memory and newborn neurons in the adult rat hippocampus. *Eur J Neurosci.* 2008;28(2):323-330.

36. Winocur G, Vardy J, Binns MA, Kerr L, Tannock I. The effects of the anti-cancer drugs, methotrexate and 5-fluorouracil, on cognitive function in mice. *Pharmacol Biochem Behav.* 2006;85(1):66-75.

37. Seigers R, Schagen SB, Beerling W, Boogerd W, van Tellingen O, van Dam FS, Koolhaas JM, Buwalda B. Long-lasting suppression of hippocampal cell proliferation and impaired cognitive performance by methotrexate in the rat. *Behav Brain Res.* 2008;186(2):168-175.

38. Lomeli N, Di K, Czerniawski J, Guzowski JF, Bota DA. Cisplatin-induced mitochondrial dysfunction is associated with impaired cognitive function in rats. *Free radical biology & medicine.* 2017;102:274-286.

39. Gaman AM, Uzoni A, Popa-Wagner A, Andrei A, Petcu EB. The Role of Oxidative Stress in Etiopathogenesis of Chemotherapy Induced Cognitive Impairment (CICI)-"Chemobrain". *Aging and disease.* 2016;7(3):307-317.

40. Joshi G, Sultana R, Tangpong J, Cole MP, St Clair DK, Vore M, Estus S, Butterfield DA. Free radical mediated oxidative stress and toxic side effects in brain induced by the anti cancer drug adriamycin: insight into chemobrain. *Free radical research.* 2005;39(11):1147-1154.

41. Konat GW, Kraszpulski M, James I, Zhang HT, Abraham J. Cognitive dysfunction induced by chronic administration of common cancer chemotherapeutics in rats. *Metabolic brain disease.* 2008;23(3):325-333.

42. Tangpong J, Cole MP, Sultana R, Joshi G, Estus S, Vore M, St Clair W, Ratanachaiyavong S, St Clair DK, Butterfield DA. Adriamycin-induced, TNF-alpha-mediated central nervous system toxicity. *Neurobiology of disease.* 2006;23(1):127-139.

43. Kaya E, Keskin L, Aydogdu I, Kuku I, Bayraktar N, Erkut MA. Oxidant/antioxidant parameters and their relationship with chemotherapy in Hodgkin's lymphoma. *The Journal of international medical research.* 2005;33(6):687-692.

44. Kasapovic J, Pejic S, Stojiljkovic V, Todorovic A, Radosevic-Jelic L, Saicic ZS, Pajovic SB. Antioxidant status and lipid peroxidation in the blood of breast cancer patients of different ages after chemotherapy with 5-fluorouracil, doxorubicin and cyclophosphamide. *Clinical biochemistry.* 2010;43(16-17):1287-1293.

45. Joshi G, Aluise CD, Cole MP, Sultana R, Pierce WM, Vore M, St Clair DK, Butterfield DA. Alterations in brain antioxidant enzymes and redox proteomic identification of oxidized brain proteins induced by the anti-cancer drug adriamycin: implications for oxidative stress-mediated chemobrain. *Neuroscience.* 2010;166(3):796-807.

46. Joshi G, Hardas S, Sultana R, St Clair DK, Vore M, Butterfield DA. Glutathione elevation by gamma-glutamyl cysteine ethyl ester as a potential therapeutic strategy for preventing oxidative stress in brain mediated by in vivo administration of adriamycin: Implication for chemobrain. *Journal of neuroscience research.* 2007;85(3):497-503.

47. Zhang H, Davies KJ, Forman HJ. Oxidative stress response and Nrf2 signaling in aging. *Free radical biology & medicine.* 2015;88(Pt B):314-336.

48. Trachootham D, Lu W, Ogasawara MA, Nilsa RD, Huang P. Redox regulation of cell survival. *Antioxidants & redox signaling.* 2008;10(8):1343-1374.

49. Davies KJ. Oxidative stress, antioxidant defenses, and damage removal, repair, and replacement systems. *IUBMB life.* 2000;50(4-5):279-289.

50. Pickering AM, Koop AL, Teoh CY, Ermak G, Grune T, Davies KJ. The immunoproteasome, the 20S proteasome and the PA28alphabeta proteasome regulator are oxidative-stress-adaptive proteolytic complexes. *The Biochemical journal.* 2010;432(3):585-594.

51. Pickering AM, Davies KJ. Degradation of damaged proteins: the main function of the 20S proteasome. *Progress in molecular biology and translational science.* 2012;109:227-248.

52. Lomeli N, Bota DA, Davies KJA. Diminished stress resistance and defective adaptive homeostasis in age-related diseases. *Clin Sci (Lond).* 2017;131(21):2573-2599.

53. Ngo JK, Davies KJ. Mitochondrial Lon protease is a human stress protein. *Free radical biology & medicine.* 2009;46(8):1042-1048.

54. Ngo JK, Pomatto LC, Davies KJ. Upregulation of the mitochondrial Lon Protease allows adaptation to acute oxidative stress but dysregulation is associated with chronic stress, disease, and aging. *Redox biology.* 2013;1:258-264.

55. Rolfe DF, Brown GC. Cellular energy utilization and molecular origin of standard metabolic rate in mammals. *Physiological reviews.* 1997;77(3):731-758.

56. Raefsky SM, Mattson MP. Adaptive responses of neuronal mitochondria to bioenergetic challenges: Roles in neuroplasticity and disease resistance. *Free radical biology & medicine.* 2017;102:203-216.

57. Stone JB, DeAngelis LM. Cancer-treatment-induced neurotoxicity—focus on newer treatments. *Nature Reviews Clinical Oncology.* 2015;13:92.

58. Monje ML, Vogel H, Masek M, Ligon KL, Fisher PG, Palmer TD. Impaired human hippocampal neurogenesis after treatment for central nervous system malignancies. *Ann Neurol.* 2007;62(5):515-520.

59. Andres AL, Gong X, Di K, Bota DA. Low-doses of cisplatin injure hippocampal synapses: a mechanism for 'chemo' brain? *Experimental neurology.* 2014;255:137-144.

60. Gong X, Schwartz PH, Linskey ME, Bota DA. Neural stem/progenitors and glioma stem-like cells have differential sensitivity to chemotherapy. *Neurology.* 2011;76(13):1126-1134.

61. Boukelmoune N, Chiu GS, Kavelaars A, Heijnen CJ. Mitochondrial transfer from mesenchymal stem cells to neural stem cells protects against the neurotoxic effects of cisplatin. *Acta neuropathologica communications.* 2018;6(1):139.

62. Zhou W, Kavelaars A, Heijnen CJ. Metformin Prevents Cisplatin-Induced Cognitive Impairment and Brain Damage in Mice. *PLoS One.* 2016;11(3):e0151890.

63. Chiu GS, Maj MA, Rizvi S, Dantzer R, Vichaya EG, Laumet G, Kavelaars A, Heijnen CJ. Pifithrin-mu Prevents Cisplatin-Induced Chemobrain by Preserving Neuronal Mitochondrial Function. *Cancer Res.* 2017;77(3):742-752.

64. Chiu GS, Boukelmoune N, Chiang ACA, Peng B, Rao V, Kingsley C, Liu HL, Kavelaars A, Kesler SR, Heijnen CJ. Nasal administration of mesenchymal stem cells restores cisplatin-induced cognitive impairment and brain damage in mice. *Oncotarget.* 2018;9(85):35581-35597.

65. Argyriou AA, Assimakopoulos K, Iconomou G, Giannakopoulou F, Kalofonos HP. Either called "chemobrain" or "chemofog," the long-term chemotherapy-induced cognitive decline in cancer survivors is real. *Journal of pain and symptom management.* 2011;41(1):126-139.

66. Weiss B. Chemobrain: a translational challenge for neurotoxicology. *Neurotoxicology.* 2008;29(5):891-898.

67. Screnci D, McKeage MJ, Galettis P, Hambley TW, Palmer BD, Baguley BC. Relationships between hydrophobicity, reactivity, accumulation and peripheral nerve toxicity of a series of platinum drugs. *British journal of cancer.* 2000;82(4):966-972.

68. Koppen C, Reifschneider O, Castanheira I, Sperling M, Karst U, Ciarimboli G. Quantitative imaging of platinum based on laser ablation-inductively coupled plasma-mass spectrometry to investigate toxic side effects of cisplatin. *Metallomics : integrated biometal science.* 2015;7(12):1595-1603.

69. Dzagnidze A, Katsarava Z, Makhalova J, Liedert B, Yoon MS, Kaube H, Limmroth V, Thomale J. Repair Capacity for Platinum-DNA Adducts Determines the Severity of Cisplatin-Induced Peripheral Neuropathy. *J Neurosci* 2007;27(35):9451-9457.

70. Todd RC, Lippard SJ. Inhibition of transcription by platinum antitumor compounds. *Metallomics : integrated biometal science.* 2009;1(4):280-291.

71. Yang Z, Schumaker LM, Egorin MJ, Zuhowski EG, Guo Z, Cullen KJ. Cisplatin preferentially binds mitochondrial DNA and voltage-dependent anion channel

protein in the mitochondrial membrane of head and neck squamous cell carcinoma: possible role in apoptosis. *Clin Cancer Res.* 2006;12(19):5817-5825.

72. Podratz JL, Knight AM, Ta LE, Staff NP, Gass JM, Genelin K, Schlattau A, Lathroum L, Windebank AJ. Cisplatin induced mitochondrial DNA damage in dorsal root ganglion neurons. *Neurobiology of disease.* 2011;41(3):661-668.

73. Areti A, Yerra VG, Naidu V, Kumar A. Oxidative stress and nerve damage: role in chemotherapy induced peripheral neuropathy. *Redox biology.* 2014;2:289-295.

74. Kim HJ, Lee JH, Kim SJ, Oh GS, Moon HD, Kwon KB, Park C, Park BH, Lee HK, Chung SY, Park R, So HS. Roles of NADPH oxidases in cisplatin-induced reactive oxygen species generation and ototoxicity. *The Journal of neuroscience : the official journal of the Society for Neuroscience.* 2010;30(11):3933-3946.

75. Correa DD, Hess LM. Cognitive function and quality of life in ovarian cancer. *Gynecologic oncology.* 2012;124(3):404-409.

76. Hess LM, Chambers SK, Hatch K, Hallum A, Janicek MF, Buscema J, Borst M, Johnson C, Slayton L, Chongpison Y, Alberts DS. Pilot study of the prospective identification of changes in cognitive function during chemotherapy treatment for advanced ovarian cancer. *The journal of supportive oncology.* 2010;8(6):252-258.

77. Verstappen CC, Heimans JJ, Hoekman K, Postma TJ. Neurotoxic complications of chemotherapy in patients with cancer: clinical signs and optimal management. *Drugs.* 2003;63(15):1549-1563.

78. Schagen SB, Muller MJ, Boogerd W, Mellenbergh GJ, Van Dam FS. Change in Cognitive Function After Chemotherapy: a Prospective Longitudinal Study in Breast Cancer Patients. *J Natl Cancer Inst.* 2006;98(23):1742-1745.

79. Czerniawski J, Guzowski JF. Acute neuroinflammation impairs context discrimination memory and disrupts pattern separation processes in hippocampus. *The Journal of neuroscience : the official journal of the Society for Neuroscience.* 2014;34(37):12470-12480.

80. Czerniawski J, Miyashita T, Lewandowski G, Guzowski JF. Systemic lipopolysaccharide administration impairs retrieval of context-object discrimination, but not spatial, memory: Evidence for selective disruption of specific hippocampus-dependent memory functions during acute neuroinflammation. *Brain Behav Immun.* 2015;44:159-166.

81. Barker GR, Warburton EC. When is the hippocampus involved in recognition memory? *The Journal of neuroscience : the official journal of the Society for Neuroscience.* 2011;31(29):10721-10731.

82. Andres AL, Regev L, Phi L, Seese RR, Chen Y, Gall CM, Baram TZ. NMDA Receptor Activation and Calpain Contribute to Disruption of Dendritic Spines by the Stress Neuropeptide CRH. *J Neurosci* 2013;33(43):16945-16960.

83. Santos JH, Meyer JN, Mandavilli BS, Van Houten B. Quantitative PCR-based measurement of nuclear and mitochondrial DNA damage and repair in mammalian cells. *Methods in molecular biology (Clifton, NJ).* 2006;314:183-199.

84. Dranka BP, Benavides GA, Diers AR, Giordano S, Zelickson BR, Reily C, Zou L, Chatham JC, Hill BG, Zhang J, Landar A, Darley-Usmar VM. Assessing bioenergetic function in response to oxidative stress by metabolic profiling. *Free Radic Biol Med.* 2011;51:1621-1635.

85. Zhang J, Nuebel E, Wisidagama DR, Setoguchi K, Hong JS, Van Horn CM, Imam SS, Vergnes L, Malone CS, Koehler CM, Teitell MA. Measuring energy metabolism in cultured cells, including human pluripotent stem cells and differentiated cells. *Nature Protoc.* 2012;7(6):1068-1085.

86. Reagan-Shaw S, Nihal M, Ahmad N. Dose translation from animal to human studies revisited. *FASEB J.* 2007;22:659-661.

87. Rene NJ, Cury FB, Souhami L. Conservative treatment of invasive bladder cancer. *Current oncology (Toronto, Ont).* 2009;16(4):36-47.

88. Muldoon LL, Wu YJ, Pagel MA, Neuwelt EA. N-acetylcysteine chemoprotection without decreased cisplatin antitumor efficacy in pediatric tumor models. *J Neurooncol.* 2015;121(3):433-440.

89. Rosen M, Figliomeni M, Simpkins H. The interaction of platinum antitumour drugs with mouse liver mitochondria. *International journal of experimental pathology.* 1992;73(1):61-74.

90. Clayton DA. Replication and transcription of vertebrate mitochondrial DNA. *Annual review of cell biology.* 1991;7:453-478.

91. Asin-Cayuela J, Gustafsson CM. Mitochondrial transcription and its regulation in mammalian cells. *Trends in biochemical sciences.* 2007;32(3):111-117.

92. Latcha S, Jaimes EA, Patil S, Glezerman IG, Mehta S, Flombaum CD. Long-Term Renal Outcomes after Cisplatin Treatment. *Clinical journal of the American Society of Nephrology : CJASN.* 2016;11(7):1173-1179.

93. Yoo J, Hamilton SJ, Angel D, Fung K, Franklin J, Parnes LS, Lewis D, Venkatesan V, Winquist E. Cisplatin otoprotection using transtympanic L-N-acetylcysteine: a pilot randomized study in head and neck cancer patients. *The Laryngoscope.* 2014;124(3):E87-94.

94. Lin PC, Lee MY, Wang WS, Yen CC, Chao TC, Hsiao LT, Yang MH, Chen PM, Lin KP, Chiou TJ. N-acetylcysteine has neuroprotective effects against oxaliplatin-based adjuvant chemotherapy in colon cancer patients: preliminary data. *Supportive care in cancer : official journal of the Multinational Association of Supportive Care in Cancer.* 2006;14(5):484-487.

95. Kuwahara D, Tsutsumi K, Kobayashi T, Hasunuma T, Nishioka K. Caspase-9 regulates cisplatin-induced apoptosis in human head and neck squamous cell carcinoma cells. *Cancer letters.* 2000;148(1):65-71.

96. Jiang X, Wang X. Cytochrome c promotes caspase-9 activation by inducing nucleotide binding to Apaf-1. *The Journal of biological chemistry.* 2000;275(40):31199-31203.

97. Dasari S, Tchounwou PB. Cisplatin in cancer therapy: molecular mechanisms of action. *European journal of pharmacology.* 2014;740:364-378.

98. Jamieson ER, Lippard SJ. Structure, Recognition, and Processing of Cisplatin-DNA Adducts. *Chemical reviews.* 1999;99(9):2467-2498.

99. Florea AM, Busselberg D. Cisplatin as an anti-tumor drug: cellular mechanisms of activity, drug resistance and induced side effects. *Cancers.* 2011;3(1):1351-1371.

100. Kesler S, Janelsins M, Koovakkattu D, Palesh O, Mustian K, Morrow G, Dhabhar FS. Reduced hippocampal volume and verbal memory performance associated with interleukin-6 and tumor necrosis factor-alpha levels in chemotherapy-treated breast cancer survivors. *Brain Behav Immun.* 2013;30 Suppl:S109-116.

101. de Ruiter MB, Reneman L, Boogerd W, Veltman DJ, Caan M, Douaud G, Lavini C, Linn SC, Boven E, van Dam FS, Schagen SB. Late effects of high-dose adjuvant chemotherapy on white and gray matter in breast cancer survivors: converging results from multimodal magnetic resonance imaging. *Human brain mapping.* 2012;33(12):2971-2983.

102. McDonald BC, Conroy SK, Ahles TA, West JD, Saykin AJ. Gray matter reduction associated with systemic chemotherapy for breast cancer: a prospective MRI study. *Breast cancer research and treatment.* 2010;123(3):819-828.

103. Kam JW, Boyd LA, Hsu CL, Liu-Ambrose T, Handy TC, Lim HJ, Hayden S, Campbell KL. Altered neural activation during prepotent response inhibition in breast cancer survivors treated with chemotherapy: an fMRI study. *Brain Imaging Behav.* 2016;10(3):840-848.

104. Kam JW, Brenner CA, Handy TC, Boyd LA, Liu-Ambrose T, Lim HJ, Hayden S, Campbell KL. Sustained attention abnormalities in breast cancer survivors with cognitive deficits post chemotherapy: An electrophysiological study. *Clinical neurophysiology : official journal of the International Federation of Clinical Neurophysiology.* 2016;127(1):369-378.

105. Amidi A, Agerbaek M, Wu LM, Pedersen AD, Mehlsen M, Clausen CR, Demontis D, Borglum AD, Harboll A, Zachariae R. Changes in cognitive functions and cerebral grey matter and their associations with inflammatory markers, endocrine markers, and APOE genotypes in testicular cancer patients undergoing treatment. *Brain Imaging Behav.* 2016.

106. Stewart DJ, Leavens M, Maor M, Feun L, Luna M, Bonura J, Caprioli R, Loo TL, Benjamin RS. Human central nervous system distribution of cis-diamminedichloroplatinum and use as a radiosensitizer in malignant brain tumors. *Cancer Res.* 1982;42(6):2474-2479.

107. Gregg RW, Molepo JM, Monpetit VJ, Mikael NZ, Redmond D, Gadia M, Stewart DJ. Cisplatin neurotoxicity: the relationship between dosage, time, and platinum concentration in neurologic tissues, and morphologic evidence of toxicity. *J Clin Oncol.* 1992;10(5):795-803.

108. Pereira Dias G, Hollywood R, Bevilaqua MC, da Luz AC, Hindges R, Nardi AE, Thuret S. Consequences of cancer treatments on adult hippocampal neurogenesis: implications for cognitive function and depressive symptoms. *Neuro-oncology.* 2014;16(4):476-492.

109. Seigers R, Fardell JE. Neurobiological basis of chemotherapy-induced cognitive impairment: a review of rodent research. *Neuroscience and biobehavioral reviews.* 2011;35(3):729-741.

110. Schneiderman B. Hippocampal volumes smaller in chemotherapy patients. *Lancet Oncol.* 2004;5(4):202.

111. Oz M, Nurullahoglu AKE, Yerlikaya FH, Demir EA. Curcumin alleviates cisplatin-induced learning and memory impairments. *Neurobiology of learning and memory.* 2015;123:43-49.

112. Pompella A, Visvikis A, Paolicchi A, Tata VD, Casini AF. The changing faces of glutathione, a cellular protagonist. *Biochemical Pharmacology.* 2003;66(8):1499-1503.

113. McLellan LI, Lewis AD, Hall DJ, Ansell JD, Wolf CR. Uptake and distribution of N-acetylcysteine in mice: tissue-specific effects on glutathione concentrations. *Carcinogenesis.* 1995;16(9):2099-2106.

114. Adair JC, Knoefel JE, Morgan N. Controlled trial of N-acetylcysteine for patients with probable Alzheimer's disease. *Neurology.* 2001;57(8):1515-1517.

115. Millea PJ. N-acetylcysteine: multiple clinical applications. *American family physician.* 2009;80(3):265-269.

116. Sandhir R, Sood A, Mehrotra A, Kamboj SS. N-Acetylcysteine reverses mitochondrial dysfunctions and behavioral abnormalities in 3-nitropropionic acid-induced Huntington's disease. *Neurodegener Dis.* 2012;9(3):145-157.

117. Cascinu S, Catalano V, Cordella L, Labianca R, Giordani P, Baldelli AM, Beretta GD, Ubiali E, Catalano G. Neuroprotective Effect of Reduced Glutathione on Oxaliplatin-Based Chemotherapy in Advanced Colorectal Cancer: A Randomized, Double-Blind, Placebo-Controlled Trial. *Journal of Clinical Oncology.* 2002;20(16):3478-3483.

118. Estensen RD, Levy M, Klopp SJ, Galbraith AR, Mandel JS, Blomquist JA, Wattenberg LW. N-acetylcysteine suppression of the proliferative index in the colon of patients with previous adenomatous colonic polyps. *Cancer letters.* 1999;147(1-2):109-114.

119. Holoye PY. "Ifosfamide plus N-acetylcysteine in the treatment of small cell and non-small cell carcinoma of the lung: a Southeastern Cancer Study Group Trial". *Cancer treatment reports.* 1987;71(4):431-432.

120. Morgan LR, Donley PJ, Harrison EF, Hunter HL. Protective effect of N-acetylcysteine on the urotoxicity produced by oxazaphosphorine without interference with anticancer activity. *European journal of cancer & clinical oncology.* 1982;18(1):113-114.

121. Myers JS. Chemotherapy-related cognitive impairment: the breast cancer experience. *Oncol Nurs Forum.* 2012;39(1):E31-40.

122. Anderson FS, Kunin-Batson AS. Neurocognitive late effects of chemotherapy in children: the past 10 years of research on brain structure and function. *Pediatric blood & cancer.* 2009;52(2):159-164.

123. Anderson-Hanley C, Sherman ML, Riggs R, Agocha VB, Compas BE. Neuropsychological effects of treatments for adults with cancer: a meta-analysis and review of the literature. *Journal of the International Neuropsychological Society : JINS.* 2003;9(7):967-982.

124. Wefel JS, Witgert ME, Meyers CA. Neuropsychological sequelae of non-central nervous system cancer and cancer therapy. *Neuropsychol Rev.* 2008;18(2):121-131.

125. Iyer NS, Balsamo LM, Bracken MB, Kadan-Lottick NS. Chemotherapy-only treatment effects on long-term neurocognitive functioning in childhood ALL survivors: a review and meta-analysis. *Blood.* 2015;126(3):346-353.

126. Duffner PK, Armstrong FD, Chen L, Helton KJ, Brecher ML, Bell B, Chauvenet AR. Neurocognitive and neuroradiologic central nervous system late effects in children treated on Pediatric Oncology Group (POG) P9605 (standard risk) and P9201 (lesser risk) acute lymphoblastic leukemia protocols (ACCL0131): a methotrexate

consequence? A report from the Children's Oncology Group. *Journal of pediatric hematology/oncology.* 2014;36(1):8-15.

127. Conklin HM, Krull KR, Reddick WE, Pei D, Cheng C, Pui CH. Cognitive outcomes following contemporary treatment without cranial irradiation for childhood acute lymphoblastic leukemia. *Journal of the National Cancer Institute.* 2012;104(18):1386-1395.

128. Kadan-Lottick NS, Zeltzer LK, Liu Q, Yasui Y, Ellenberg L, Gioia G, Robison LL, Krull KR. Neurocognitive functioning in adult survivors of childhood non-central nervous system cancers. *Journal of the National Cancer Institute.* 2010;102(12):881-893.

129. Vardy J, Tannock I. Cognitive function after chemotherapy in adults with solid tumours. *Critical reviews in oncology/hematology.* 2007;63(3):183-202.

130. John TD, Sender LS, Bota DA. Cognitive Impairment in Survivors of Adolescent and Early Young Adult Onset Non-CNS Cancers: Does Chemotherapy Play a Role? *J Adolesc Young Adult Oncol.* 2016.

131. Pizzo PA, Poplack DG. *Principles and practice of pediatric oncology.* 6th ed. Philadelphia, PA: Wolters Kluwer/Lippincott Williams & Wilkins Health; 2011.

132. Nakagawa H, Fujita T, Kubo S, Tokiyoshi K, Yamada M, Kanayama T, Hagiwara Y, Nakanomyo H, Hiraoka M. Difference in CDDP penetration into CSF between selective intraarterial chemotherapy in patients with malignant glioma and intravenous or intracarotid administration in patients with metastatic brain tumor. *Cancer Chemother Pharmacol.* 1996;37(4):317-326.

133. Howlader N, Noone AM, Krapcho M, Miller D, Bishop K, Kosary CL, Yu M, Ruhl J, Tatalovich Z, Mariotto A, Lewis DR, Chen HS, Feuer EJ, Cronin KA. *SEER Cancer Statistics Review, 1975-2014.* 2017.

134. Sengupta P. The Laboratory Rat: Relating Its Age With Human's. *International journal of preventive medicine.* 2013;4(6):624-630.

135. Andreollo NA, Santos EF, Araujo MR, Lopes LR. Rat's age versus human's age: what is the relationship? *Arquivos brasileiros de cirurgia digestiva : ABCD = Brazilian archives of digestive surgery.* 2012;25(1):49-51.

136. Rzeski W, Pruskil S, Macke A, Felderhoff-Mueser U, Reiher AK, Hoerster F, Jansma C, Jarosz B, Stefovska V, Bittigau P, Ikonomidou C. Anticancer agents are potent neurotoxins in vitro and in vivo. *Ann Neurol.* 2004;56(3):351-360.

137. Reiriz AB, Reolon GK, Preissler T, Rosado JO, Henriques JA, Roesler R, Schwartsmann G. Cancer chemotherapy and cognitive function in rodent models: memory impairment induced by cyclophosphamide in mice. *Clin Cancer Res.* 2006;12(16):5000.

138. Bisen-Hersh EB, Hineline PN, Walker EA. Effects of early chemotherapeutic treatment on learning in adolescent mice: implications for cognitive impairment and remediation in childhood cancer survivors. *Clin Cancer Res.* 2013;19(11):3008-3018.

139. Barker GR, Bird F, Alexander V, Warburton EC. Recognition memory for objects, place, and temporal order: a disconnection analysis of the role of the medial prefrontal cortex and perirhinal cortex. *The Journal of neuroscience : the official journal of the Society for Neuroscience.* 2007;27(11):2948-2957.

140. Baxter MG. "I've seen it all before": explaining age-related impairments in object recognition. Theoretical comment on Burke et al. (2010). *Behav Neurosci.* 2010;124(5):706-709.

141. Mumby DG, Gaskin S, Glenn MJ, Schramek TE, Lehmann H. Hippocampal damage and exploratory preferences in rats: memory for objects, places, and contexts. *Learn Mem.* 2002;9(2):49-57.

142. Phillips RG, LeDoux JE. Differential contribution of amygdala and hippocampus to cued and contextual fear conditioning. *Behav Neurosci.* 1992;106(2):274-285.

143. Maren S, Aharonov G, Fanselow MS. Neurotoxic lesions of the dorsal hippocampus and Pavlovian fear conditioning in rats. *Behav Brain Res.* 1997;88(2):261-274.

144. Konrad K, Firk C, Uhlhaas PJ. Brain development during adolescence: neuroscientific insights into this developmental period. *Dtsch Arztebl Int.* 2013;110(25):425-431.

145. van Praag H, Qu PM, Elliott RC, Wu H, Dreyfus CF, Black IB. Unilateral hippocampal lesions in newborn and adult rats: effects on spatial memory and BDNF gene expression. *Behav Brain Res.* 1998;92(1):21-30.

146. Alhadeff AL, Holland RA, Nelson A, Grill HJ, De Jonghe BC. Glutamate Receptors in the Central Nucleus of the Amygdala Mediate Cisplatin-Induced Malaise and Energy Balance Dysregulation through Direct Hindbrain Projections. *The Journal of neuroscience : the official journal of the Society for Neuroscience.* 2015;35(31):11094-11104.

147. Semple BD, Blomgren K, Gimlin K, Ferriero DM, Noble-Haeusslein LJ. Brain development in rodents and humans: Identifying benchmarks of maturation and vulnerability to injury across species. *Progress in neurobiology.* 2013;106-107:1-16.

148. Giedd JN, Blumenthal J, Jeffries NO, Castellanos FX, Liu H, Zijdenbos A, Paus T, Evans AC, Rapoport JL. Brain development during childhood and adolescence: a longitudinal MRI study. *Nature neuroscience.* 1999;2(10):861-863.

149. Micheva KD, Beaulieu C. Quantitative aspects of synaptogenesis in the rat barrel field cortex with special reference to GABA circuitry. *The Journal of comparative neurology.* 1996;373(3):340-354.

150. Zhong J, Carrozza DP, Williams K, Pritchett DB, Molinoff PB. Expression of mRNAs encoding subunits of the NMDA receptor in developing rat brain. *Journal of neurochemistry.* 1995;64(2):531-539.

151. Huttenlocher PR. Synaptic density in human frontal cortex - developmental changes and effects of aging. *Brain research.* 1979;163(2):195-205.

152. Stavraka C, Ford A, Ghaem-Maghami S, Crook T, Agarwal R, Gabra H, Blagden S. A study of symptoms described by ovarian cancer survivors. *Gynecologic oncology.* 2012;125(1):59-64.

153. Pearre DC, Bota DA. Chemotherapy-related cognitive dysfunction and effects on quality of life in gynecologic cancer patients. *Expert Rev Qual Life Cancer Care.* 2018;3(1):19-26.

154. John T, Lomeli N, Bota DA. Systemic cisplatin exposure during infancy and adolescence causes impaired cognitive function in adulthood. *Behav Brain Res.* 2017;319:200-206.

155. Zafarullah M, Li WQ, Sylvester J, Ahmad M. Molecular mechanisms of N-acetylcysteine actions. *Cellular and Molecular Life Sciences CMLS.* 2003;60(1):6-20.

156. Abdel-Wahab WM, Moussa FI, Saad NA. Synergistic protective effect of N-acetylcysteine and taurine against cisplatin-induced nephrotoxicity in rats. *Drug Des Devel Ther.* 2017;11:901-908.

157. Huang S, You J, Wang K, Li Y, Zhang Y, Wei H, Liang X, Liu Y. N-Acetylcysteine Attenuates Cisplatin-Induced Acute Kidney Injury by Inhibiting the C5a Receptor. *Biomed Res Int.* 2019;2019:4805853.

158. Dickey DT, Wu YJ, Muldoon LL, Neuwelt EA. Protection against cisplatin-induced toxicities by N-acetylcysteine and sodium thiosulfate as assessed at the molecular, cellular, and in vivo levels. *J Pharmacol Exp Ther.* 2005;314(3):1052-1058.

159. D'Andrea GM. Use of antioxidants during chemotherapy and radiotherapy should be avoided. *CA Cancer J Clin.* 2005;55(5):319-321.

160. Dickey DT, Muldoon LL, Doolittle ND, Peterson DR, Kraemer DF, Neuwelt EA. Effect of N-acetylcysteine route of administration on chemoprotection against cisplatin-induced toxicity in rat models. *Cancer Chemother Pharmacol.* 2008;62(2):235-241.

161. Yu D, Wolf JK, Scanlon M, Price JE, Hung MC. Enhanced c-erbB-2/neu expression in human ovarian cancer cells correlates with more severe malignancy that can be suppressed by E1A. *Cancer Res.* 1993;53(4):891-898.

162. Lecuru F, Agostini A, Camatte S, Robin F, Aggerbeck M, Jais JP, Vilde F, Taurelle R. Impact of pneumoperitoneum on tumor growth. *Surg Endosc.* 2002;16(8):1170-1174.

163. Lecuru F, Guilbaud N, Agostini A, Augereau C, Vilde F, Taurelle R. Description of two new human ovarian carcinoma models in nude rats suitable for laparoscopic experimentation. *Surg Endosc.* 2001;15(11):1346-1352.

164. Owen JB, Butterfield DA. Measurement of oxidized/reduced glutathione ratio. *Methods in molecular biology (Clifton, NJ).* 2010;648:269-277.

165. Rahman I, Kode A, Biswas SK. Assay for quantitative determination of glutathione and glutathione disulfide levels using enzymatic recycling method. *Nature Protocols.* 2006;1(6):3159-3165.

166. Wu YJ, Muldoon LL, Neuwelt EA. The Chemoprotective Agent N-Acetylcysteine Blocks Cisplatin-Induced Apoptosis through Caspase Signaling Pathway. *Journal of Pharmacology and Experimental Therapeutics.* 2005;312(2):424-431.

167. Luo J, Tsuji T, Yasuda H, Sun Y, Fujigaki Y, Hishida A. The molecular mechanisms of the attenuation of cisplatin-induced acute renal failure by N-acetylcysteine in rats. *Nephrol Dial Transplant.* 2008;23(7):2198-2205.

168. Beeson CC, Beeson GC, Schnellmann RG. A high-throughput respirometric assay for mitochondrial biogenesis and toxicity. *Anal Biochem.* 2010;404(1):75-81.

169. Gorgun MF, Zhuo M, Englander EW. Cisplatin Toxicity in Dorsal Root Ganglion Neurons Is Relieved by Meclizine via Diminution of Mitochondrial Compromise and Improved Clearance of DNA Damage. *Molecular neurobiology.* 2016.

170. Fernandez-Fernandez S, Bobo-Jimenez V, Requejo-Aguilar R, Gonzalez-Fernandez S, Resch M, Carabias-Carrasco M, Ros J, Almeida A, Bolaños JP. Hippocampal neurons require a large pool of glutathione to sustain dendrite integrity and cognitive function. *Redox biology.* 2018;19:52-61.

171. Winocur G, Johnston I, Castel H. Chemotherapy and cognition: International cognition and cancer task force recommendations for harmonising preclinical research. *Cancer treatment reviews.* 2018;69:72-83.

172. Winocur G, Berman H, Nguyen M, Binns MA, Henkelman M, van Eede M, Piquette-Miller M, Sekeres MJ, Wojtowicz JM, Yu J, Zhang H, Tannock IF. Neurobiological Mechanisms of Chemotherapy-induced Cognitive Impairment in a Transgenic Model of Breast Cancer. *Neuroscience.* 2018;369:51-65.

173. Khynriam D, Prasad SB. Hematotoxicity and blood glutathione levels after cisplatin treatment of tumor-bearing mice. *Cell Biol Toxicol.* 2001;17(6):357-370.

174. Green JL, Heard KJ, Reynolds KM, Albert D. Oral and Intravenous Acetylcysteine for Treatment of Acetaminophen Toxicity: A Systematic Review and Meta-analysis. *West J Emerg Med.* 2013;14(3):218-226.

175. Ishikawa T, Ali-Osman F. Glutathione-associated cis-diamminedichloroplatinum(II) metabolism and ATP-dependent efflux from leukemia cells. Molecular characterization of glutathione-platinum complex and its biological significance. *The Journal of biological chemistry.* 1993;268(27):20116-20125.

176. Ezerina D, Takano Y, Hanaoka K, Urano Y, Dick TP. N-Acetyl Cysteine Functions as a Fast-Acting Antioxidant by Triggering Intracellular H2S and Sulfane Sulfur Production. *Cell Chem Biol.* 2018;25(4):447-459.e444.

177. Zhang S, Hu X, Guan W, Luan L, Li B, Tang Q, Fan H. Isoflurane anesthesia promotes cognitive impairment by inducing expression of β-amyloid protein-related factors in the hippocampus of aged rats. *PloS one.* 2017;12(4):e0175654-e0175654.

178. Cimprich B, Reuter-Lorenz P, Nelson J, Clark PM, Therrien B, Normolle D, Berman MG, Hayes DF, Noll DC, Peltier S, Welsh RC. Prechemotherapy alterations in brain function in women with breast cancer. *J Clin Exp Neuropsychol.* 2010;32(3):324-331.

179. Vardy JL, Dhillon HM, Pond GR, Rourke SB, Bekele T, Renton C, Dodd A, Zhang H, Beale P, Clarke S, Tannock IF. Cognitive Function in Patients With Colorectal Cancer Who Do and Do Not Receive Chemotherapy: A Prospective, Longitudinal, Controlled Study. *Journal of clinical oncology : official journal of the American Society of Clinical Oncology.* 2015;33(34):4085-4092.

180. Taphoorn MJ, Klein M. Cognitive deficits in adult patients with brain tumours. *The Lancet Neurology.* 2004;3(3):159-168.

181. Krebber AM, Buffart LM, Kleijn G, Riepma IC, de Bree R, Leemans CR, Becker A, Brug J, van Straten A, Cuijpers P, Verdonck-de Leeuw IM. Prevalence of depression in cancer patients: a meta-analysis of diagnostic interviews and self-report instruments. *Psycho-oncology.* 2014;23(2):121-130.

182. Steinbach JP, Blaicher HP, Herrlinger U, Wick W, Nagele T, Meyermann R, Tatagiba M, Bamberg M, Dichgans J, Karnath HO, Weller M. Surviving glioblastoma for more than 5 years: the patient's perspective. *Neurology.* 2006;66(2):239-242.

183. Hottinger AF, Yoon H, DeAngelis LM, Abrey LE. Neurological outcome of long-term glioblastoma survivors. *J Neurooncol.* 2009;95(3):301-305.

184. Allen DH, Loughan AR. Impact of Cognitive Impairment in Patients with Gliomas. *Seminars in oncology nursing.* 2018;34(5):528-546.

185. Abrey LE. The impact of chemotherapy on cognitive outcomes in adults with primary brain tumors. *J Neurooncol.* 2012;108(2):285-290.

186. Wu PH, Coultrap S, Pinnix C, Davies KD, Tailor R, Ang KK, Browning MD, Grosshans DR. Radiation induces acute alterations in neuronal function. *PLoS One.* 2012;7(5):e37677.

187. Parihar VK, Limoli CL. Cranial irradiation compromises neuronal architecture in the hippocampus. *Proceedings of the National Academy of Sciences of the United States of America.* 2013;110(31):12822-12827.

188. Nolen SC, Lee B, Shantharam S, Yu HJ, Su L, Billimek J, Bota DA. The effects of sequential treatments on hippocampal volumes in malignant glioma patients. *J Neurooncol.* 2016;129(3):433-441.

189. Acharya MM, Christie LA, Lan ML, Giedzinski E, Fike JR, Rosi S, Limoli CL. Human neural stem cell transplantation ameliorates radiation-induced cognitive dysfunction. *Cancer Res.* 2011;71(14):4834-4845.

190. Agnihotri S, Burrell KE, Wolf A, Jalali S, Hawkins C, Rutka JT, Zadeh G. Glioblastoma, a brief review of history, molecular genetics, animal models and novel therapeutic strategies. *Archivum immunologiae et therapiae experimentalis.* 2013;61(1):25-41.

191. Di K, Lomeli N, Wood SD, Vanderwal CD, Bota DA. Mitochondrial Lon is over-expressed in high-grade gliomas, and mediates hypoxic adaptation: potential role of Lon as a therapeutic target in glioma. *Oncotarget.* 2016;7(47):77457-77467.

192. Oliva CR, Nozell SE, Diers A, McClugage SG, 3rd, Sarkaria JN, Markert JM, Darley-Usmar VM, Bailey SM, Gillespie GY, Landar A, Griguer CE. Acquisition of temozolomide chemoresistance in gliomas leads to remodeling of mitochondrial electron transport chain. *The Journal of biological chemistry.* 2010;285(51):39759-39767.

193. Egeland M, Guinaudie C, Du Preez A, Musaelyan K, Zunszain PA, Fernandes C, Pariante CM, Thuret S. Depletion of adult neurogenesis using the chemotherapy drug temozolomide in mice induces behavioural and biological changes relevant to depression. *Translational psychiatry.* 2017;7(4):e1101.

194. Pereira-Caixeta AR, Guarnieri LO, Medeiros DC, Mendes E, Ladeira LCD, Pereira MT, Moraes MFD, Pereira GS. Inhibiting constitutive neurogenesis compromises long-term social recognition memory. *Neurobiology of learning and memory.* 2018;155:92-103.

195. Niibori Y, Yu TS, Epp JR, Akers KG, Josselyn SA, Frankland PW. Suppression of adult neurogenesis impairs population coding of similar contexts in hippocampal CA3 region. *Nature communications.* 2012;3:1253.

196. Garthe A, Behr J, Kempermann G. Adult-generated hippocampal neurons allow the flexible use of spatially precise learning strategies. *PLoS One.* 2009;4(5):e5464.

197. Schmidt-Hieber C, Jonas P, Bischofberger J. Enhanced synaptic plasticity in newly generated granule cells of the adult hippocampus. *Nature.* 2004;429(6988):184-187.

198. Snyder JS, Kee N, Wojtowicz JM. Effects of adult neurogenesis on synaptic plasticity in the rat dentate gyrus. *Journal of neurophysiology.* 2001;85(6):2423-2431.

199. Lin MT, Beal MF. Mitochondrial dysfunction and oxidative stress in neurodegenerative diseases. *Nature.* 2006;443:787.

200. Schon EA, Manfredi G. Neuronal degeneration and mitochondrial dysfunction. *The Journal of clinical investigation.* 2003;111(3):303-312.

201. Commandeur JN, Stijntjes GJ, Vermeulen NP. Enzymes and transport systems involved in the formation and disposition of glutathione S-conjugates. Role in bioactivation and detoxication mechanisms of xenobiotics. *Pharmacological reviews.* 1995;47(2):271-330.

202. Raefsky SM, Mattson MP. Adaptive responses of neuronal mitochondria to bioenergetic challenges: Roles in neuroplasticity and disease resistance. *Free Radical Biology and Medicine.* 2017;102:203-216.

203. Oboh G, Ogunruku OO. Cyclophosphamide-induced oxidative stress in brain: protective effect of hot short pepper (Capsicum frutescens L. var. abbreviatum). *Experimental and toxicologic pathology : official journal of the Gesellschaft fur Toxikologische Pathologie.* 2010;62(3):227-233.

204. Keeney JTR, Ren X, Warrier G, Noel T, Powell DK, Brelsfoard JM, Sultana R, Saatman KE, Clair DKS, Butterfield DA. Doxorubicin-induced elevated oxidative stress and neurochemical alterations in brain and cognitive decline: protection by MESNA and insights into mechanisms of chemotherapy-induced cognitive impairment ("chemobrain"). *Oncotarget.* 2018;9(54):30324-30339.

205. Tangpong J, Cole MP, Sultana R, Estus S, Vore M, St Clair W, Ratanachaiyavong S, St Clair DK, Butterfield DA. Adriamycin-mediated nitration of manganese superoxide dismutase in the central nervous system: insight into the mechanism of chemobrain. *Journal of neurochemistry.* 2007;100(1):191-201.

206. Hess JA, Khasawneh MK. Cancer metabolism and oxidative stress: Insights into carcinogenesis and chemotherapy via the non-dihydrofolate reductase effects of methotrexate. *BBA Clinical.* 2015;3:152-161.

207. Schwartz PH, Bryant PJ, Fuja TJ, Su H, O'Dowd DK, Klassen H. Isolation and characterization of neural progenitor cells from post-mortem human cortex. *Journal of neuroscience research.* 2003;74(6):838-851.

208. Lee SY. Temozolomide resistance in glioblastoma multiforme. *Genes & Diseases.* 2016;3(3):198-210.

209. Larsen NB, Rasmussen M, Rasmussen LJ. Nuclear and mitochondrial DNA repair: similar pathways? *Mitochondrion.* 2005;5(2):89-108.

210. Acin-Perez R, Bayona-Bafaluy MP, Fernandez-Silva P, Moreno-Loshuertos R, Perez-Martos A, Bruno C, Moraes CT, Enriquez JA. Respiratory complex III is required to maintain complex I in mammalian mitochondria. *Molecular cell.* 2004;13(6):805-815.

211. Budde SM, van den Heuvel LP, Janssen AJ, Smeets RJ, Buskens CA, DeMeirleir L, Van Coster R, Baethmann M, Voit T, Trijbels JM, Smeitink JA. Combined enzymatic complex I and III deficiency associated with mutations in the nuclear encoded NDUFS4 gene. *Biochemical and biophysical research communications.* 2000;275(1):63-68.

212. Blakely EL, Mitchell AL, Fisher N, Meunier B, Nijtmans LG, Schaefer AM, Jackson MJ, Turnbull DM, Taylor RW. A mitochondrial cytochrome b mutation causing severe respiratory chain enzyme deficiency in humans and yeast. *The FEBS journal.* 2005;272(14):3583-3592.

213. Anderson S, Bankier AT, Barrell BG, de Bruijn MHL, Coulson AR, Drouin J, Eperon IC, Nierlich DP, Roe BA, Sanger F, Schreier PH, Smith AJH, Staden R, Young IG. Sequence and organization of the human mitochondrial genome. *Nature.* 1981;290:457.

214. Wu L, Guo D, Liu Q, Gao F, Wang X, Song X, Wang F, Zhan R-Z. Abnormal Development of Dendrites in Adult-Born Rat Hippocampal Granule Cells Induced by Cyclophosphamide. *Frontiers in Cellular Neuroscience.* 2017;11:171.

215. Manchon JFM, Dabaghian Y, Uzor N-E, Kesler SR, Wefel JS, Tsvetkov AS. Levetiracetam mitigates doxorubicin-induced DNA and synaptic damage in neurons. *Scientific Reports.* 2016;6:25705.

216. Seigers R, Schagen SB, Van Tellingen O, Dietrich J. Chemotherapy-related cognitive dysfunction: current animal studies and future directions. *Brain Imaging and Behavior.* 2013;7(4):453-459.

217. Latzer P, Schlegel U, Theiss C. Morphological Changes of Cortical and Hippocampal Neurons after Treatment with VEGF and Bevacizumab. *CNS neuroscience & therapeutics.* 2016;22(6):440-450.

218. Newpher TM, Ehlers MD. Spine microdomains for postsynaptic signaling and plasticity. *Trends in cell biology.* 2009;19(5):218-227.

219. Sturgill JF, Steiner P, Czervionke BL, Sabatini BL. Distinct domains within PSD-95 mediate synaptic incorporation, stabilization, and activity-dependent trafficking. *The Journal of neuroscience : the official journal of the Society for Neuroscience.* 2009;29(41):12845-12854.

220. Zhang WB, Wang Z, Shu F, Jin YH, Liu HY, Wang QJ, Yang Y. Activation of AMP-activated protein kinase by temozolomide contributes to apoptosis in glioblastoma cells via p53 activation and mTORC1 inhibition. *The Journal of biological chemistry.* 2010;285(52):40461-40471.

221. Oliva CR, Moellering DR, Gillespie GY, Griguer CE. Acquisition of Chemoresistance in Gliomas Is Associated with Increased Mitochondrial Coupling and Decreased ROS Production. *PLOS ONE.* 2011;6(9):e24665.

222. Resende FFB, Titze-de-Almeida SS, Titze-de-Almeida R. Function of neuronal nitric oxide synthase enzyme in temozolomide-induced damage of astrocytic tumor cells. *Oncology letters.* 2018;15(4):4891-4899.

223. Boatright KM, Salvesen GS. Mechanisms of caspase activation. *Current opinion in cell biology.* 2003;15(6):725-731.

224. Agarwala SS, Kirkwood JM. Temozolomide in combination with interferon alpha-2b in patients with metastatic melanoma: a phase I dose-escalation study. *Cancer.* 2003;97(1):121-127.

225. Prust MJ, Jafari-Khouzani K, Kalpathy-Cramer J, Polaskova P, Batchelor TT, Gerstner ER, Dietrich J. Standard chemoradiation for glioblastoma results in progressive brain volume loss. *Neurology.* 2015;85(8):683-691.

226. Karas GB, Burton EJ, Rombouts SA, van Schijndel RA, O'Brien JT, Scheltens P, McKeith IG, Williams D, Ballard C, Barkhof F. A comprehensive study of gray matter loss in patients with Alzheimer's disease using optimized voxel-based morphometry. *NeuroImage.* 2003;18(4):895-907.

227. Madsen SK, Gutman BA, Joshi SH, Toga AW, Jack CR, Jr., Weiner MW, Thompson PM. Mapping ventricular expansion onto cortical gray matter in older adults. *Neurobiology of aging.* 2015;36 Suppl 1:S32-41.

228. Bag AK, Kim H, Gao Y, Bolding M, Warren PP, Fathallah-Shaykh HM, Gurler D, Markert JM, Fiveash J, Beasley TM, Khawaja A, Friedman GK, Chapman PR, Nabors LB, Han X. Prolonged treatment with bevacizumab is associated with brain

atrophy: a pilot study in patients with high-grade gliomas. *J Neurooncol.* 2015;122(3):585-593.

229. Gilbert MR, Dignam JJ, Armstrong TS, Wefel JS, Blumenthal DT, Vogelbaum MA, Colman H, Chakravarti A, Pugh S, Won M, Jeraj R, Brown PD, Jaeckle KA, Schiff D, Stieber VW, Brachman DG, Werner-Wasik M, Tremont-Lukats IW, Sulman EP, Aldape KD, Curran WJ, Mehta MP. A Randomized Trial of Bevacizumab for Newly Diagnosed Glioblastoma. *New England Journal of Medicine.* 2014;370(8):699-708.

230. Vairano M, Graziani G, Tentori L, Tringali G, Navarra P, Russo CD. Primary cultures of microglial cells for testing toxicity of anticancer drugs. *Toxicology Letters.* 2004;148(1):91-94.

231. Norregaard A, Jensen SS, Kolenda J, Aaberg-Jessen C, Christensen KG, Jensen PH, Schroder HD, Kristensen BW. Effects of chemotherapeutics on organotypic corticostriatal slice cultures identified by a panel of fluorescent and immunohistochemical markers. *Neurotoxicity research.* 2012;22(1):43-58.

232. Eyupoglu IY, Hahnen E, Trankle C, Savaskan NE, Siebzehnrubl FA, Buslei R, Lemke D, Wick W, Fahlbusch R, Blumcke I. Experimental therapy of malignant gliomas using the inhibitor of histone deacetylase MS-275. *Molecular cancer therapeutics.* 2006;5(5):1248-1255.

233. Fung C, Dinh P, Ardeshir-Rouhani-Fard S, Schaffer K, Fossa SD, Travis LB. Toxicities Associated with Cisplatin-Based Chemotherapy and Radiotherapy in Long-Term Testicular Cancer Survivors. *Advances in Urology.* 2018;2018:20.

234. Stouten-Kemperman MM, de Ruiter MB, Caan MW, Boogerd W, Kerst MJ, Reneman L, Schagen SB. Lower cognitive performance and white matter changes in testicular cancer survivors 10 years after chemotherapy. *Human brain mapping.* 2015;36(11):4638-4647.

235. Yang M, Kim J, Kim JS, Kim SH, Kim JC, Kang MJ, Jung U, Shin T, Wang H, Moon C. Hippocampal dysfunctions in tumor-bearing mice. *Brain Behav Immun.* 2014;36:147-155.

236. Lee HC, Wei YH. Mitochondrial biogenesis and mitochondrial DNA maintenance of mammalian cells under oxidative stress. *Int J Biochem Cell Biol.* 2005;37(4):822-834.

237. Medeiros DM. Assessing mitochondria biogenesis. *Methods.* 2008;46(4):288-294.

238. Bouchez C, Devin A. Mitochondrial Biogenesis and Mitochondrial Reactive Oxygen Species (ROS): A Complex Relationship Regulated by the cAMP/PKA Signaling Pathway. *Cells.* 2019;8(4):287.

239. Schneider L, Pellegatta S, Favaro R, Pisati F, Roncaglia P, Testa G, Nicolis SK, Finocchiaro G, d'Adda di Fagagna F. DNA damage in mammalian neural stem cells leads to astrocytic differentiation mediated by BMP2 signaling through JAK-STAT. *Stem cell reports.* 2013;1(2):123-138.

240. Wang W, Osenbroch P, Skinnes R, Esbensen Y, Bjoras M, Eide L. Mitochondrial DNA Integrity Is Essential for Mitochondrial Maturation During Differentiation of Neural Stem Cells. *Stem Cells.* 2010;28:2195-2204.

241. Prozorovski T, Schulze-Topphoff U, Glumm R, Baumgart J, Schroter F, Ninnemann O, Siegert E, Bendix I, Brustle O, Nitsch R, Zipp F, Aktas O. Sirt1 contributes critically to the redox-dependent fate of neural progenitors. *Nature cell biology.* 2008;10(4):385-394.

242. Pushpakom S, Iorio F, Eyers PA, Escott KJ, Hopper S, Wells A, Doig A, Guilliams T, Latimer J, McNamee C, Norris A, Sanseau P, Cavalla D, Pirmohamed M. Drug repurposing: progress, challenges and recommendations. *Nat Rev Drug Discov.* 2019;18(1):41-58.

243. Correa DD, Root JC, Kryza-Lacombe M, Mehta M, Karimi S, Hensley ML, Relkin N. Brain structure and function in patients with ovarian cancer treated with first-line chemotherapy: a pilot study. *Brain imaging and behavior.* 2017;11(6):1652-1663.

244. Limon-Pacheco JH, Hernandez NA, Fanjul-Moles ML, Gonsebatt ME. Glutathione depletion activates mitogen-activated protein kinase (MAPK) pathways that display organ-specific responses and brain protection in mice. *Free radical biology & medicine.* 2007;43(9):1335-1347.

245. Ozkok A, Edelstein CL. Pathophysiology of Cisplatin-Induced Acute Kidney Injury. *BioMed Research International.* 2014;2014:967826.

246. Scuteri A, Galimberti A, Maggioni D, Ravasi M, Pasini S, Nicolini G, Bossi M, Miloso M, Cavaletti G, Tredici G. Role of MAPKs in platinum-induced neuronal apoptosis. *Neurotoxicology.* 2009;30(2):312-319.

247. Ki YW, Park JH, Lee JE, Shin IC, Koh HC. JNK and p38 MAPK regulate oxidative stress and the inflammatory response in chlorpyrifos-induced apoptosis. *Toxicol Lett.* 2013;218(3):235-245.

248. Wang W, Shi L, Xie Y, Ma C, Li W, Su X, Huang S, Chen R, Zhu Z, Mao Z, Han Y, Li M. SP600125, a new JNK inhibitor, protects dopaminergic neurons in the MPTP model of Parkinson's disease. *Neuroscience Research.* 2004;48(2):195-202.

249. Zhuang ZY, Wen YR, Zhang DR, Borsello T, Bonny C, Strichartz GR, Decosterd I, Ji RR. A peptide c-Jun N-terminal kinase (JNK) inhibitor blocks mechanical allodynia after spinal nerve ligation: respective roles of JNK activation in primary sensory neurons and spinal astrocytes for neuropathic pain development and

maintenance. *The Journal of neuroscience : the official journal of the Society for Neuroscience.* 2006;26(13):3551-3560.

250. Guan Q-H, Pei D-S, Zhang Q-G, Hao Z-B, Xu T-L, Zhang G-Y. The neuroprotective action of SP600125, a new inhibitor of JNK, on transient brain ischemia/reperfusion-induced neuronal death in rat hippocampal CA1 via nuclear and non-nuclear pathways. *Brain research.* 2005;1035(1):51-59.

251. Guan Q-H, Pei D-S, Liu X-M, Wang X-T, Xu T-L, Zhang G-Y. Neuroprotection against ischemic brain injury by SP600125 via suppressing the extrinsic and intrinsic pathways of apoptosis. *Brain research.* 2006;1092(1):36-46.

252. Alam J, Blackburn K, Patrick D. Neflamapimod: Clinical Phase 2b-Ready Oral Small Molecule Inhibitor of p38alpha to Reverse Synaptic Dysfunction in Early Alzheimer's Disease. *The journal of prevention of Alzheimer's disease.* 2017;4(4):273-278.

253. Scheltens P, Prins N, Lammertsma A, Yaqub M, Gouw A, Wink AM, Chu HM, van Berckel BNM, Alam J. An exploratory clinical study of p38alpha kinase inhibition in Alzheimer's disease. *Annals of clinical and translational neurology.* 2018;5(4):464-473.

254. Alam JJ. Selective Brain-Targeted Antagonism of p38 MAPKα Reduces Hippocampal IL-1β Levels and Improves Morris Water Maze Performance in Aged Rats. *Journal of Alzheimer's Disease.* 2015;48(1):219-227.